PLIOCENE STRATIGRAPHY AND GEOLOGY OF THE

NORTHEASTERN ILERET REGION, KENYA

by

Casey Lee Kidney

A thesis submitted to the faculty of
The University of Utah
in partial fulfillment of the requirements for the degree of

Master of Science

in

Geology

Department of Geology and Geophysics

The University of Utah

December 2012

The University of Utah Graduate School

STATEMENT OF THESIS APPROVAL

The thesis of **Casey Lee Kidney**

has been approved by the following supervisory committee members:

Francis H. Brown	, Chair	**October 22, 2012**
		Date Approved
Ronald L. Bruhn	, Member	**October 22, 2012**
		Date Approved
Thure E. Cerling	, Member	**October 22, 2012**
		Date Approved

and by **D. Kip Solomon** , Chair of

the Department of **Geology and Geophysics**

and by Charles A. Wight, Dean of The Graduate School.

ABSTRACT

Five members of the Koobi Fora Formation: the Lonyumun, Moiti, Lokochot, Tulu Bor, and upper Burgi members, are exposed in Areas 40 and 41 (study area) northeast of Ileret in northern Kenya. Areas 40 and 41 were first mapped using tonal contrasts on aerial photographs by Key and Watkins in their 1988 study, and were not revisited until Gathogo and Brown did a reconnaissance, broadly mapping exposures in their 2006 study.

The study area is located on the eastern margin of the Turkana Basin, where the base of the Koobi Fora Formation is in contact with volcanic rocks of Miocene age. Five tuffs are exposed in the study area. Four tuffs occur in the Lonyumun Member: the Guo Tuff, the Kanyeris Tuff, and the newly named Tukunan and Kisemei tuffs. This study, directly or indirectly provides dates for the tuffs in the Lonyumun Member and associated strata by means of magnetostratigraphy and $^{40}Ar/^{39}Ar$ dating methods. Paleomagnetic sampling and the known dates on the Moiti and Tulu Bor Tuffs of 3.4 and 4.0 Ma respectively, proved invaluable in assigning ages to strata, and was materially helped by an $^{40}Ar/^{39}Ar$ age of 4.06 ± 0.02 Ma on the Kisemei Tuff. Three tuffs known at many other localities south of the study area, the Lokochot, α-Tulu Bor and Burgi Tuffs, are missing from the study area.

Stratigraphic correlations between exposures proved difficult due to numerous and pervasive disconformable surfaces, so that significant time gaps exist in the

Lonyumun Member; all of the Moiti Member except the Moiti Tuff is missing, as is all of the lower Burgi Member.

Newly discovered fossils in the Lonyumun Member have also been indirectly dated. Initial identification suggests correlation to fossils in the Apak Member at Lothagam southwest of Lake Turkana.

In Areas 129 and 130 the Tulu Bor Member is in contact with the Lonyumun Member. Three tuffs, disconformable on the Tulu Bor Tuff allow correlation outside of these areas of which the Aberegaiye Tuff is dated to 2.70 ± 0.02 Ma on alkali feldspars contained in pumices. The other tuffs include a correlate to a tuff in submember D-5 of the Shungura Formation and a correlate to Area 116 to a tuff below the Ninikaa Tuff, the former being the first documented proof for deposition between 2.6–2.0 Ma in the Koobi Fora Formation.

TABLE OF CONTENTS

LIST OF FIGURES

viii

LIST OF TABLES

ACKNOWLEDGEMENTS

relatively unknown.

I would like to thank my family, particularly my mother and father, who have supported me financially and emotionally though out my college career. I am very grateful for what they have done for me throughout the years so I could get to where I am today, an achievement that would have been challenging without their help and constant guidance.

Lastly, I would like to add a personal thank you to Dr. Brown for including me in this study and giving me an experience of a lifetime. His 47+ years of experience in the Turkana Basin proved invaluable in understanding and noticing geological relationships in the field. I had a unique experience, while traveling to and from the Turkana Basin. Dr. Brown brought me to towns and national parks on his dime. I met wonderful people who I stay in contact with, and plan on visiting in the future. During the past two years Dr. Brown has become a very good friend and colleague. I am honored to have worked with him.

CHAPTER 1

INTRODUCTION

In northern Kenya much geological work has been done on Pliocene and

Pleistocene strata of the Turkana Basin south of Ileret, where thousands of vertebrate and

early hominid fossils have been collected. The northern exposures of the Koobi Fora

Formation in Areas 40 and 41 have long been neglected, because security in the region

was poor during the 1970s and 1980s, and because it was believed that few fossils would

be found in these areas. Recent work by Dr. Francis Kirera (Kenya National Museums)

proved that strata of Area 40 contain mammalian fossils, however they are sparse and

concentrated in only a few locations. With the existence of fossil bearing strata, the area

warranted description and mapping. Also, the nature of the basin margin has long been

unknown. It was first mapped by contrast differences using aerial photographs by Bowen

and Vondra (1973) and only briefly described by Watkins (1983) during his work on the

volcanics of the Suregei Highlands.

This study reports on the geology in the northeastern part of the Ileret Region in

the Turkana Basin. Further it discusses relation of strata exposed there to strata in the

southern part of the Koobi Fora region east of Lake Turkana, and also the geological

nature of the basin margin. The geology of the area is of special interest because

extensive disconformities remove parts of the section that are well known, and more

continuous farther toward the center of the basin.

1.1 Geography and Climate of the Study Area

The study area measures about 10 km by 15 km, and is located northeast of Ileret

in northern Kenya (Figure 1). The Omo River, which today forms a large delta at the

north end of Lake Turkana, supplies most of the sediment to the Turkana Basin and its

deposits dominate the sedimentary record. Ephemeral streams, called "lagas" in Gabra,

drain into the lake from the highland areas surrounding the basin. In the local language,

Dasanetch, large ephemeral rivers and intermediate-sized rivers are called 'Il' and

'Kolom', respectively. The Dasanetch have named these rivers, and also many

geographically distinctive hills, ridges and plains. As noted by Passey et al. (2010), the

Turkana Basin, with a mean annual high temperature of 36.9 °C and low of 25.5 °C,

places it in the hottest ~1 percent of the land area of Earth.

Exposures of the Koobi Fora Formation east of Lake Turkana are divided into

numbered paleontological collection areas (Leakey, 1978; Brown and Feibel, 1991). The

study area includes two of these numbered areas, Areas 40 and 41. The Il Eriet is a

principal ephemeral stream flowing into Lake Turkana and separates Area 40 on the west

from Area 41 on the east (Figure 1). The study area extends from the Ethiopian border

southward to Kolom Ain Borana, an eastern tributary of the Il Eriet. It is bounded on the

east by the basin margin, and on the west by a major N-S trending normal fault. Another

large stream, Il Dura, with a latitudinal course, drains from the Suregei highlands into the

Il Eriet. The drainage basin of Il Dura is principally underlain by volcanic rocks of the

Asille Group (Watkins, 1983), whereas the area drained by Il Eriet is composed

principally of metamorphic basement rocks in Ethiopia, with smaller exposures of

rhyolitic ash flows of the Asille Group. The topography of the study area is subdued with

the lowest elevation along the Il Eriet at ~460 m, and the highest elevation (~580 m) at the summit of Lala, a distinctive isolated hill near the basin margin (Figure 1).

The field area is accessible from a dirt road leading from Ileret to the north, provided the surface is dry. The road is impassable for a few days if streams are flowing, or after heavy rains. The same camp along the Il Eriet was used during both field seasons because clean water can be drawn from shallow wells in the stream bed of the Il Eriet, and it is a central location within the study area allowing access to the area by foot or 4WD vehicle.

1.2 Previous Work in the Study Area

The stratigraphic nomenclature for Pliocene and Pleistocene strata in the Ileret region was first established by Behrensmeyer (1970), revised by (Bowen and Vondra, 1973) who defined the Koobi Fora Formation, and again revised by Brown and Feibel (1986) to arrive at the current scheme. The current stratigraphic nomenclature utilizes eight members divided by chemically distinct tephra layers (Brown and Cerling, 1982; Brown and Feibel, 1986). From oldest to youngest the members are: Lonyumun, Moiti, Lokochot, Tulu Bor, Burgi, KBS, Okote, and Chari. Members are defined as strata lying between the base of one marker tuff, which gives the member its name, to the base of the next overlying marker tuff. The Koobi Fora Formation is overlain by the Galana Boi Formation that consists of lacustrine strata of Holocene age. The Galana Boi Formation was formally defined by Owen and Renaut (1986) although the term was in use much earlier.

The first report about geology and paleontology in the Ileret and Koobi Fora regions was in 1888, resulting from exploration of the area by Teleki and von Höhnel.

The lake was first named Lake Rudolf after the Crown Prince of Austria (von Höhnel, 1894), and in 1975 was renamed Lake Turkana. Aside from a disastrous visit by Fuchs (1934), the Koobi Fora region would not be revisited for geological and paleontological purposes until the late 1960's when an aerial reconnaissance in 1967 revealed extensive sediments containing mammalian fossils and stone artifacts (Leakey, 1970). Behrensmeyer (1970) proposed an informal Pliocene and Pleistocene stratigraphic nomenclature involving three units, from bottom (oldest) to top (youngest): Koobi Fora I (KF-1), Koobi Fora II (KF-2), and Koobi Fora III (KF-3). Until 1973 geological reports only covered areas as far north as the Il Eriet, and no work had been done in the study area. Bowen and Vondra (1973) revised the stratigraphic nomenclature for the Pliocene and Pleistocene sediments in the Koobi Fora region. They expanded geological work to include strata along the eastern basin margin at Ileret, Koobi Fora and Kubi Algi. Correlation between these areas was based on three tuff horizons. The lower, was designated the Suregei Tuff Complex, which they traced north to south along the western flanks of the Suregei highland and used to correlate strata from the northern end of the traverse to the southern end. The two other tuffs were the Tulu Bor Tuff and the KBS Tuff. Bowen and Vondra (1973) used the tuff sequence to divide the stratigraphic sequence into three formations: the Kubi Algi Formation (strata that lay below the Suregei Tuff Complex), the Koobi Fora Formation (strata between the basal contact of the Suregei Tuff Complex and the top of the Chari Tuff), and the Guomde Formation (strata between the top of the Chari Tuff and the base of the Galana Boi Beds).

In the early 1970s geological work began north of the Ileret area in the Suregei Highlands by Watkins (1983). In his Ph.D. dissertation Watkins, mapped and proposed a

formal stratigraphic nomenclature for the Cenozoic volcanic and sedimentary strata in the area between Lake Turkana and Chew Bahir (Lake Stefanie). In mapping the western margin of the highland, he noted Pliocene aged lacustrine sediments overlying an older surface with angular debris.

The need to revise Vondra and Bowen's stratigraphic scheme came after Cerling and Brown (1982) showed by X-ray fluorescence (XRF) analysis that many tuffs correlated with the Tulu Bor Tuff were, in fact, different chemically. They also noted that the Suregei Tuff complex is not tuffaceous, instead being a diatomite. The current stratigraphic scheme by Brown and Feibel (1986) combines the Kubi Algi, Koobi Fora, and Guomde Formations into a single formation designated the Koobi Fora Formation.

The first published geologic map to incorporate the study area (Areas 40 and 41) was that of Key and Watkins (1988). They described strata in Area 40 as mostly superficial deposits of Pleistocene to recent age with some exposures of upper Koobi Fora and Guomde Formations (KBS, Okote and Chari Members). In Area 41 they mapped strata as Upper Koobi Fora and Guomde Formations with some exposures south of Il Dura belonging to the Lower Koobi Fora Formation (Lonyumun, Moiti, Lokochot, Tulu Bor, and Burgi Members). The map also shows the contact between sedimentary strata of the Koobi Fora Formation and volcanic rocks of the Asille Group (Watkins, 1983). This thesis maps the study area differently than Key and Watkins (1988), as is shown by the geological map in Appendix A.

Gathogo (2003) described the stratigraphy and paleoenvironments of the Koobi Fora Formation of the Ileret area, but concentrated his work south of the Il Eriet. The Lonyumun Member was described in Areas 13, 14, 15, and 41 where strata, of the

Lonyumun Member overlie Asille Group volcanics. These strata are similar to those in the study area, which include olive claystones with diatomaceous intervals that grade to sandstones rich in gypsum, ostracods and fish fossils. Gathogo (2003) also noted that exposures of the Lonyumun Member extend north of Il Biliet into Area 41.

Gathogo and Brown (2006) published the stratigraphy of the Ileret region principally on the basis of Gathogo (2003). Gathogo and Brown (2006) named and assigned the Guo and Kanyeris tuffs to undifferentiated Moiti and Lokochot Members in Areas 13 and 138, respectively, a placement that this study shows to be incorrect. The Guo Tuff had been noted in Area 13 by Bowen (1974), though not by that name.

Gathogo and Brown (2006) also did reconnaissance mapping in Areas 40 and 41 as far north as Il Dura. There they noted strata below the unconformity at the base of the upper Burgi Member, and above the local top of the Lonyumun Member noting that the sediments might belong to the Moiti, Lokochot, Tulu Bor or lower Burgi Members. They also noted an exposure of the Moiti Tuff in the northeastern part of Area 40 confirming the presence of Lonyumun and Moiti Members in that region.
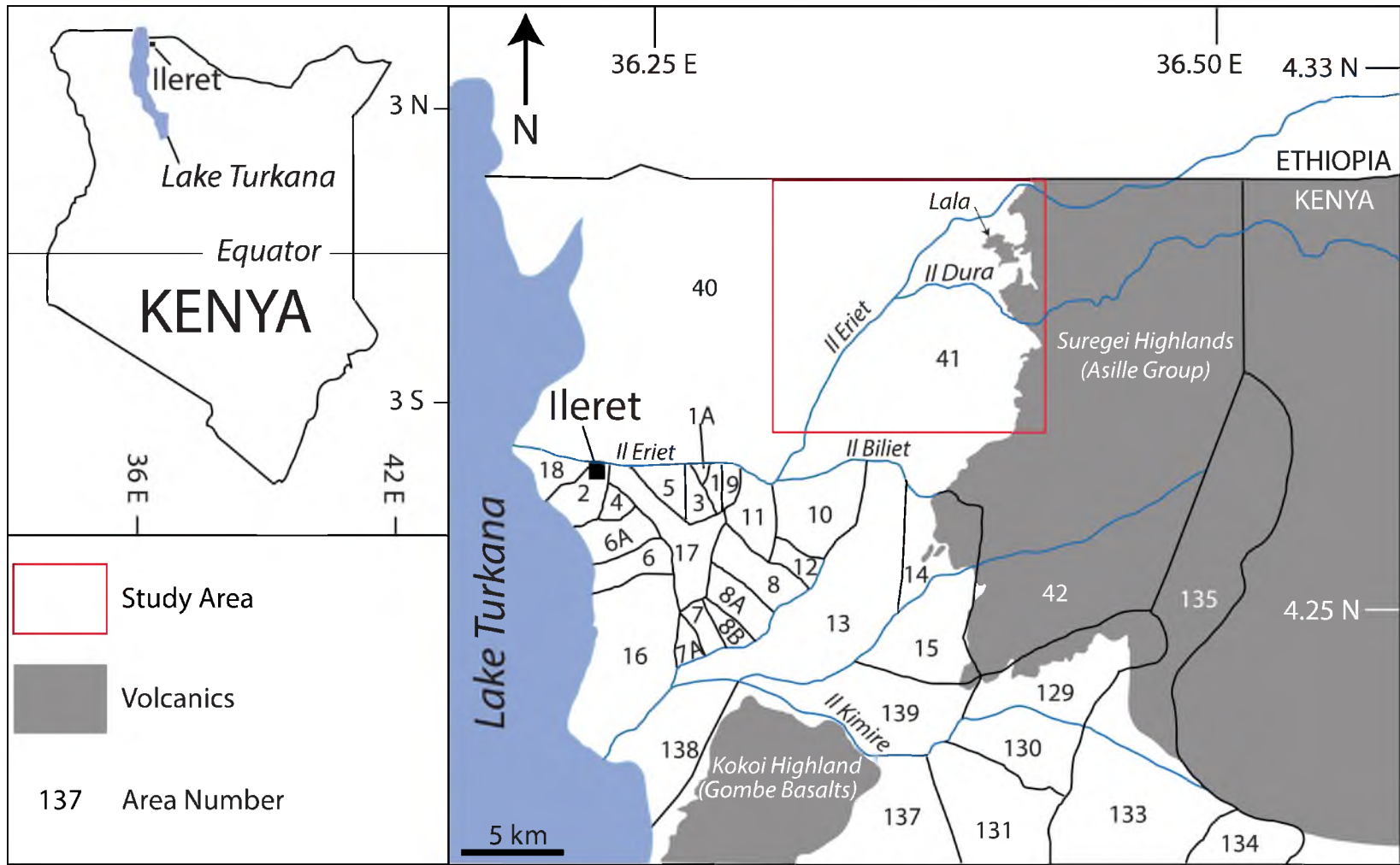
Figure 1. Overview of the study area and major geographical features. Paleontological collection sites in the Ileret region are numbered.

CHAPTER 2

REGIONAL GEOLOGIC SETTING

The study area lies in a lowland known as the Turkana depression, containing the

now closed Omo-Turkana Basin. Mammalian fossils have been recovered from strata of

Oligocene to Pleistocene age in the basin and include many hominids found in Pliocene

and early Pleistocene strata (Boschetto et al., 1992; Leakey and Leakey, 1978). Brown

and McDougall (2011) review geochronological control on all rock units within the basin.

2.1 Structural-Tectonic Setting

The Omo-Turkana Basin is part of the regional East African Rift System (EARS),

a 50–150 km wide zone of normal faulting spanning 3,500 km in a N-S direction from

the Afar Triple Junction to Mozambique (Figure 2). The Omo-Turkana Basin lies in the

Kenyan-Ethiopian rift and is part of the Turkana depression, a larger regional feature.

The Turkana depression lies between two lithospheric domes, the Afar Dome and the

East African Dome both of which probably formed by magmatic underplating (Morley et

al., 1999a). The northern, Afar dome, and the southern East African dome have average

elevations of 1,500 m and 1,200 m, respectively (Morley et al., 1999a).

The Kenya Rift, including the Omo-Turkana Basin, runs N-S from the Omo Rift

Basin in Kenya/southern Ethiopia to Lake Baringo in central Kenya (Morley et al., 1992;

Rosendahl, 1987; Ebinger et al., 2000). The Turkana Basin is the broadest stretch of the

EARS (150 km), containing three or four half-grabens in the widest portion. Half-graben formation may be caused by thinning of the crust to 18–20 km (Morley et al., 1999b). The basin also has many N-S trending normal faults, which in the Koobi Fora region are generally dropped down to the east.

Eocene volcanism in the northwestern Turkana depression is perhaps the earliest onset of rifting in this part of the East African Rift System (McDougall and Brown, 2008). Volcanic activity migrated northwest to the southern Ethiopian rift system during the early Oligocene (Ebinger et al., 2000; WoldeGabriel et al., 1990) and by Late Oligocene–Middle Miocene time, half-graben systems had formed west of Lake Turkana. Rifting migrated southward during the Middle–Late Miocene, N-S trending normal faults formed, and volcanism occurred in the central part of the rift, eventually migrating eastward. According to Haileab et al. (2004) normal faults must have been active after Middle Pleistocene time because faulting has occurred in the Silbo Tuff (0.74 Ma) in the Chari Member of the Koobi Fora Formation, and Gathogo (2004) showed that faulting also occurred during Okote Member times ~1.5 Ma ago. This study also notes good evidence for faulting of the Tulu Bor Tuff in Area 129 prior to deposition of the upper Burgi Member 2 Ma ago (see below). By the end of the Pliocene epoch about 35–40 km of extension had occurred in the central part of the Turkana Basin which is believed to have eventuated in short lived eruptions of basaltic material called the Gombe Basalts about 4.0 Ma (Haileab et al., 2004).

More information and much greater detail about the evolution of the Kenyan rift and greater EARS is presented in Morley (1999) "Geoscience of Rift Systems – Evolution of East Africa".

2.2 Stratigraphic Setting

Four major geological units make up the Turkana depression, they are: Early Paleozoic metamorphic crystalline basement; Cretaceous arkosic sandstones and conglomerates containing dinosaur fossils (western Turkana Basin); Oligocene and Miocene volcanic rocks intercalated with terrestrial sediments; and Pliocene and Pleistocene strata of the Omo-Turkana Basin that are termed the Omo Group and Turkana Group (de Heinzelin, 1983).

Sedimentation in the Koobi Fora region began in the Early Pliocene (~ 4.5 Ma) following capture of the Omo River by basin subsidence due to half-graben formation (Bruhn et al., 2011). Five major depositional environments dominate the geological record in the Koobi Fora Formation: fluvial channel, fluvial floodplain, delta, lake margin and lake basin. After capture of the Omo River at 4.5 Ma, a lake with an area about 3 times the size of the current lake formed that spread across the entire basin, reaching its maximum extent about 4.2 Ma. By the time of Moiti Tuff deposition (~ 4 Ma) the lake had filled in, and the Omo River, with its accompanying floodplain, meandered through the basin and exited to the southeast. Another short-lived lake, the Lokochot Lake, replaced the Omo River system around 3.5 Ma, however it was not as large as the Lonyumun Lake. From 3.45 - 2.0 Ma the Omo River again flowed from north to south through the basin exiting to the southeast. This exiting river has been given the name the Turkana River (Feibel, 1988). The Turkana River is believed to have flowed through the region now occupied by the Chalbi Desert, thence most likely through the valley of Lakh Dera, finally terminating in the Indian Ocean. Evidence for the existence of this river is plentiful, and includes small pumice clasts in the Tulu Bor Tuff

(3.43 Ma) north of Loiyangalani, large pumices in the Lokalalei Tuff (2.5 Ma) northwest of Loiyangalani, the existence of *Euthecodon brumpti*, a central African crocodilian, at Marsabit Road site near the southern end of the Chalbi Desert, and the appearance of the fossil stingray, *Dasyatis africana* in the basin ~2 Ma ago (Bruhn et al., 2011; Feibel, 1988). The stingray fossils offer substantial proof that the Turkana Basin and the Indian Ocean were once hydrologically connected. At about 2 Ma volcanic activity blocked the Turkana River, closing the basin, and causing the lake to become a permanent feature so long as sufficient water was provided (Bruhn et al., 2011). Once the basin was closed, lake levels rose and fell as a result of tectonic movements and climatic changes. The last large lake deposited the Galana Boi Formation about 10 ka ago when lake level reached an elevation of 457 m, during which time sediment input from the Omo River to the Koobi Fora region (and indeed, the current site of Lake Turkana) decreased dramatically when the lake overflowed to the northwest into the White Nile catchment (Brown and Feibel, 1991; Harris et al., 2006; Brown and Fuller, 2008) and sedimentation took place in the Kibish region rather than in the region of the current delta.

Brown and Feibel (1991) provide additional information on the stratigraphy, depositional environments and paleogeography of the Koobi Fora Formation, and illustrate paleogeographic reconstructions in the Turkana Basin through a series of maps.
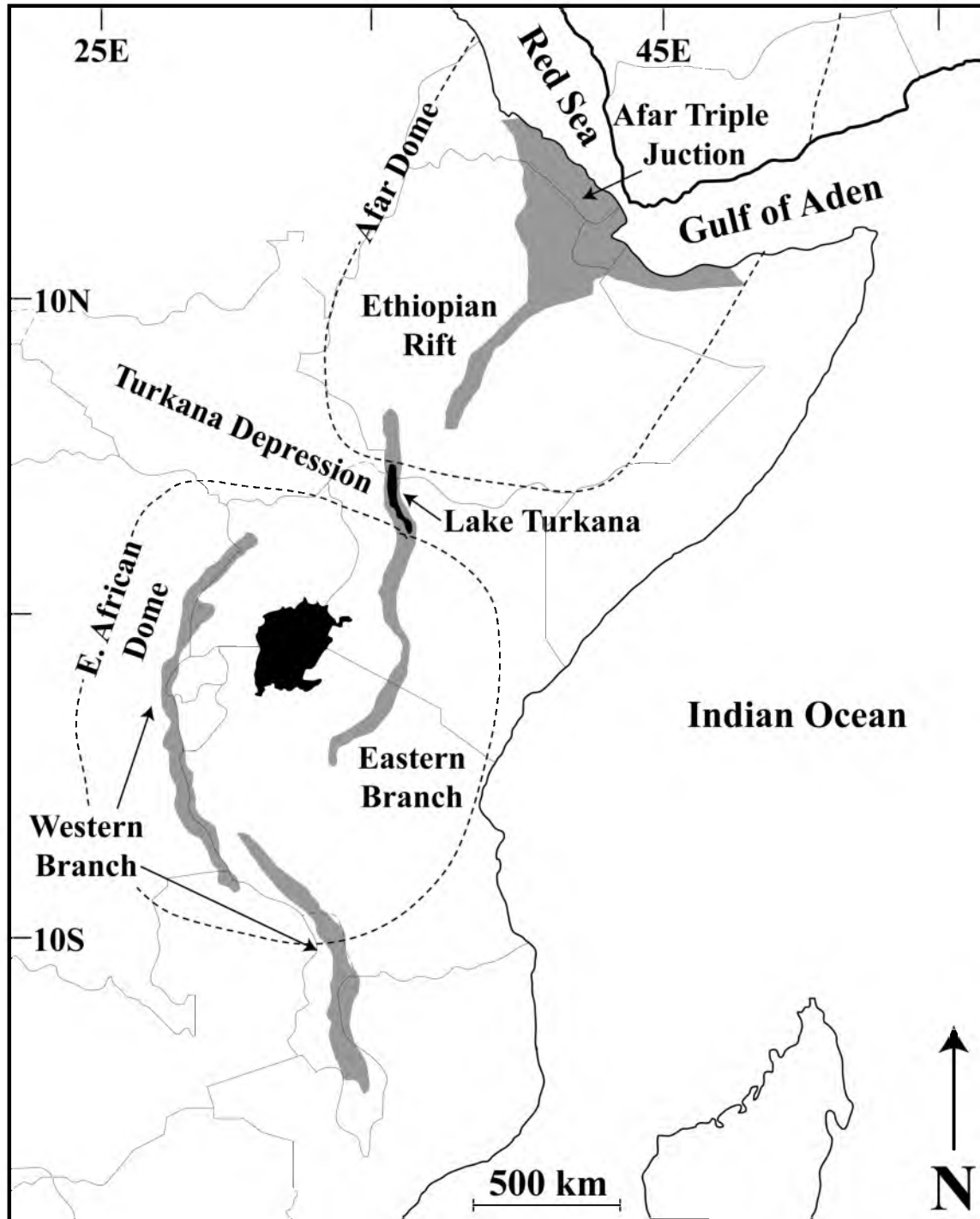
Figure 2. East African Rift System (EARS) showing the eastern and western branches, the Turkana Depression, and approximate location of the Afar and East African Domes (after Ebinger et al., 1989)

CHAPTER 3

OBJECTIVES

The purpose of this study was to map and describe in detail the strata in Areas 40
and 41 as well as trace out the basin margin, with the intent of correlating strata exposed
in Areas 40 and 41 with other, better studied parts of the Koobi Fora Formation in order
to establish their age. Specific objectives were as follows:

1. Map in detail Pliocene and Pleistocene strata from the eastern basin margin to the
   N-S trending, North Gele Fault;

2. Assign strata in the region to the appropriate member(s) of the Koobi Fora
   Formation, revising work as necessary;

3. Link strata along basin margin (Lonyumun Member) in the study area to sections
   measured by Gathogo (2003) in Area 15, and to sections established in Areas 129,
   135, and 139;

4. Assign ages to strata and faunal assemblage in the study area through $^{40}Ar/^{39}Ar$
   dating, tephrostratigraphic correlations, and magnetostratigraphy;

5. Create a geologic map for the region.

CHAPTER 4

METHODOLOGY

4.1 Field Work

Fieldwork was done over two 8-week periods during the summers of 2010 and

2011. Work was conducted from a temporary fly camp located in Area 41 on the eastern

bank of the Il Eriet. The camp consisted of six people, two Dasanetch field guides from

Ileret (Kokoi and Mutua); a Turkana camp manager from Loiyangalani (Simon Ilar) and

a Kamba mechanic from Nairobi (Lucas Mulinge) who was brought to maintain the field

vehicle, the author, and his advisor, F.H. Brown (University of Utah). Techniques used

to accomplish the objectives are described below.

4.1.1 Stratigraphic Sections

Stratigraphic sections were measured using a Jacob's staff and Brunton compass.

A machete and hoe were used to clear outcrops of thin overburden in order to expose

fresh surfaces for description of strata by their color, grain size, and lithology. A Brunton

compass was used to measure directional information on sedimentary bedding surfaces.

Beginning and ending GPS points were recorded for each measured section and sample

locations.

4.1.2 Collection of Samples for Paleomagnetic Study

An effort was made to sample the section from the bottom of the Koobi Fora

Formation up to the Tulu Bor Tuff. Samples were collected at intervals of a few meters

where sections had already been measured. Where exposure lacked, or because strata

were too coarse, the vertical sampling interval was variable

Outcrops were cleaned using a hoe and machete, in some locations requiring that

much material be removed. Directional arrows (north) were scribed on top of the

bedding surface, as the dips in the regions are very shallow except near faults. Thus dip

was not important in establishing the paleomagnetic polarity direction. Samples were

shaped in the field using hacksaws and sandpaper to make 2.5 x 2.5 cm cylinders, which

were then packed, and sent to the University of Utah for measurement.

4.1.3 Geologic Mapping

Stereographic aerial photographs (series HSL KEN 70) by Hunting NS and

Google Earth imagery with latitude and longitudinal lines were used for mapping in the

field. A GPS (Geographical Positioning System) receiver was used to record sample

locations and points of interest. The GPS device was set to decimal degrees (DD), and

the World Geodetic Survey 1984 (WGS 1984) reference ellipsoid is used for all locations

listed in the appendices.

4.2 Laboratory Analysis

All laboratory work was done at the University of Utah with the exception of

^{40}Ar/^{39}Ar dating which was done at the University of Wisconsin-Madison. Some sample

preparation was done in the field such as initial crushing and sieving of tephra samples, and shaping of paleomagnetic blocks.

4.2.1 Tuffaceous Samples

Tuffs and tuffaceous sandstones were prepared in the field by crushing them with a mortar and pestle then sieving through #60 (250 μm) and #120 (125 μm) mesh sieves, normally taking the -60+120 fraction for further treatment. Where there was insufficient material in the -60+120 mesh fraction, the finer material <125 μm was processed without further sieving.

Separates were cleaned in the laboratory by first washing and decanting them with deionized water to remove dust from the sample. Then all carbonate was removed from the sample using 10% nitric acid (HNO_3) to prevent formation of fluorite (CaF_2) during hydrofluoric acid cleaning. Once all carbonate had been removed then each sample was washed three times with deionized water. Next 5% hydrofluoric acid (HF) was added to the sample and put in an ultrasonic bath for five minutes to remove clay from glass shards. In some cases this step needed to be repeated. Samples were then dried and observed under a polarizing microscope to determine glass content. If needed, the glass was further concentrated by removing minerals using a Frantz Isodynamic Separator.

Microprobe mounts were then prepared for the glass concentrates, with eleven samples and a standard (mm3) in each mount and cemented using a two-part epoxy resin. A carbon coating was applied to the mount in a Denton Desk II Evaporator to ensure electrical conductivity under the electron beam of the microprobe.

Samples were analyzed on a Cameca SX-50 electron microprobe (EMP) equipped with four wavelength-dispersive spectrometers. Beam diameters between 5 and 25 μm were used with a voltage of 15 kV and a current of 25 nA. Natural obsidian (mm3) is used as the standard for O, Si, Al and K. Standards used for other elements are given in Brown and Fuller (2008). At least twenty glass shards were analyzed for each sample.

The resulting data were cleaned by removing analyses of glass with totals <98.5% or >101.5%, and analyses of mineral grains. Remaining analyses on glass were separated into modes by visual inspection, and each mode was averaged separately. The analyses were compared with analyses of other tuffs from the Omo-Turkana Basin using a database maintained by Dr. Francis H. Brown.

4.2.2 Paleomagnetic Samples

Paleomagnetic measurement was done at the University of Utah's Cryogenic Magnetometer Laboratory/Magnetically Shielded Room by the author. Dr. Susan Halgedahl and Dr. Richard Jarrard (both of the University of Utah) instructed the author in use of the machine and interpretation of results.

Cylindrical rock samples for measurement of paleomagnetism were prepared for measurement on a 2G Enterprises 760-3.0 Cryogenic Magnetometer equipped with three (x, y, and z) direct current superconducting quantum interference devices (DC SQUID). The instrument was installed in 1995 and is set up for manual measurement of single samples. For thermal demagnetization, all samples were heated from $100^{\circ}C - 650^{\circ}C$ at 14 temperatures to remove secondary remanent magnetism (Tauxe et al., 2010). If the magnetic moment of a sample approached zero at elevated temperatures ($>500^{\circ}C$), then it was only heated to $600^{\circ}C$.

4.2.3 ^{40}Ar/^{39}Ar Dating

Sanidine feldspars were dated using the ^{40}Ar/^{39}Ar dating method from two pumice-bearing tuffs. Pumices were crushed and sieved, obtaining the largest feldspar grains possible. A 100–200 μm fraction was used for all samples sent for dating. The cleaning process is the same for feldspars as that described for glass above. A binocular microscope was used to pick feldspars with no visible inclusions or glass rind. Once a pure separate was obtained, further cleaning and picking produced the cleanest possible grains. Picked grains were then stained with sodium cobaltinitrite to distinguish plagioclase and alkali feldspars. Alkali feldspars with high potassium content take up the stain and appear bright yellow, while plagioclase is dull white. Details and procedure for staining are given in Hynek et al. (2011).

Potassium-rich alkali feldspars were sent to the University of Wisconsin-Madison for dating at the Rare Gas Laboratory by Dr. Brian Jicha. From there, samples were sent to Oregon State University where they were irradiated for 3 hours in a cadmium-lined in-core irradiation tube in the TRIGA reactor (Salisbury et al., 2011). At the University of Wisconsin-Madison, single-crystal laser fusion was performed and in the case of smaller sanidines (<150 μm diameter), multiple crystals were fused together. All ages were calculated relative to 28.201 Ma for the Fish Canyon sanidine (Kuiper et al., 2008) using decay constants of Min et al. (2000). Age determinations are based on single crystal (bulk when single crystals were too small) feldspar analysis using the ^{40}Ar/^{39}Ar method. Feldspars were isolated from pumices within volcanic tuffs that were compositionally similar to the tuff. McDougall and Brown (2008) discuss in detail the chronology of the pre-KBS Tuff sequence.

CHAPTER 5

STRATIGRAPHIC DESCRIPTIONS AND INTERPRETATIONS

Five members of the Koobi Fora Formation are represented by ~190 m of strata in

Areas 40 and 41. From oldest to youngest they are: the Lonyumun Member (4.49 – 3.97

Ma), Moiti Member (3.97 – 3.60 Ma), Lokochot Member (3.60 – 3.43 Ma), Tulu Bor

Member (3.43 – 2.64 Ma) and the upper Burgi member (2.05 – 1.87 Ma) (McDougall and

Brown, 2008; McDougall and Brown, 2012). The upper Burgi member is the youngest

member of the Koobi Fora Formation in the study area and unconformably overlies lower

members. The unconformity is marked by the sharp onset of deposition of lacustrine

laminated siltstones and claystones that contain abundant fossil fish bones. A main focus

of this study was to map and measure in detail the stratigraphy of Areas 40 and 41. As

work progressed, considerable attention was afforded to the Lonyumun Member, which

makes up most of the strata in the region, and in a single isolated area, contains a rich

mammalian fossil fauna assemblage. Quaternary deposits include active ephemeral sand

streams and surficial cover comprised of fine- to coarse-grained sand, with clasts of

Asille Group volcanics derived from the Suregei Highlands. Most of the study area lies

above 460 m, so that the Galana Boi Formation, if present, would be confined to the

southwestern most part of the mapped area. However, no strata definitely attributable to

the Galana Boi Formation were noted.

At this point it seems sensible to introduce names and ages of some stratigraphic units that will be defined in the stratigraphic descriptions of individual sections in order that the reader will be able to follow the text more easily.

Several volcanic ash layers with glass compositions not previously encountered in the Turkana Basin were noted during the course of this work. Two of these are named in this thesis: the Tukunan Tuff, and the Kisemei Tuff. In addition the stratigraphic order of tuffs previously known has been confirmed, or re-evaluated. As these units and other marker beds are all important to correlating between sections within the study area and also more widely, and because $^{40}Ar/^{39}Ar$ ages measured on them are of importance to the chronostratigraphy of the area, they are presented in Figure 3 as a stratigraphic chart.

Because several of the tuffs are known from only one or a few outcrops, determining their relative age is not possible from field data alone. Each analyzed tuff, has a dominant mode, which is taken as the composition associated with its eruption. Many tuffs also contain subsidiary modes that are viewed as contaminants from older tuffs in the region. Where these subsidiary modes correspond to the dominant mode of another tuff, their presence allows the inference that a tuff containing such modes is younger than the contaminant. In this way, it is possible to state securely that the Kisemei Tuff is younger than the Kanyeris, Tukunan, and Guo tuffs. Similarly, the Kanyeris Tuff is younger than the Tukunan and Guo tuffs. The Tukunan and Guo tuffs contain only a single compositional mode, because they are the oldest of the tuffs in the Lonyumun Member. However, their ages relative to each other remain unknown, because neither contains a minor contaminant of the other.

Strata were assigned to members of the Koobi Fora Formation as defined by Brown and Feibel (1986) and are shown on the geologic map in Appendix A. Interpretation of depositional environments was done using the lithologic facies described by Brown and Feibel (1991) and followed their models of paleogeographic reconstructions.

Correlated columnar sections of the entire study area are given in Figure 4 and their locations are shown in Figure 5, with lithologic symbols used on the sections explained in Figure 6.

5.1 The Lonyumun Member

The Lonyumun Member constitutes the thickest and most laterally extensive strata exposed in the study area. It is defined as those strata above the contact with Miocene volcanic rocks to the base of the Moiti Tuff (Brown and Feibel, 1986). From bottom to top this member consists mainly of strata deposited in lacustrine, deltaic, and fluvial environments.

The base of the Lonyumun Member extends from the Ethiopian border southward through southern Area 41, and into Areas 15 and 129 (Figure 1) where it correlates to sections of Gathogo (2003), CLK10-S1, and CLK-129.1, -129.2, -135.1 respectively. Here, the Lonyumun Member is described in three intervals: a lower lacustrine interval from the Asille Group volcanics to a widespread conglomeratic sandstone, a middle deltaic interval from the top of the conglomeratic sandstone to a bivalve-packed sandstone, and finally an upper fluvial interval from the bivalve-packed sandstone to a disconformity or to the base of the Moiti Tuff depending on location within the study area.

Brown claystones and siltstones that contain diatomites characterize the lower interval in the study area and were deposited in a lacustrine environment associated with the Lonyumun Lake. Strata in the middle interval are mainly deltaic deposits of limonite-rich muddy sandstones, interbedded with invertebrate packed calcium-carbonate cemented sandstones. The middle interval grades upward to strata indicative of fluvial environments. Strata of the upper interval are mostly muddy sandstones with intervals of calcium-carbonate cemented channel sandstones. This interval includes all the tuffs in the Lonyumun Member and is the only interval that contains mammalian fossils. At the base of the upper interval a large assemblage of mammalian fossils was discovered during the 2011 field season in Area 40 north of Namorotukunan.

The Guo, Tukunan, Kanyeris, and Kisemei tuffs occur in the upper interval. The Tukunan Tuff is named after Namorotukunan hill near its only locality and similarly for the Kisemei Tuff which was found in the Kisemei drainage area. Feldspars from pumices within the Kisemei Tuff were dated to 4.06 ± 0.03 Ma by $^{40}Ar/^{39}Ar$ method placing the tuff in the Lonyumun Member because it is of greater antiquity than the Moiti Tuff

Assigning ages to the various sections through the Lonyumun Member is achieved here through the date on the Kisemei Tuff and by paleomagnetic sampling from the base of the Lonyumun Member to the base of the Tulu Bor Tuff. Estimating ages for the other tuffs (Kanyeris, Guo, and Tukunan tuffs) in the Lonyumun Member is important because they are exposed in other locations south of the study area where mammalian (including hominin) fossils have been discovered.

5.1.1 Lithologic Description - The Lower Interval

The base of the Lonyumun Member is in contact with Miocene Asille Group volcanic rocks (Figure 7), and colluvium (Figure 8) that make up the eastern basin margin. It is best exposed on the western slope of the Suregei Highland, and north of Il Eriet where it extends northward to (and across) the Ethiopian border (Figure 1). The base of the member is characterized by diatomaceous siltstones overlain by ~ 20 m of laminated claystones that are capped by a widespread orange conglomeratic sandstone rich in quartz, feldspar, and biotite (Figure 9). Sections CLK11-S5, and CLK10-S12, and -S2 (Figure 10) correlate to this lower interval. Here the diatomaceous layer in CLK11-S5 and the lowest diatomite in CLK10-S12, and -S2 are correlated to the lower diatomite in PNG-14.1, -14.2 and in CLK10-S1 (Figure 11). The diatomites at the bottom of section CLK10-S1 are in contact with colluvium developed on Asille Group volcanics along the eastern basin margin (Figure 12).

The lower interval extends from the basin margin westward where it crops out between Lala and a syncline containing the Moiti Tuff. Exposures continue north of the Il Eriet to the Ethiopian border where the lower diatomite allows correlation of CLK11-S16 to CLK10-S12, -S2, -S7 and CLK11-S5 (Figure 10). The lower interval north of the Il Eriet contains large-scale internal folding in strata associated with the widespread conglomeratic sandstone. Sandy section adjacent to, and sandwiched between, horizontal strata make up the top 12 m of the lower interval in CLK11-S16 (Figure 13). CLK11-S16 represents a minimum thickness of ~ 40 m for the conglomeratic sandstone that caps the lower interval. The total thickness of the sandy section is unknown because no marker bed could be correlated to another section. Instead CLK10-S16 is measured to a

geographical high. The total thickness (minimum) of the lower interval is then ~60 m in Area 41, determined by using the thicknesses of CLK10-S12, -S2 and CLK11-S5.

In the Kisemei drainage, west of Na'uko (Figure 4) the bottom 5 m of CLK10-S9 (Figure 14) correlates to the lower interval. This condensed interval contains gastropod-packed cobble (~15 m) conglomerates with clasts derived from Asille Group basalts (Figure 15). The top of the lower interval is marked by a carbonate-rich fine-grained sandstone that overlies the conglomerates at the base. The carbonate-rich sandstone is packed with ostracods and correlates southward to the top of PNG-14.2 (Figure 11), which then correlates to the lower ostracodite containing gastropods and fish bone in PNG 41.2 (Figure 14).

The lower interval extends northeast into southern Ethiopia where it may correlate to the Ileret sediments described by Davidson (1983). Davidson (1983) correlated these strata to the Ileret sediments of Vondra and Bowen (1976) and described the exposures as well-bedded claystones rich in gypsum, siltstones, sandstones, gravels and tuffs. Only the existence of tuffs noted in this description differentiates these strata from those of the lower Lonyumun interval. Coarse clastic rocks are noted to lie against basalts in Ethiopia just north of the study area and are unconformable on Asille Group volcanics, but contain few volcanic clasts. If Davidson's correlation is correct, then either the sediments in Ethiopia at an elevation of ~600 m have been uplifted since deposition or strata in the Turkana basin have dropped down. This is because they lie ~140 m above the elevation of the drainage divide (457 m) into the White Nile from the Turkana Basin. However, the presence of tuffs in the Ethiopian sections may suggest that deposits there were laid down at a different time.

Davidson's work on the area also provides insight to the source of biotite in clastic rocks exposed in the study area. The probable source is the biotite- and hornblende- gneisses north of the study area in Ethiopia which possibly provide the abundant biotite found in the orange conglomeratic sandstone.

5.1.2 Lithologic Description - The Middle Interval

The lower interval is overlain by a middle interval that is the most invertebrate-rich of all strata in the study area. The interval consists mainly of limonite-rich thinly bedded siltstones and claystone with minor laminated claystone intervals and well-cemented sandstones. Most interbedded siltstones and claystones are pale-yellow to light brown (Figure 16), laminated claystones are pale olive brown, and calcite-cemented sandstones are light grey to very pale yellow.

Only section CLK11-S7 (Figure 10) links the top of the lower interval to the bottom of the middle interval. The upper sandy section of the lower interval is represented here as long ribbons of sandstone exposed on the surface (Figure 17). In section CLK11-S7 a gastropod-rich sandstone and a diatomaceous layer are overlain by 28 m of muddy sandstone that make up the middle interval. The lower 16 m of CLK11-S6 is correlated with the middle interval, and with CLK11-S7 by an ostracodite through the intervening section CLK11-S8 (Figure 18). The top of the middle interval is marked by a sandstone packed with shells of the bivalve *Pseudobovaria* sp. (Figure 19). The *Pseudobovaria* sp. packed sandstone extends from the top of CLK11-S7 to CLK10-S4a in Area 41 (Figure 18). In CLK10-S4a and CLK10-S3 the middle interval (~ 33 m) from bottom to top includes a 4 m thick muddy sandstone with very well preserved wood

fragments, a sandstone packed with gastropods, bivalves, fish bone, and a 10 m thick interval with lenses of calcite-cemented sandstones at the top (Figure 20).

In the Kisemei drainage area ~ 35 m of muddy sandstones with abundant carbonate concretion layers correlate to the middle interval (Figure 14). The middle interval extends southward where it correlates to the 23 m of strata above the youngest ostracodite in PNG-41.2 (Figure 14).

5.1.3 Lithologic Description - The Upper Interval

The upper interval of the member was deposited under fluvial conditions, includes all the tuffs in the member, and is the only interval in which vertebrate fossils were noted in abundance. Tuffs in the upper interval from oldest to youngest are: the Guo Tuff (Area 40), Tukunan Tuff (Area 40), Kanyeris Tuff (Areas 40 and 41), and the Kisemei Tuff (Area 41).

At Namorotukunan the top 9 m of CLK11-S6, and section CLK10-S7 make up the bottom of the upper interval (Figure 21). At these localities, fine grained, limonite-rich cross-bedded sands grade up to siltstones in fining upward sequences. There is a large well-preserved vertebrate fossil assemblage in strata of the lower 6 m of CLK11-S6. The probable age of this assemblage is discussed in Chapter 9.

Section CLK11-S13 (Figure 21) correlates to the top portion of the upper interval of the Lonyumun Member where the Kanyeris Tuff caps a small remnant hill that exposes 16 m of claystone, siltstone, and muddy thin-bedded sandstone containing minor gypsum. In section CLK10-S11 the Tukunan Tuff is overlain by 8 m of muddy sandstone with abundant calcite concretions and then by the Kanyeris Tuff (Figure 21). This section is important because it establishes the stratigraphic level of the Tukunan

Tuff relative to the Kanyeris Tuff and the β-Tulu Bor Tuff. The top of the Lonyumun

Member is marked by a disconformity above the Kanyeris Tuff in sections CLK10-S11, -

S10 and CLK11-S13 (Figure 21) and recognized by a change in paleomagnetic polarity.

In section CLK10-S8 (Figure 21) the top of the Lonyumun Member is placed at the top of

a layer rich in calcite concretions (caliche layer). The formal top of the Lonyumun

Member is defined as the base of the Moiti Tuff, however this tuff does not occur at these

localities and the disconformity it used as the top of the member in its place. The Moiti

Tuff is, however, present in CLK11-S15 where it overlies ~ 9 m of muddy sandstone of

the upper interval (Figure 21).

East of Il Eriet the Moiti Tuff overlies ~ 37 m of strata in the upper interval, and

is expressed as a plateau at the top of a synclinal structure. The upper interval is

composed mostly of medium to fine grained sandy section with intervals of thinly bedded

to laminated siltstones, and cemented discontinuous sandstones laterally containing

gastropods and bivalves (Figure 22). The bottom portion of the upper interval is made up

of coarsening upward sequences that grade to siltstones with lenticular sandstones that

contain mammalian teeth. The top part of the upper interval contains a calcite-cemented

sandstone with large bivalves, ostracods and gastropods. This is overlain by fining

upward sequences that are capped by the Moiti Tuff, the base of which marks the top of

the Lonyumun Member in this locality (Figure 22).

In the Kisemei drainage the upper interval of the Lonyumun Member includes the

Kisemei, Kanyeris and Guo tuffs. These tuffs allow correlation of the strata in the

Kisemei drainage area to those north of Il Dura and north of Namorotukanan by the Moiti

Tuff (Figure 23). To the north, the section at Kisemei is contiguous with a section that is drained by a small tributary of Il Dura.

The upper interval of the Lonyumun Member in the Kisemei area (Figure 23) is made up of calcified sandy mudstones locally rich in gypsum that contain sparse well-preserved vertebrate bones (Figure 24). To the south, the section contains a cemented sandstone packed with rhizoliths and gastropods. The bottom half of the strata described above is present below the Guo Tuff in CLK10-S9 and CLK11-S14. The top half of the upper interval is taken as the base of the Guo Tuff. The bottom of section CLK11-S4 correlates to the top half where the Guo Tuff is overlain by 9 m of muddy sandstone and calcified sandstone, and then by the Kanyeris Tuff establishing the relationship between the Guo and Kanyeris Tuffs. The Kisemei Tuff lies 5 m above the Guo in CLK10-S14. CLK11-S2 correlates to the upper interval by the Kisemei Tuff at its base where it lies 18 m below a prominent gastropod packed cemented sandstone. In section CLK11-S1 the Moiti Tuff lies 11m below the same gastropod packed sandstone, allowing correlation of the Kisemei, Kanyeris and Guo tuffs to exposures of the Moiti Tuff.

The Kisemei Tuff is newly defined here, with the type locality given as a small exposure on the northern bank of one of the streams that makes up Kisemei at 4.3792 N latitude, and 36.3700 E longitude. At the type locality it is about 2 m thick, and composed principally of small pumice clasts set in a sandy matrix composed mainly of glass shards. It is named here because alkali feldspars from the pumice clasts have been dated to 4.06 ± 0.02 Ma, and it therefore provides important temporal control on this part of the section.

The Tukunan Tuff is also defined in this study. This is a local unit and shards of its composition make up as a minor component of the Kisemei Tuff (see above), but because it is compositionally closely similar to the α-Tulu Bor Tuff (see Table 1), it is named here in order to prevent confusion with that unit. The type locality of this tuff is designated as an outcrop in the upper reaches of Il Gele at 4.4043 N, 36.3269 E, where the tuff is exposed. At the type locality it has a maximum thickness of 2.5 m, and demonstrably lies below the Kanyeris Tuff. It is composed of nearly pure glass shards of only one composition, and differs from the α-Tulu Bor Tuff principally in its higher TiO_2 content and lower Cl content.

As shown by Gathogo and Brown (2006), the Guo Tuff and the Kanyeris Tuff are of very distinct composition, notably in their rather high CaO content. Thus far, the Guo and Kanyeris tuffs are known only from the northernmost part of the Koobi Fora region, and have not been recognized in strata of broadly comparable age anywhere else in the Omo-Turkana Basin. Analyses of tuffs from the study area spanning the interval from the Guo Tuff to the β-Tulu Bor Tuff are arranged stratigraphically in Table 1 along with comparative analyses from Gathogo and Brown (2006) where appropriate. Compositions of the α- and β-Tulu Bor tuffs are well known (Cerling and Brown, 1982), and need no comment. They are included because the Tukunan Tuff has a composition closely similar to that of the α-Tulu Bor Tuff. Similarly the composition of the Moiti Tuff is well known (Brown et al., 1992), including the minor modes, which are similar to that of pumices within the tuff.

The Kisemei Tuff is, in fact, a pumice gravel that lies near the level of the Kanyeris Tuff in the section. Unlike the units just discussed, it contains glass of several

compositions that are quite different. With the data currently available, it is not possible

to say whether the principal modes of many of the samples actually represent discrete

compositions, or whether they are part of a continuum of compositions from a zoned

magma. Of importance, though, is that samples of the Kisemei Tuff contained glass

shards with compositions that correspond closely to those of the Guo, Tukunan and

Kanyeris Tuffs, suggesting that the Kisemei Tuff was deposited following eruption of

those two units. Four shards have compositions most similar to glass of the Naibar Tuff,

but as this tuff has been dated at 4.02 ± 0.02 Ma, they perhaps belong instead to yet

another older tuffaceous unit.

Gathogo and Brown (2006) first named the Guo and Kanyeris tuffs and assigned

both to an undifferentiated Moiti/Lokochot member. At Kisemei, however the Guo and

Kanyeris Tuffs can be shown to lie below the Moiti Tuff, and by definition they must

belong to the Lonyumun Member (Figure 23). This thesis thus revises the stratigraphic

placement of Gathogo and Brown (2006) and reassigns the Guo and Kanyeris Tuffs to the

Lonyumun Member.

5.1.4 Interpretation

During initial deposition of the Lonyumun Member a large lake had inundated the

study area. Evidence of this lake has been recorded along the eastern basin margin to the

south (Gathogo, 2003; Gathogo and Brown, 2006) as well as still farther south beyond

the Ileret Region (Brown and Feibel, 1986, 1991; Feibel et al., 1991).

Lonyumun Member sediments in Area 41 along the basin margin comprise ~ 20

m of laminated, iron rich, olive brown claystones and siltstones with two distinct

diatomaceous siltstones near the base, which are indicative of a pelagic lacustrine

environment. As discussed above, these layers are also present south into Areas 14 and

15 (Figure 11) where Gathogo (2003) also described deposits of the Lonyumun Lake.

Northeast of Lala, coarser sandstones and conglomerates with significant components of

basalt, and metamorphic basement derived from the northeast are intercalated in thick

layers of claystone. Coarser sediment introduced into the basin from the northeast may

have been blocked by Lala, thus accumulating only in the northeast, depriving the basin

margin south of Lala of coarse-grained material.

The lower interval grades abruptly from laminated claystones to a conglomeratic

sandstone in northern Area 40 and north of Il Dura in Area 41. The conglomeratic

sandstone overlies Asille group volcanics, and dips gently away from the Suregei

Highland, suggesting uplift sometime after deposition. In this interval, large scale

internal folding within the unit has a variety of orientations. Yet in places its strata are

not deformed, and wherever there are overlying and underlying strata the unit is preceded

and followed by undeformed strata. Folds generally trend east-west suggesting a slope

from north to south, given that sediment was sourced from the north. Soft sediment

deformation is also prevalent in the coarse sands suggesting rapid deposition (Figure 25).

The biotite and hornblende grains were probably delivered to the Omo River system from

marginal streams draining the gneissic basement in southern Ethiopia north of the study

area.

The deformed unit may be a deltaic slump deposit that formed during the time the

Lonyumun Lake was receding from the study area. Recent articles on slump folding

describe characteristics similar to the structures and sediment deformation observed in

this interval. Given the tectonic history of the Turkana Basin the suggested mechanism for producing the slumps is seismicity (Alsop and Marco, 2012; Gibert et al., 2005).

The middle interval of the Lonyumun Member records a deltaic environment. The Omo Delta progrades farther south after the slumping event deposited thinly bedded fine sands and silts very rich in limonite in Areas 40 and 41. Similar deposits of much younger age are present in the Kibish Formation (southern Ethiopia) with each layer being a yearly deposit (Brown and Fuller, 2008). Still later the lake receded farther south as shown by the presence of beach and marginal lacustrine environments in the Kisemei drainage area, and distributary channels developed in the area north of Namorotukanan. Bivalves occupy the distributary channels or broad delta flats, corresponding to the widespread bivalve packed sandstone in sections CLK10-S4a and CLK11-S7 (Figure 18). During this time, but before deposition of the Guo Tuff, fairly complete vertebrate fossils, such as the crocodilian noted in section CLK10-S9, are preserved in muddy sandstones that are laterally transitional to beach deposits. This area was most likely a marginal lacustrine environment with an ephemeral stream delivering coarse sediment into the lake in a way similar to the that of the modern Il Eriet.

Still later, the Lonyumun Lake continued to drop and the deltaic environments are replaced by fluvial channel and fluvial floodplain environments. This is consonant with Brown and Feibel (1991) who state that by 3.9 Ma the Lonyumun Lake was filled in and the Omo River flowed through the basin as a meandering river. The Guo, Kisemei and Moiti tuffs all contain pumices and have internal ripple structures suggesting that these tuffs are derived from the Omo-River. The Kanyeris and Tukunan tuffs vary in thickness

laterally and are associated with muddy sandstone deposits containing rhizoliths, suggesting they too are fluvially deposited.

An unconformable surface or the base of the Moiti Tuff (depending on locality within the study area) represents the top of the Lonyumun Member. The unconformity occurs throughout the study area and marked by either a paleomagnetic reversal or a caliche surface.

5.2 Moiti Member

By definition, the Moiti Member includes all strata that lie between the base of the Moiti Tuff and the base of the Lokochot Tuff (Brown and Feibel, 1986). The Moiti Tuff is present in three places within the study area: in Area 41 between Lala and Il Eriet (Figure 22) and the Kisemei drainage (Figure 21), and in Area 40 northeast of Namorotukanan (Figure 23). A tuff with a composition most similar to that of the Wargolo Tuff (Table 2) lies disconformably on the Moiti Tuff at the first two locations listed above. deMenocal and Brown (1999) provide an orbitally tuned age for the Wargolo Tuff of 3.80 ± 0.01 Ma.

5.2.1 Lithologic Description

In Area 41, the Moiti Tuff ranges from 2–4 m thick from south to north respectively and caps a small plateau in a syncline bounded by normal faults. At the southern end of the plateau thin patches of the Wargolo Tuff lie disconformably on the Moiti Tuff (CLK11-177, -178; Table 2; Figure 22). Little overlying section is exposed, but the surfaces of both tuffs are covered with coarse quartzo-feldspathic sandstone that contains large subrounded cobbles (≤ 10 cm) of quartz and perthitic feldspar. At this

locality the Moiti Tuff overlies fluvial deposits of the upper part of the Lonyumun

Member. South of Il Dura on the northern slope of Na'uko there is a small exposure of

the Wargolo Tuff where Moiti Member strata may be preserved. After hours of

inspection the exposure yielded a small pumice compositionally the same as the Wargolo

Tuff (CLK11-196; Table 2).

Northeast of Namorotukanan in Area 40, the Moiti Tuff (~ 4 m) also forms a

plateau above fluvial deposits in the upper part of the Lonyumun Member. The tuff is

also fault bounded here at its eastern extremity. At the northern end of the plateau, the

tuff contains a gravel bar made up of pumices up to ~8 cm in maximum dimension

(Figure 26), but elsewhere on this outcrop, the tuff contains accretionary lapilli. At this

locality the Wargolo (CLK11-159; Table 2) also overlies the Moiti Tuff in a similar

fashion as Area 41 and the surface is covered with materials similar to those described for

Area 41. Of importance is that the β-Tulu Bor Tuff appears to lie disconformably on the

Moiti Tuff and the underlying section. It is also important to point out that west of the

Moiti Tuff in Area 40, the Wargolo Tuff lies disconformably on the Kanyeris Tuff in a

small northern facing outcrop. The implication is that the Wargolo rests disconformably

on the Lonyumun Member in a thin section of Moiti Member strata.

At Kisemei, the Moiti Tuff is exposed at the bottom of an ephemeral stream for

only a few tens of meters laterally. This latter location is important because strata above

the Moiti Tuff may belong to the Moiti Member. These consist of coarse fluvial

sandstones similar to those that overlie the Moiti Tuff in the other two areas, but lack the

quartz and perthite cobbles.

The Moiti Member is known to exist in Areas 40 and 41, but is limited in its expression mainly as the Moiti and Wargolo tuffs. It may be that in the past, as today, these tuffs were resistant enough to erosion to form plateaus similar to those in the present landscape that were then buried by subsequent deposition associated with the β-Tulu Bor Tuff. Currently we have no evidence that there was ever a substantial section of the Moiti Member, however, if this was the case, those strata have subsequently been removed by erosion.

5.2.2 Interpretation

In the two plateau sections, the Moiti Tuff was fluvially deposited either in a single channel or in two related channels when the ancient Omo River flowed as a meandering river through the basin (see Brown and Feibel, 1991). The pumice deposit in Area 40 suggests that this may have been the lowest part of the topography, and that the plateau in Area 41 represents deposition on a related floodplain. If this is the case, then the topographically low area was at least 3 km in dimension from east to west. The occurrence of the Moiti Tuff in the Kisemei drainage may represent the eastern edge of deposition of this unit, but a thin fluvial section of the Moiti Member may exist in this latter locality.

Following deposition of the Moiti Tuff was a depositional hiatus until the Wargolo Tuff, brought by the Omo River, was deposited on the Moiti Tuff at ~3.8 Ma. Because the Wargolo Tuff lies almost directly on the Kanyeris Tuff, it follows that if strata were deposited in the area, then those strata must have been removed exposing the Moiti Tuff plateaus and the Lonyumun Member in western Area 40 before its deposition.

5.3 Undifferentiated Lokochot and Tulu Bor Members

The Lokochot Member is defined as those strata that lie between the base of the Lokochot Tuff and the base of the α-Tulu Bor Tuff (Brown and Feibel, 1986). The Lokochot and α-Tulu Bor do not occur in the study area, but there are up to 26 m of strata between the β-Tulu Bor Tuff and the underlying Kanyeris Tuff in Area 40 that are of normal polarity (see Chapter 6), which suggests that they belong to either the Lokochot or Tulu Bor members. From studies elsewhere in the basin (Hillhouse et al., 1986; Brown, Shuey & Croes, 1978), the transition from reversed polarity below to normal above is known to occur at the level of the Lokochot Tuff, coinciding with the boundary between the Gilbert and Gauss Chrons. In Area 41 strata above the Kanyeris Tuff in sections CLK11-S1, -S2, -S3, -S4, and -S14 and in section CLK10-S9 are constrained only to lie between the Kanyeris Tuff and the disconformity at the base of the upper Burgi Member, therefore they may belong to the Moiti, Lokochot, Tulu Bor, or lower Burgi members. Their paleomagnetic polarities were not measured, but doing so would limit the possible placement of strata to those members.

5.3.1 Lithologic Description

Thickness of the undifferentiated Lokochot/Tulu Bor Member decreases from east ($\sim$ 20 m) to west ($\sim$ 5 m) in Area 40. The bottom of the member is provisionally placed at a prominent paleosol carbonate (caliche) layer in section CLK10-S8 and at the top of the Kanyeris Tuff in sections CLK10-S10 and CLK11-S11 (Figures 27). Sediments are fairly homogenous pale brown sandy mudstones that become sandier to the west. The bases of these sandy mudstones include pebbles of quartz and feldspar set in a fine-grained matrix. Calcium carbonate concretions exist throughout the undifferentiated

member, with some forming grey, cemented concretionary layers. No vertebrate or invertebrate fossils are known in these strata.

5.3.2 Interpretation

Fluvial and fluvial floodplain deposits continue above the Moiti Tuff to the base of the Tulu Bor Tuff making up the undifferentiated Lokochot/Tulu Bor Member. Caliche surfaces are present throughout the entire section occurring in muddy sandstones rich in rhizoliths. Dry stream beds would have been prominent in this area probably accounting for the lack of fossils in this member.

5.4 Tulu Bor Member

The Tulu Bor Member is defined as those strata from the base of the Tulu Bor Tuff to the bottom of the Burgi Tuff (Brown and Feibel, 1986). The Burgi Member is divided into two parts, the lower Burgi being from the base of the Burgi Tuff to a widespread disconformity first recognized by Bowen (1974), then later revised by Brown and Feibel (1986) and finally dated at 2 Ma by Gathogo (2003). The upper Burgi is defined as those strata from the 2 Ma disconformity to the base of the KBS Tuff (Brown and Feibel, 1986). The Burgi Tuff does not occur in the study area, but the 2 Ma disconformity is prominent in Area 40 around Namorotukunan and in Area 41 around a hill south of the Il Dura and Il Eriet confluence. Here strata that lie between the base of the β-Tulu Bor Tuff and the 2 Ma disconformity can confidently be assigned to the Tulu Bor Member.

5.4.1 Lithologic Description

Strata of the Tulu Bor Member (45 m) are much coarser than underlying strata in the study area and are best represented in section CLK10-S10 (Figure 27). In this section the β-Tulu Bor Tuff is expressed as a tuffaceous sandstone about 20 cm thick that contains quartz, biotite, rhizoliths, and white, flat, spherical, and bubble junction glass shards. The β-Tulu Bor Tuff is overlain by 8 m of pale brown, poorly sorted, medium sandstone with rounded to angular grains, and contains abundant calcite concretions. The rest of the section (37 m) is made up of coarse conglomeratic sandstones with occasional thin sandy mudstones having quartz and feldspar pebbles near their bases. Conglomeratic sandstones are reddish brown, rich in rhizoliths, contain some clay and are weakly cemented. Thin ledge-forming cemented sandstones are prominent at the top of the member. Overlying the lower sediments is the disconformity at the base of the upper Burgi member, marked by a heavily cemented fining upward medium sandstone containing abundant fish bones and some gastropods. The highest bed below the disconformity is taken as the top of the Tulu Bor Member in CLK10-S10 (Figure 27).

Also assigned to the Tulu Bor Member in Area 41 are ~ 13 m of coarse grained conglomeratic sandstones similar to the ones described in Area 40 are exposed on a cliff along the Il Eriet (Figure 28). At the base of the cliff there are well-cemented cobble conglomerates overlain by channelized conglomeratic sandstones. These conglomerates continue south along the western slope of the hill where they are overlain by strata above the upper Burgi disconformity

5.4.2 Interpretation

Coarse gravels with short intervals of muddy sandstones both containing calcite concretions and cemented channelized sandstones characterize the Tulu Bor Member in the Namorotukunan area and along the western edge of Area 41. The coarse gravels are mainly composed of quartz and feldspar with minor metamorphic and volcanic fragments. Given the mineralogical and lithological composition of this interval, the source for sediment is likely the biotite and hornblende gneisses in southern Ethiopia. These coarse deposits reflect periods of intermittent flow from the northeast by an ephemeral stream similar to the Il Eriet, the seasonal nature of the area may have allowed abundant calcium carbonate concretions to form in these sediments during dry periods.

This depositional environment during this time for the Tulu Bor Member is consistent with the paleogeographic descriptions of Brown and Feibel (1991). Farther south in the basin, there is evidence for a lake, the Lokochot Lake, smaller than that of the Lonyumun Lake that had formed before deposition of the Tulu Bor Tuff, however there is no evidence that this lake existed in the study area. Either the Lokochot Lake did not extend this far northward (or eastward) or evidence for its existence was removed by erosion at a disconformity below the β-Tulu Bor Tuff. At the time of Tulu Bor Tuff deposition, the lake had filled in and the Omo River flowed from north to south through the basin. The tuffaceous sandstone containing the β-Tulu Bor Tuff may have been deposited on the sides of the Omo River on its associated floodplain. It is of significance that neither the α-Tulu Bor Tuff nor the Lokochot Tuff have been identified in this region. The implication is that following erosion of the Lonyumun and Moiti Members, deposition ensues shortly before the β-Tulu Bor Tuff.

5.5 Burgi Member

The Burgi Member is defined as those strata that lie between the base of the Burgi

Tuff and the base of the KBS Tuff (Brown and Feibel, 1986). Within the study area,

there is no evidence for deposition during lower Burgi Member times, and only part of

the upper Burgi Member is present. Upper Burgi Member strata are exposed at two

localities: Namorotukunan (Figure 27) and at the western edge of Area 41.

5.5.1 Lithologic Description

As mentioned above, disconformity marking the base of the upper Burgi Member

is exposed on the western slope of a hill at the western edge of Area 41 (Appendix A).

Strata overlying this disconformable surface are assigned to the upper Burgi Member.

No stratigraphic section was measured at this locality, however the section above the

disconformity includes a gastropod packed sandstone (Figure 29) that wraps around the

hill and is overlain by fine-grained muddy sandstones (Figure 30).

At Namorotukanan, the upper Burgi Member (~ 18 m) is assigned to strata

between the disconformity and the top of the hill (Figure 27). The bottom of the upper

Burgi Member is a ledge-forming, well-cemented medium sandstone fining upwards to

fine grained sandstone with sparse gastropods and abundant fish bones. Overlying

sediments are laminated brown mudstones with sparse limonite staining containing a 1.5

m thick laminated diatomaceous siltstone layer 6 m above the disconformity. These

mudstones are capped by terrace gravels at the top of Namorotukanan and mark the end

of Burgi Member strata, or lie disconformably on it.

5.5.2 Interpretation

By ~ 2.0 Ma another lake, the Lorenyang Lake, had formed in the basin which extended northward into southern Ethiopia, but was not present in the southern parts of the Koobi Fora region (Brown and Feibel, 1991). Strata assigned to this interval are, however, present much farther south, northwest of Loiyangalani (Gathogo et al., 2008). The inundation of the lake is marked by lacustrine strata and fossil fish bones in the study area. A layer fining upward from medium- to fine-grained sand contains fish bones and gastropods that formed in a lake margin environment with coarse sediment input from a marginal stream. Laminated mudstones higher in the section in the Namorotukanan area likely reflect continued rising of the lake. A diatomaceous siltstone ~ 6 m above the base of this member indicates local fluctuations in lake level, as diatomites are interpreted as lake margin facies in bays where clastic detrital influx is limited.

In the western part of Area 41, strata are similar to those in Area 40 at Namorotukunan, however they are somewhat coarser grained and lack diatomites. They are therefore interpreted as having been deposited in a lake margin environment with substantial clastic input.

In both areas the top of the Burgi Member is marked by terrace gravels with coarse volcanic and metamorphic clasts that were deposited on an erosional surface, which must postdate the upper Burgi member. It is likely that these coarse grained units were deposited by the streams ancestral to Il Dura (volcanic source) and Il Eriet (rhyolitic and metamorphic source)

Table 1. Electron microprobe analyses of the α-Tulu Bor, β-Tulu Bor, Moiti, Kisemei, Kanyeris, Tukunan and Guo tuffs

Name/sample	M,N	No	SiO_2	TiO_2	ZrO_2	Al_2O_3	Fe_2O_3	MnO	MgO	CaO	Na_2O	K_2O	F	Cl	Sum	less O	H_2O	Total
Principal compositional mode of the β-Tulu Bor Tuff																		
CLK10-048	1,1	14	72.26	0.16	0.04	12.31	1.55	0.05	0.06	0.30	3.24	3.06	0.05	0.10	93.19	0.05	7.20	100.35
CLK10-058	1,1	15	73.54	0.15	0.03	12.45	1.51	0.05	0.05	0.30	2.86	2.46	0.12	0.10	93.65	0.08	7.69	101.26
CLK10-064	1,1	16	72.25	0.14	0.03	12.27	1.53	0.05	0.06	0.31	3.17	2.66	0.12	0.10	92.70	0.07	7.40	100.03
CLK10-073	1,1	15	73.66	0.14	0.05	12.25	1.56	0.05	0.06	0.31	3.54	2.74	0.13	0.10	94.59	0.08	5.54	100.06
CLK10-080	1,1	15	75.52	0.14	0.04	12.43	1.50	0.05	0.06	0.29	3.48	3.08	0.16	0.09	96.85	0.09	4.35	101.12
CLK10-099	1,3	9	73.17	0.15	0.05	12.25	1.63	0.05	0.06	0.30	2.78	4.91	0.13	0.10	95.58	0.08	5.83	101.33
CLK11-149	1,1	14	73.42	0.14	0.04	12.09	1.33	0.07	0.06	0.28	3.93	2.92	0.13	0.10	94.52	0.08	5.03	99.47
CLK11-150	1,1	20	73.54	0.15	0.06	12.29	1.24	0.06	0.06	0.29	3.60	2.63	0.08	0.10	94.10	0.06	5.42	99.46
CLK11-151	1,1	20	73.35	0.14	0.04	12.09	1.37	0.06	0.06	0.28	3.97	2.93	0.14	0.10	94.52	0.08	6.13	100.57
CLK11-153	1,1	20	73.62	0.15	0.05	12.24	1.20	0.05	0.06	0.28	3.77	2.87	0.16	0.09	94.56	0.09	4.65	99.12
CLK11-155	1,1	21	73.21	0.13	0.05	12.09	1.34	0.05	0.06	0.28	3.84	2.67	0.14	0.10	93.98	0.08	6.35	100.24
CLK11-200	1,1	21	73.37	0.14	0.04	12.11	1.33	0.06	0.06	0.28	3.48	2.72	0.15	0.10	93.84	0.09	6.36	100.12
CLK11-201	1,2	18	73.79	0.15	0.03	12.17	1.30	0.06	0.06	0.28	3.16	2.36	0.11	0.10	93.55	0.07	6.59	100.08
CLK11-202	1,2	19	73.72	0.15	0.05	12.20	1.27	0.07	0.06	0.30	3.32	2.47	0.13	0.10	93.83	0.08	6.28	100.04
Minor compositional modes in samples assigned to the β-Tulu Bor Tuff																		
CLK10-099	3,3	3	69.28	0.31	0.19	13.47	3.11	0.12	0.13	0.57	2.06	4.50	0.13	0.08	94.02	0.07	6.67	100.61
CLK10-099	2,3	3	71.33	0.27	0.06	13.20	1.89	0.07	0.16	0.61	3.00	4.78	0.14	0.09	95.62	0.08	5.70	101.24
CLK11-150	1,1	4	65.12	0.38	0.14	15.93	7.29	0.32	0.17	0.81	6.03	5.02	0.24	0.24	101.82	0.23	0.56	102.15
CLK11-201	2,2	3	72.07	0.25	0.07	12.81	1.23	0.04	0.13	0.56	3.18	2.12	0.05	0.09	92.61	0.04	7.45	100.02
CLK11-202	2,2	2	69.87	0.30	0.10	13.27	2.43	0.10	0.12	0.51	2.77	2.28	0.12	0.08	91.96	0.07	7.75	99.64
Principal compositional mode of the α-Tulu Bor Tuff																		
CLK10-001	1,1	12	71.83	0.20	0.04	12.63	1.36	0.03	0.11	0.47	2.93	4.25	0.09	0.09	94.07	0.06	7.74	101.75
CLK10-002	1,1	13	71.32	0.25	0.04	13.14	1.52	0.06	0.14	0.58	2.50	3.80	0.01	0.09	93.45	0.02	8.46	101.89
CLK10-003	1,1	15	71.01	0.23	0.06	13.08	1.50	0.05	0.14	0.57	1.92	4.44	0.10	0.09	93.22	0.06	9.00	102.16
CLK10-004	1,1	16	70.62	0.25	0.06	12.83	1.54	0.04	0.14	0.55	2.15	4.22	0.09	0.08	92.60	0.06	8.96	101.50
CLK10-005	1,1	15	71.01	0.24	0.03	12.99	1.44	0.05	0.13	0.55	2.22	3.81	0.04	0.09	92.64	0.04	9.92	102.52

Table 1. continued.

Name/sample	M,N	No	SiO$_2$	TiO$_2$	ZrO$_2$	Al$_2$O$_3$	Fe$_2$O$_3$	MnO
Principal compositional mode of the α-Tulu Bor Tuff								
CLK10-006	1,1	15	71.11	0.25	0.07	13.09	1.50	0.06
CLK10-009	1,1	15	71.09	0.23	0.07	12.84	1.65	0.05
CLK10-010	1,1	12	71.28	0.24	0.05	13.16	1.57	0.04
CLK10-014	1,1	16	70.95	0.24	0.05	13.13	1.52	0.05
CLK10-019	1,2	12	71.31	0.21	0.03	12.63	1.34	0.05
CLK10-020	1,1	15	72.52	0.21	0.05	12.71	1.37	0.04
CLK10-023	1,2	10	72.64	0.20	0.02	12.73	1.36	0.04
CLK10-024	1,1	14	73.31	0.21	0.04	12.84	1.31	0.04
CLK10-029	1,1	15	70.19	0.21	0.04	12.68	1.38	0.05
CLK10-039	1,1	14	70.71	0.22	0.04	12.65	1.44	0.05
CLK10-041	1,1	8	71.02	0.20	0.04	12.73	1.32	0.04
CLK10-044	1,1	14	71.30	0.20	0.02	12.54	1.36	0.04
CLK10-051	1,1	19	73.10	0.23	0.03	12.86	1.45	0.05
CLK10-054	1,2	11	71.97	0.20	0.04	12.71	1.38	0.04
CLK10-055	1,1	15	70.20	0.24	0.02	12.82	1.47	0.04
CLK10-057	1,2	11	71.94	0.22	0.03	12.61	1.34	0.04
CLK10-098	1,1	15	72.16	0.19	0.06	12.73	1.32	0.05
CLK10-100	1,1	16	71.42	0.22	0.02	12.97	1.40	0.04
CLK10-101	1,1	15	73.51	0.19	0.03	12.78	1.35	0.05
CLK11-120	1,1	13	72.12	0.24	0.05	12.82	1.54	0.05
Minor compositional modes in samples assigned to the α-Tulu Bor Tuff								
CLK10-019	2,2	2	71.76	0.19	0.07	10.56	3.29	0.13
CLK10-023	2,2	4	73.55	0.18	0.08	10.56	3.36	0.11
CLK10-041	2,3	4	72.44	0.15	0.13	10.96	2.38	0.06
CLK10-054	2,2	2	72.80	0.18	0.11	10.38	3.33	0.13
CLK10-057	2,2	4	72.96	0.18	0.13	10.51	3.28	0.11
CLK10-041	3,3	3	71.81	0.20	0.12	10.46	3.30	0.09

MgO	CaO	Na$_2$O	K$_2$O	F	Cl	Sum	less O	H$_2$O	Total
0.14	0.58	2.55	3.78	0.11	0.09	93.35	0.06	8.11	101.40
0.13	0.54	2.81	3.97	0.13	0.09	93.61	0.07	7.91	101.44
0.15	0.59	2.67	4.07	0.13	0.09	94.05	0.07	7.93	101.90
0.14	0.59	2.23	4.29	0.13	0.09	93.43	0.07	8.51	101.86
0.11	0.46	3.17	4.37	0.11	0.09	93.89	0.06	7.46	101.28
0.12	0.48	2.89	3.84	0.07	0.09	94.40	0.05	7.83	102.18
0.11	0.47	3.11	3.58	0.09	0.09	94.47	0.06	7.37	101.79
0.12	0.49	3.01	3.16	0.12	0.09	94.76	0.07	6.08	100.77
0.13	0.51	3.00	2.83	0.06	0.09	91.20	0.05	8.97	100.12
0.13	0.53	2.80	3.25	0.12	0.09	92.06	0.07	8.10	100.10
0.11	0.48	2.94	4.34	0.09	0.09	93.42	0.06	7.85	101.21
0.11	0.45	3.01	4.27	0.11	0.09	93.52	0.07	7.43	100.88
0.11	0.52	3.79	3.89	0.05	0.08	96.15	0.04	4.79	100.90
0.11	0.48	3.08	4.26	0.11	0.09	94.48	0.07	7.07	101.48
0.14	0.56	2.47	3.09	0.09	0.10	91.27	0.06	9.08	100.29
0.11	0.45	3.08	2.62	0.11	0.08	92.67	0.07	6.92	99.53
0.14	0.51	2.52	3.89	0.15	0.08	93.80	0.08	7.06	100.78
0.13	0.52	2.73	4.70	0.12	0.09	94.38	0.07	7.75	102.06
0.12	0.48	2.63	4.87	0.12	0.08	96.24	0.07	5.73	101.90
0.14	0.56	2.64	1.88	0.05	0.09	92.18	0.04	7.70	99.84
0.02	0.19	3.05	4.01	0.20	0.11	93.58	0.11	7.97	101.43
0.02	0.20	2.71	2.88	0.19	0.12	93.95	0.11	7.80	101.64
0.02	0.17	3.40	4.60	0.10	0.11	94.55	0.07	6.27	100.75
0.01	0.21	1.18	2.38	0.21	0.10	91.01	0.11	9.11	100.01
0.00	0.17	2.95	3.03	0.14	0.13	93.59	0.09	5.79	99.30
0.02	0.21	2.57	3.90	0.15	0.12	92.95	0.09	8.64	101.49

Table 1. continued.

Name/sample	M,N	No	SiO_2	TiO_2	ZrO_2	Al_2O_3	Fe_2O_3	MnO	MgO	CaO	Na_2O	K_2O	F	Cl	Sum	less O	H_2O	Total
Principal compositional mode of the Moiti Tuff																		
CLK10-065	1,1	13	72.45	0.17	0.12	10.82	2.60	0.08	0.00	0.20	3.46	3.24	0.09	0.12	93.40	0.07	6.70	100.03
CLK10-115	1,1	15	73.53	0.17	0.12	11.06	2.74	0.08	0.01	0.21	3.39	2.90	0.17	0.12	94.52	0.10	6.44	100.86
CLK-148A	1,2	13	72.99	0.15	0.14	10.49	2.67	0.09	0.01	0.21	3.57	3.34	0.09	0.11	93.86	0.06	6.69	100.48
CLK10-063	1,2	11	74.19	0.19	0.10	11.03	2.62	0.10	0.00	0.21	3.42	3.42	0.04	0.12	95.47	0.05	6.42	101.85
Minor compositional modes in samples assigned to the Moiti Tuff																		
CLK10-063	2,2	3	72.72	0.35	0.12	10.33	4.38	0.18	0.01	0.29	2.94	2.98	0.01	0.09	94.42	0.02	6.94	101.33
CLK11-148A	2,2	4	71.97	0.26	0.11	9.91	4.36	0.12	0.00	0.27	2.67	2.66	0.08	0.07	92.49	0.05	7.64	100.09
Compositions of principal modes of shards and pumice fragments measured within the Kisemei Tuff																		
CLK11-206A	1,2	6	70.13	0.43	0.04	12.46	2.27	0.13	0.22	0.71	2.39	2.03	0.15	0.05	91.00	0.07	7.88	98.81
CLK10-036	1,1	15	71.31	0.35	0.13	11.81	2.42	0.16	0.17	0.17	2.21	3.90	0.20	0.15	92.96	0.12	8.35	101.19
CLK11-128	2,3	2	72.81	0.34	0.15	11.91	2.63	0.13	0.17	0.20	3.98	3.44	0.15	0.16	96.07	0.10	3.91	99.88
CLK11-138A(1)	1,1	12	70.43	0.28	0.09	12.85	2.59	0.12	0.13	0.31	3.58	2.43	0.17	0.11	93.08	0.10	7.07	100.06
CLK11-138A(2)	1,1	11	71.58	0.26	0.07	12.11	3.07	0.14	0.11	0.19	4.16	3.28	0.05	0.13	95.14	0.05	4.97	100.06
CLK11-138A(3)	1,1	12	70.90	0.24	0.10	12.14	2.84	0.14	0.11	0.21	4.74	4.05	0.18	0.12	95.76	0.10	4.51	100.17
CLK11-138B	1,1	9	72.06	0.24	0.13	12.11	2.97	0.12	0.11	0.21	3.87	3.25	0.20	0.13	95.38	0.11	4.87	100.14
CLK11-206C	1,1	13	71.12	0.24	0.11	11.82	3.07	0.13	0.11	0.19	3.31	1.98	0.22	0.12	92.42	0.12	6.77	99.08
CLK11-128	1,3	12	73.97	0.19	0.18	10.56	3.39	0.16	0.06	0.13	3.03	2.78	0.15	0.20	94.80	0.11	4.89	99.57
CLK11-140	1,1	14	71.43	0.32	0.11	10.83	3.82	0.21	0.14	0.18	3.89	3.30	0.12	0.14	94.50	0.08	4.77	99.18
CLK11-206	1,3	14	72.13	0.32	0.12	10.87	3.55	0.19	0.12	0.17	2.58	2.17	0.17	0.15	92.55	0.10	7.28	99.72
CLK11-139	1,3	12	71.86	0.32	0.12	10.55	3.71	0.21	0.12	0.17	2.65	2.39	0.09	0.15	92.32	0.07	6.52	98.77
CLK11-206B	1,1	6	71.77	0.27	0.10	10.42	4.28	0.19	0.12	0.15	2.37	1.18	0.18	0.15	91.16	0.11	7.50	98.55
CLK11-206A	2,2	3	71.57	0.25	0.08	10.37	4.34	0.16	0.10	0.15	2.39	1.44	0.21	0.15	91.22	0.12	7.60	98.71
CLK11-138B	3,4	2	72.03	0.25	0.15	10.62	4.17	0.17	0.13	0.13	3.37	3.19	0.21	0.13	94.54	0.12	4.85	99.27

Table 1. continued.

Name/sample	M,N	No	SiO_2	TiO_2	ZrO_2	Al_2O_3	Fe_2O_3	MnO	MgO	CaO	Na_2O	K_2O	F	Cl	Sum	less O	H_2O	Total
Minor mode within the Kisemei Tuff corresponding to composition of the Tukunan Tuff																		
CLK11-138B	4,4	2	73.76	0.34	0.03	12.29	1.72	0.09	0.14	0.43	3.52	2.62	0.14	0.03	95.12	0.07	4.75	99.80
CLK11-139	3,3	2	72.51	0.40	0.06	12.33	1.53	0.10	0.19	0.52	3.08	2.41	0.15	0.05	93.31	0.07	6.04	99.27
Minor mode within the Kisemei Tuff corresponding to composition of the Kanyeris Tuff																		
CLK11-206	2,3	2	71.47	0.32	0.07	12.75	2.01	0.15	0.17	0.63	3.22	2.58	0.15	0.06	93.57	0.08	6.47	99.97
CLK11-139	2,3	3	70.46	0.47	0.09	12.55	2.04	0.13	0.26	0.77	2.90	2.29	0.09	0.05	92.10	0.05	7.16	99.20
Minor modes of high Al content within the Kisemei Tuff																		
CLK11-206	3,3	2	71.03	0.28	0.11	13.29	2.09	0.12	0.14	0.35	3.73	3.14	0.18	0.11	94.58	0.10	6.43	100.91
CLK11-138B	2,4	3	70.83	0.25	0.09	13.39	2.55	0.12	0.12	0.35	3.69	2.80	0.18	0.11	94.49	0.10	5.73	100.12
CLK11-128	3,3	2	65.89	0.75	0.06	15.43	3.50	0.17	0.57	0.78	5.37	3.91	0.13	0.07	96.62	0.07	3.89	100.45
Principal compositional mode of the Kanyeris Tuff																		
CLK10-056	1,1	14	69.02	0.44	0.06	12.62	2.09	0.13	0.22	0.73	1.57	1.81	0.09	0.05	88.84	0.05	10.16	98.95
CLK10-075	1,1	17	71.15	0.43	0.08	12.63	2.21	0.12	0.24	0.77	2.33	2.06	0.12	0.05	92.19	0.06	8.35	100.48
CLK10-076	1,1	15	69.13	0.46	0.09	12.73	2.23	0.12	0.26	0.82	2.32	2.05	0.11	0.05	90.39	0.06	9.29	99.62
CLK10-077	1,1	15	70.47	0.46	0.09	12.86	2.19	0.13	0.26	0.81	2.34	2.11	0.11	0.05	91.87	0.06	8.84	100.66
CLK10-079	1,1	14	69.06	0.45	0.10	12.43	2.23	0.12	0.27	0.81	1.87	1.77	0.09	0.04	89.24	0.05	10.05	99.24
CLK10-079	1,1	10	69.19	0.49	0.08	12.62	2.54	0.14	0.36	0.88	2.26	1.68	0.02	0.04	90.29	0.02	9.15	99.42
CLK11-161	1,1	12	70.23	0.47	0.09	12.55	1.94	0.13	0.25	**0.71**	2.20	1.69	0.13	0.05	90.43	0.07	9.77	100.13
CLK11-185	1,1	18	70.88	0.44	0.07	12.65	1.94	0.12	0.26	**0.75**	2.34	1.40	0.11	0.05	91.01	0.06	8.35	99.30
CLK11-129	1,2	8	71.50	0.43	0.07	12.65	2.29	0.12	0.24	0.77	2.63	2.18	0.11	0.05	93.04	0.06	6.37	99.35
Minor modes within the Kanyeris Tuff																		
CLK10-075	2,2	2	73.70	0.26	0.13	10.16	4.34	0.20	0.04	0.20	3.62	3.58	0.18	0.15	96.56	0.11	4.85	101.30
CLK11-129	2,2	2	69.90	0.47	0.05	12.79	2.62	0.13	0.33	0.96	2.43	1.92	0.06	0.05	91.72	0.04	7.18	98.86
Principal compositional mode of the Tukunan Tuff																		
CLK10-078	1,1	16	70.88	0.38	0.09	12.30	1.75	0.09	0.16	0.53	2.53	2.32	0.14	0.05	91.23	0.07	8.59	99.75
CLK11-160	1,1	21	71.97	0.36	0.07	12.09	1.53	0.09	0.17	0.49	3.07	2.36	0.16	0.04	92.41	0.08	7.79	100.12

Table 1. continued.

Name/sample	M,N	No	SiO$_2$	TiO$_2$	ZrO$_2$	Al$_2$O$_3$	Fe$_2$O$_3$	MnO	MgO	CaO	Na$_2$O	K$_2$O	F	Cl	Sum	less O	H$_2$O	Total
Principal compositional mode of the Guo Tuff																		
CLK10-070	1,1	14	69.57	0.49	0.09	13.00	2.44	0.13	0.33	0.98	2.15	2.09	0.13	0.05	91.46	0.07	8.68	100.07
CLK10-071A	1,1	20	70.79	0.52	0.11	12.98	2.58	0.14	0.33	0.98	3.34	3.13	0.13	0.04	95.07	0.07	5.89	100.90
CLK10-071B	1,1	19	70.64	0.50	0.11	12.94	2.55	0.14	0.33	0.99	3.41	3.21	0.13	0.04	94.99	0.06	5.89	100.82
CLK10-071C	1,1	19	70.93	0.49	0.11	12.99	2.57	0.14	0.33	0.99	3.61	3.59	0.14	0.04	95.92	0.07	5.29	101.14
CLK10-081	1,1	15	69.48	0.51	0.09	12.92	2.43	0.14	0.32	0.97	1.85	1.79	0.14	0.04	90.68	0.07	9.58	100.19
CLK11-131	1,1	19	69.96	0.50	0.09	12.76	2.56	0.14	0.33	0.96	2.51	1.91	0.17	0.04	91.92	0.08	7.33	99.17
CLK11-136	1,1	17	70.35	0.52	0.11	12.85	2.55	0.14	0.33	0.94	2.70	2.27	0.17	0.04	92.96	0.08	6.47	99.35
CLK11-141	1,1	19	69.62	0.51	0.10	12.63	2.13	0.14	0.33	0.92	2.92	2.49	0.12	0.04	91.95	0.06	6.79	98.68
CLK11-161	1,1	6	69.47	0.50	0.09	12.67	2.17	0.12	0.32	0.91	1.91	1.78	0.09	0.05	90.08	0.05	9.61	99.65
CLK11-187	1,1	14	70.09	0.48	0.10	12.87	2.43	0.13	0.32	0.87	1.62	1.33	0.08	0.05	90.39	0.05	6.90	97.24
CLK11-187	1,1	6	71.42	0.46	0.08	13.04	2.30	0.13	0.24	0.79	2.15	1.74	0.13	0.05	92.51	0.06	6.24	98.69

Table 2. Electron microprobe analyses of the Wargolo Tuff

Name/sample	M,N	No	SiO_2	TiO_2	ZrO_2	Al_2O_3	Fe_2O_3	MnO	MgO	CaO	Na_2O	K_2O	F	Cl	Sum	less O	H_2O	Total
Principal compositional mode of the Wargolo Tuff																		
CLK11-152	1,2	15	74.32	0.17	0.14	10.75	2.32	0.09	0.01	0.19	3.96	3.64	0.10	0.11	95.80	0.07	4.90	100.64
CLK11-159	1,3	7	73.79	0.19	0.13	10.57	2.33	0.08	0.01	0.19	3.62	3.03	0.16	0.12	94.21	0.09	6.35	100.46
CLK11-177	1,2	14	74.50	0.18	0.13	10.80	2.27	0.08	0.01	0.20	3.78	3.48	0.09	0.11	95.64	0.07	4.70	100.27
CLK11-178	1,1	19	74.25	0.16	0.13	10.75	2.28	0.09	0.01	0.19	3.89	3.77	0.12	0.12	95.75	0.08	4.19	99.86
CLK11-193	1,1	19	74.05	0.18	0.15	10.76	2.16	0.10	0.01	0.19	3.98	3.98	0.12	0.12	95.81	0.08	3.28	99.01
CLK11-194	1,2	19	74.20	0.19	0.17	10.85	2.11	0.09	0.00	0.19	3.94	3.91	0.15	0.12	95.91	0.09	4.69	100.50
CLK11-196	1,1	13	73.69	0.16	0.14	10.65	2.65	0.08	0.01	0.21	3.60	3.76	0.04	0.12	95.12	0.05	5.32	100.38
K81-485	1,1	16	71.93	0.11		10.52	2.31	0.07	0.02	0.18	3.38	3.89			92.14			
K81-485	1,1	22	75.10	0.14	0.00	10.92	2.35	0.07	0.02	0.18	2.62	3.99	0.36	0.11	95.85	0.18	7.27	102.94
K81-558	1,1	16	73.85	0.14		10.53	2.55	0.07	0.02	0.19	2.82	3.60			93.77			
Minor compositional modes in samples assigned to the Wargolo Tuff																		
CLK11-152	2,2	3	73.11	0.35	0.13	10.27	4.04	0.17	0.02	0.28	4.06	3.60	0.09	0.09	96.20	0.06	4.33	100.48
CLK11-159	3,3	5	69.60	0.48	0.14	12.67	2.09	0.13	0.33	0.89	2.16	1.86	0.12	0.04	90.52	0.06	9.15	99.60
CLK11-159	2,3	6	70.55	0.42	0.07	12.57	1.85	0.14	0.25	0.72	2.56	1.64	0.13	0.05	90.95	0.06	8.71	99.59
CLK11-177	2,2	5	73.48	0.32	0.14	10.20	3.77	0.15	0.01	0.29	3.60	3.57	0.09	0.09	95.70	0.06	4.42	100.07
CLK11-194	2,2	2	72.78	0.30	0.19	10.07	3.43	0.19	0.01	0.25	2.35	2.59	0.10	0.09	92.35	0.06	7.24	99.53

Marker Bed	N	R	Age (Ma)	Member
KBS Tuff	■		1.87	KBS
		■		U. Burgi
Disconformity			0.77	
Lokalalei Tuff		■		L. Burgi
Burgi Tuff	■		2.64	
Aberegaiye Tuff	■		2.7	Tulu Bor
Disconformity			0.73	
β-Tulu Bor	■			Tulu Bor
α-Tulu Bor	■		3.43	
Lokochot	■		3.6	Lokochot
Wargolo		■	3.8	Moiti
Disconformity			0.46	
Moiti Tuff		■	3.97	Moiti
Naibar Tuff		■	4.02	
Kisemei Tuff		■	4.06 ± 0.03	Lonyumun
Kanyeris Tuff		■	4.12 ± 0.06	
Disconformity			0.11	
Tukunan Tuff	■		4.29–4.18	
Guo Tuff	■		4.29–4.18	
Pseudobovaria Bed		■	4.29–4.49	Lonyumun
U. Diatomite		■	4.29–4.49	
L. Diatomite		■	4.29–4.49	
Unconformity				
Asille Group Volcanics			Miocene	

Figure 3. General stratigraphic column from Miocene basalts to the top of the KBS Tuff. Probable durations of hiatuses are given for disconformities in the column labeled "Age."
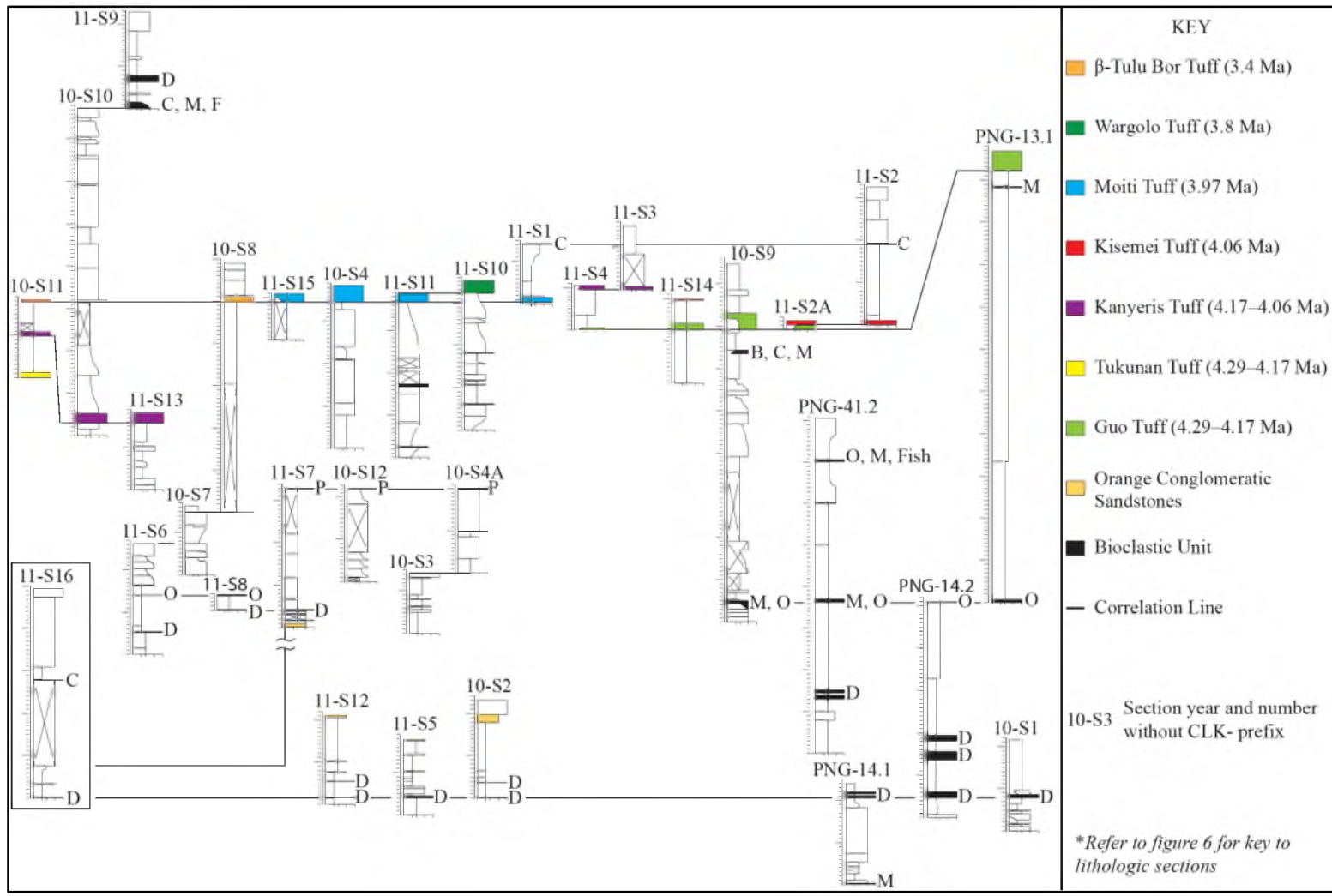
Figure 4. Correlated stratigraphic sections of the Koobi Fora Formation in Areas 15, 40 and 41, including sections in Areas 41, and 14 by Gathogo (2003).
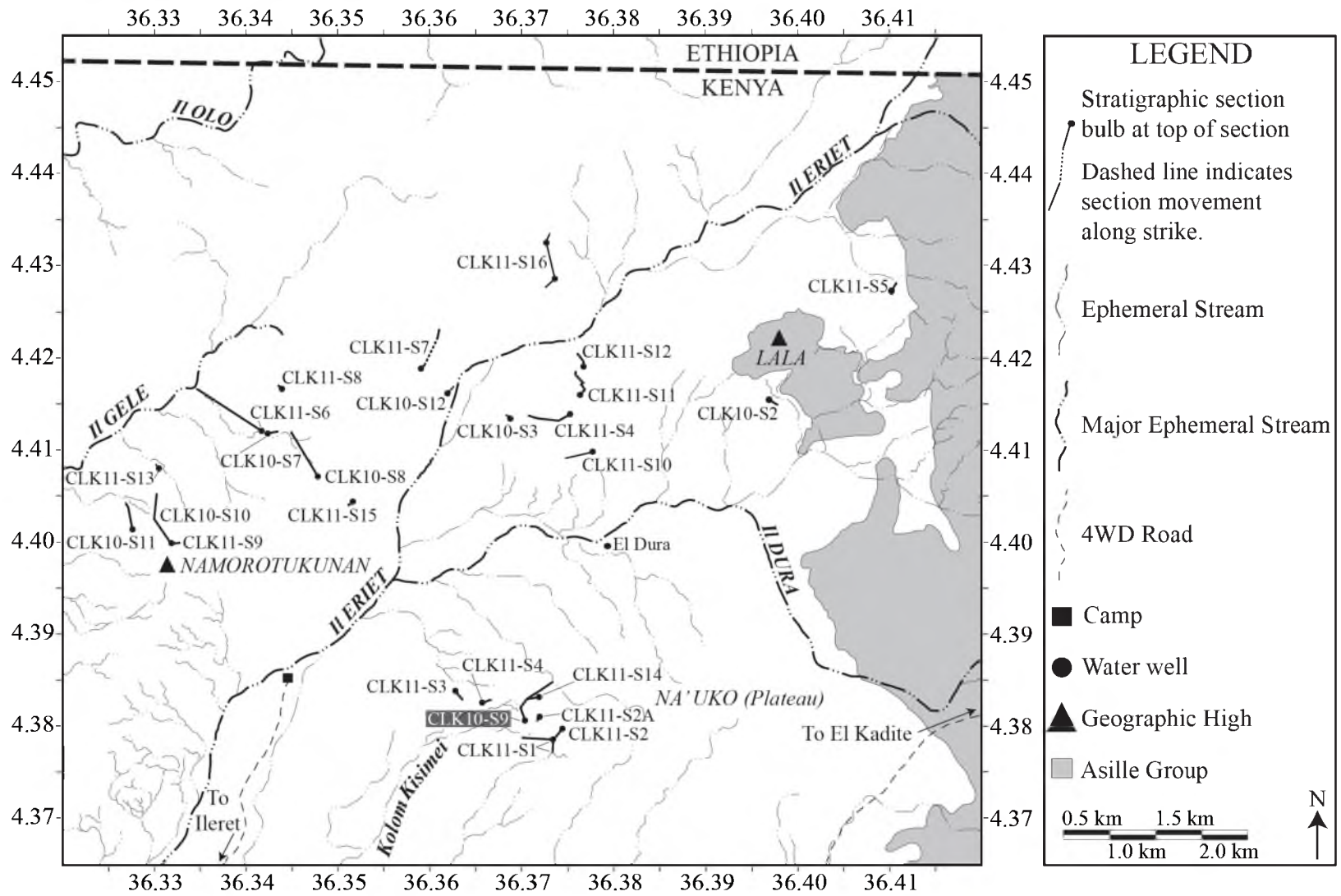
Figure 5. Locations of stratigraphic columns of the Koobi Fora Formation in Areas 40 and 41.

Paleontologic Symbols

D	Diatomites
O	Ostracodite
F	Fish Bone
W	Petrified Wood
B	Bellamya sp.
Pl	Pleiodon ovata sp.
C	Cleopatra sp.
M	Melanoides sp.
P	Pseudobovaria sp.

β-Tulu Bor (*β-TB*)

Wargolo Tuff (*WRG*)

Moiti Tuff (*MOI*)

Kisemei Tuff (*KIS*)

Kanyeris Tuff (*KAN*)

Tukunan Tuff (*TUK*)

Guo Tuff (*GUO*)

Orange Conglomeratic Sandstone (*OCS*)

Lithologic Symbols

Fe	Iron Oxides and Hydroxides
SPC	Soil Pebble Conglomerate
Ca	Carbonate Concretions
MnO2	Maganese Oxides
	Fossil Wood
	Root Casts
	Gypsum
	Halite

Internal Structures

Herringbone Ripples

Desiccation Cracks

Fluvial Ripples

Claystone

Siltstone

Sandstone

Conglomerate

Tuffaceous sandstone

Tuff

Bioclastic unit

Basalt pebble conglomerate

Sandy claystone and mudstone

Cross-bedded sandstone

Cross-bedded clayey sandstone

Interbedded sandstone and claystone

Thinly bedded clayey sandstone

Laminated claystone and siltstone

Sandstone with interbeds of siltstone

Laminated sandstone and siltstone

Figure 6. Key to lithologic symbols used in the stratigraphic sections of the Koobi Fora Formation in Areas 40 and 41. After Brown and Feibel (1986).

Figure 7. The contact between strata at the bottom of the Lonyumun Member and Miocene rhyolites. Located north of Lala on the east side of Il Eriet.

Figure 8. View to the north of the basin margin in Area 41 half way up Lala (4.4239 N, 36.3981 E)

Figure 9. Blocks of conglomeratic sandstone at the top of the lower interval of the Lonyumun Member. View is to the north-northwest (4.4479 N, 36.4159 E).

Figure 10. Stratigraphic sections of the lower interval of the Lonyumun Member in Areas 41 and 40. Section CLK10-S7 illustrates the correlation between the lower and middle intervals.
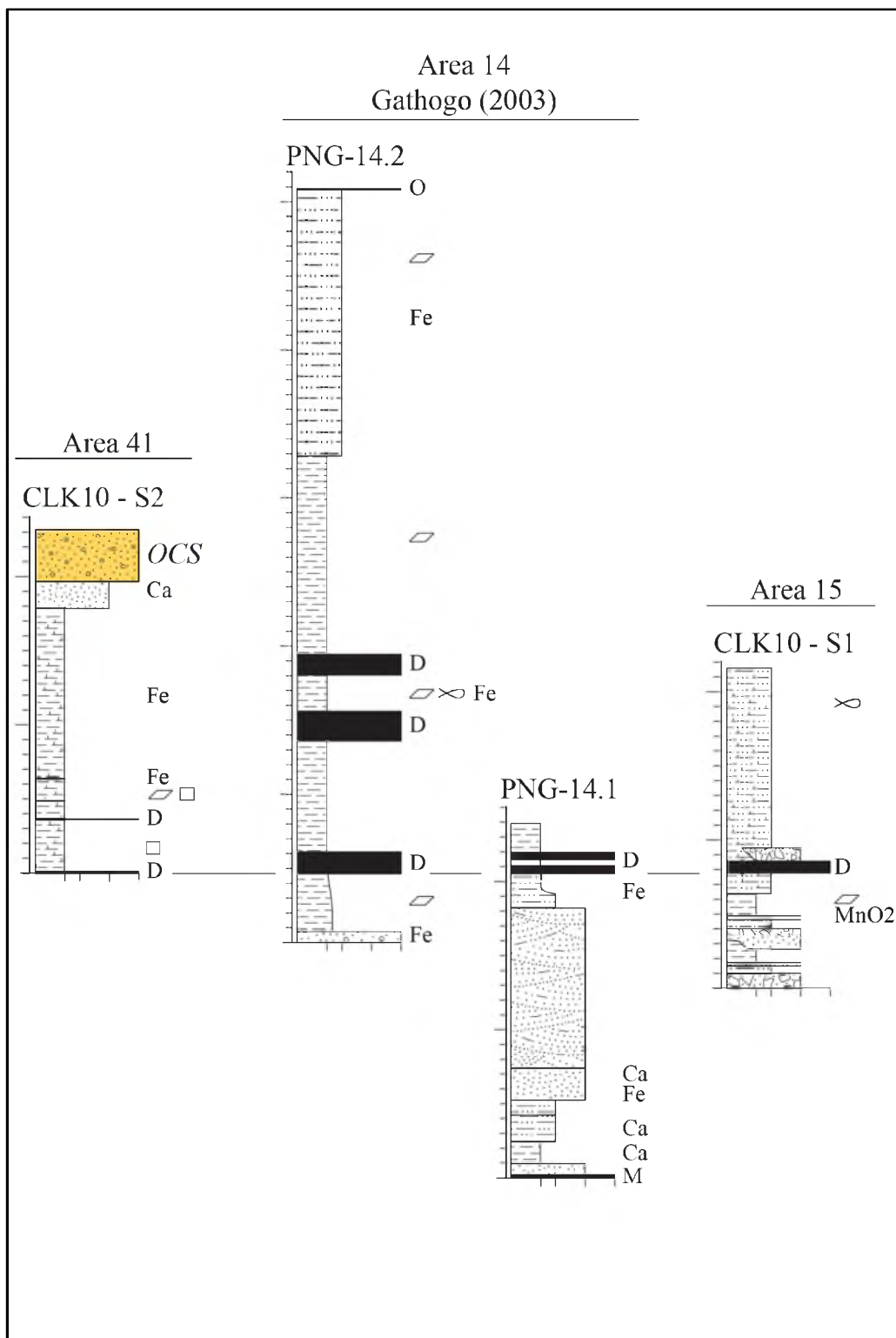
Figure 11. Stratigraphic sections of the lower interval of the Lonyumun Member in Area 41 with correlation to sections in Areas 14 and 15. Area 14 sections are after Gathogo (2003).

Figure 12. Diatomites disconformably lying on Asille Group volcanic rocks and dipping away from the basin margin in Area 15 (4.2427 N, 36.3862 E).

Figure 13. Internal structures within the slumped interval displaying high dip angles (left) sandwiched between non-dipping strata (right). Location: 4.4396 N, 36.3764 E
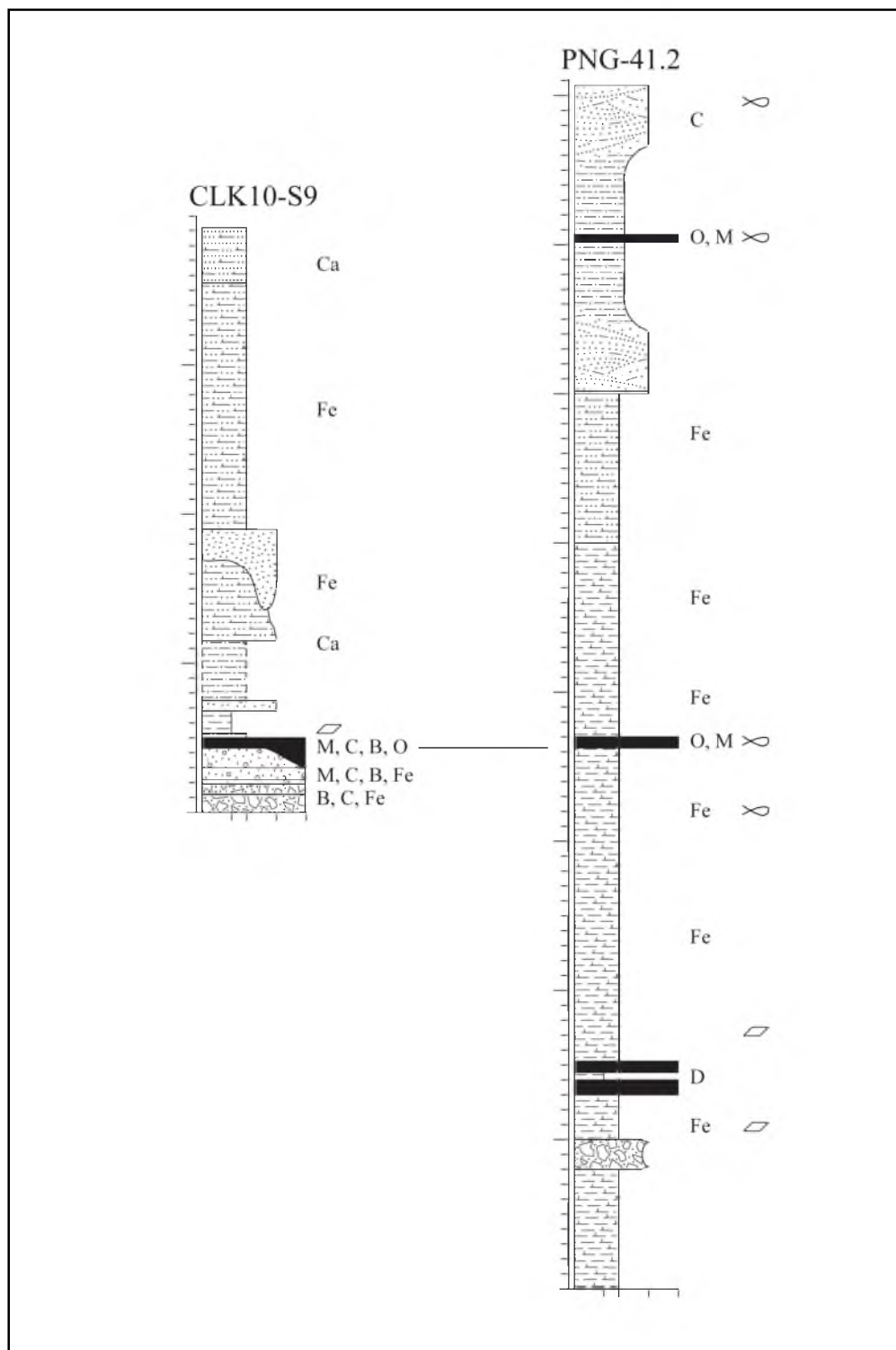
Figure 14. Lower and middle intervals of the Lonyumun Member in section CLK10-S9 correlated to section PNG-41.2 (Gathogo, 2003) in southern Area 41 near Il Biliet

Figure 15. Conglomerates packed with gastropods at the bottom of CLK10-S9. Exposure is on the southern cut-bank of a small tributary of Il Dura in the Kisemei drainage area at 4.3848 N, 36.3734 E.

Figure 16. Thin-bedded claystones and siltstones of the middle interval of the Lonyumun Member (4.4232 N, 36.3610 E).

Figure 17. Ribbon sandstones cropping out at the bottom of section CLK11-S7 in Area 40. Ribbons are part of the orange sandstone conglomerate at the top of the lower interval of the Lonyumun Member (4.4234 N, 36.3614 E).
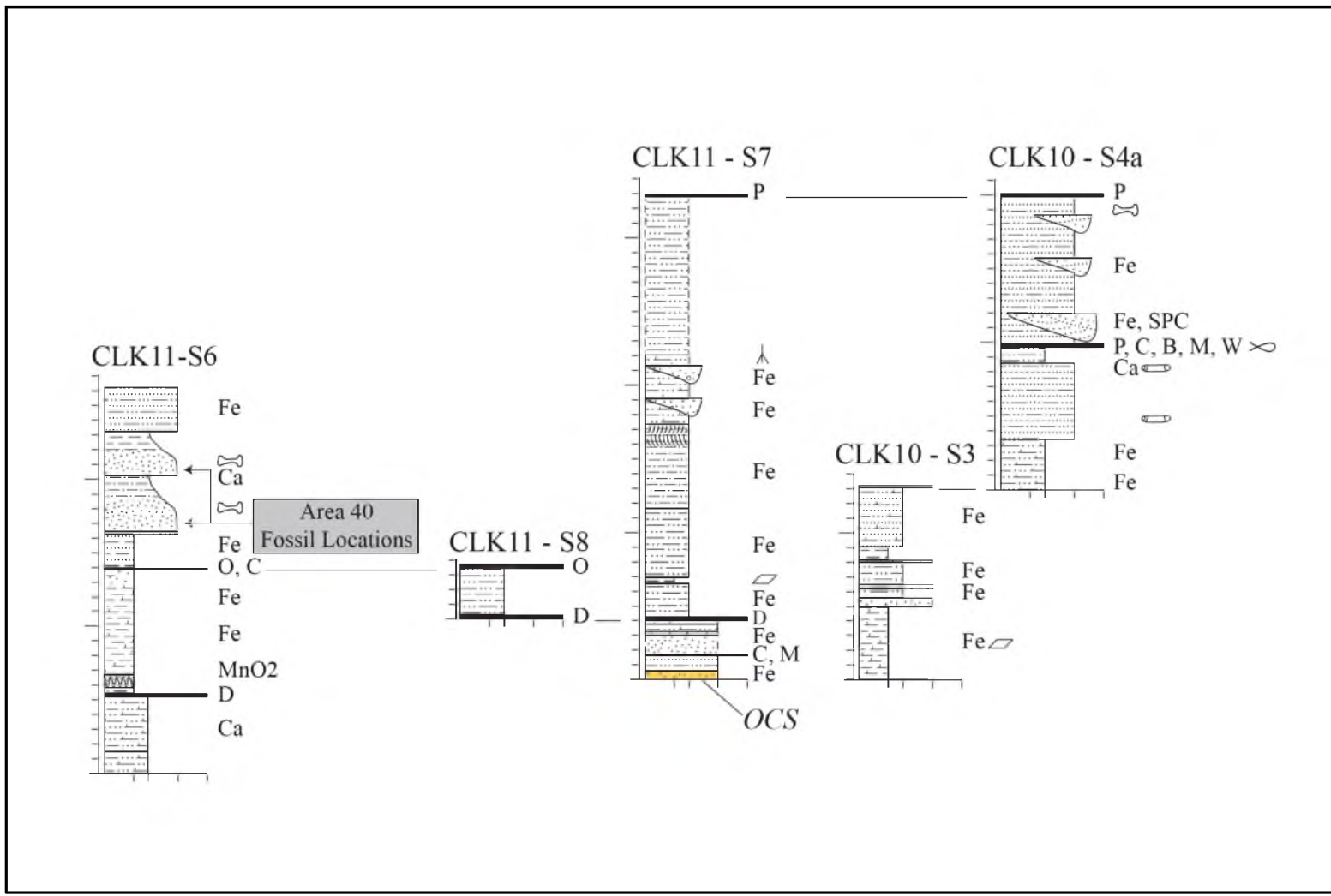
Figure 18. Stratigraphic sections of the middle interval of the Lonyumun Member in Areas 40 and 41.

Figure 19. *Pseudobovaria* sp. packed sandstone at the top of the middle interval of the Lonyumun Member. This marker bed is continuous between Areas 40 and 41 (4.4097 N, 36.3686 E).

Figure 20. Channelized calcite cemented sandstones typical of the middle interval of the Lonyumun Member in Area 41 (4.3989 N, 36.3619 E).
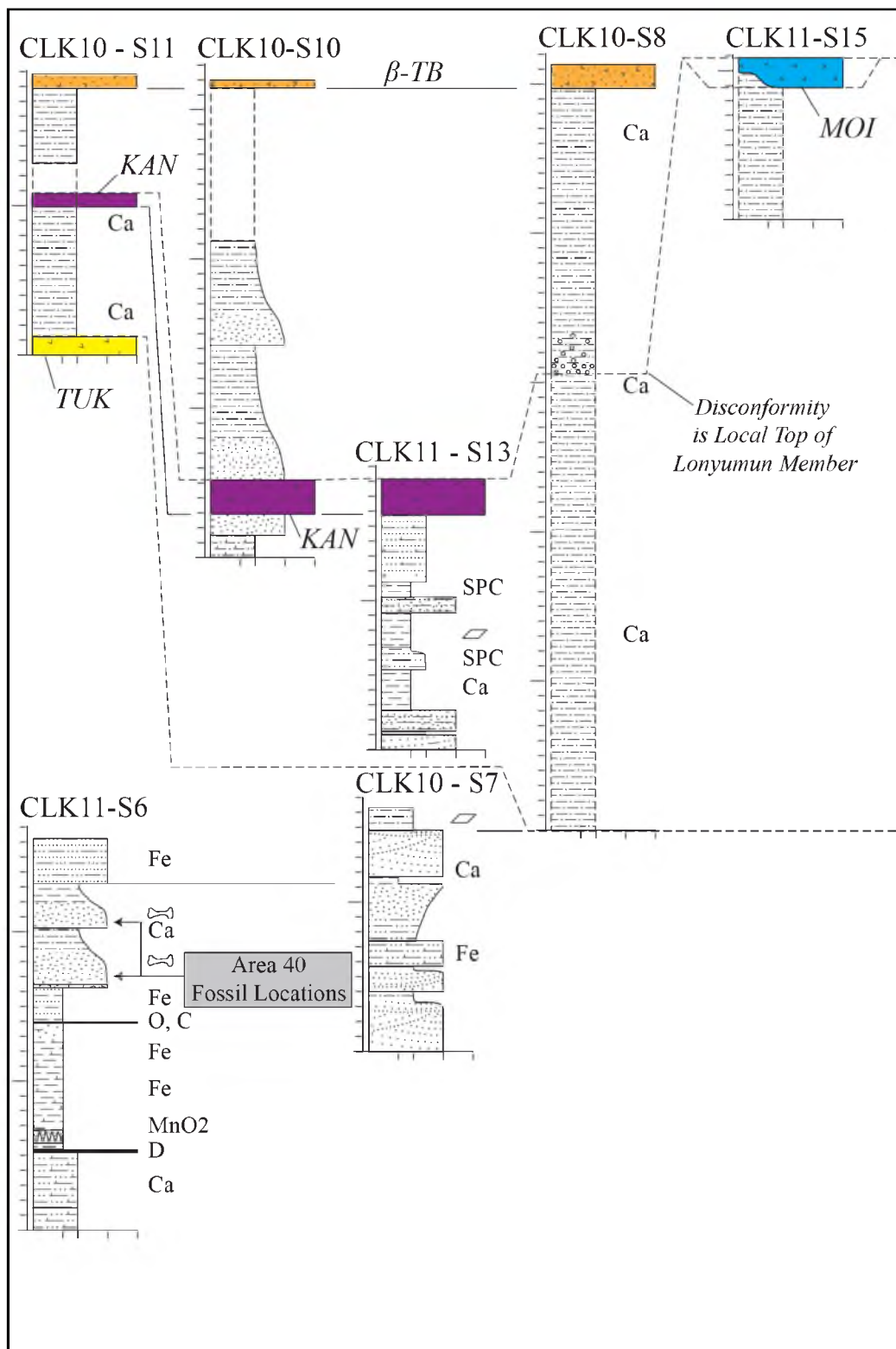
Figure 21. Stratigraphic sections of the upper interval of the Lonyumun Member, and undifferentiated Lokochot/Tulu Bor Members in the Namorotukunan area.
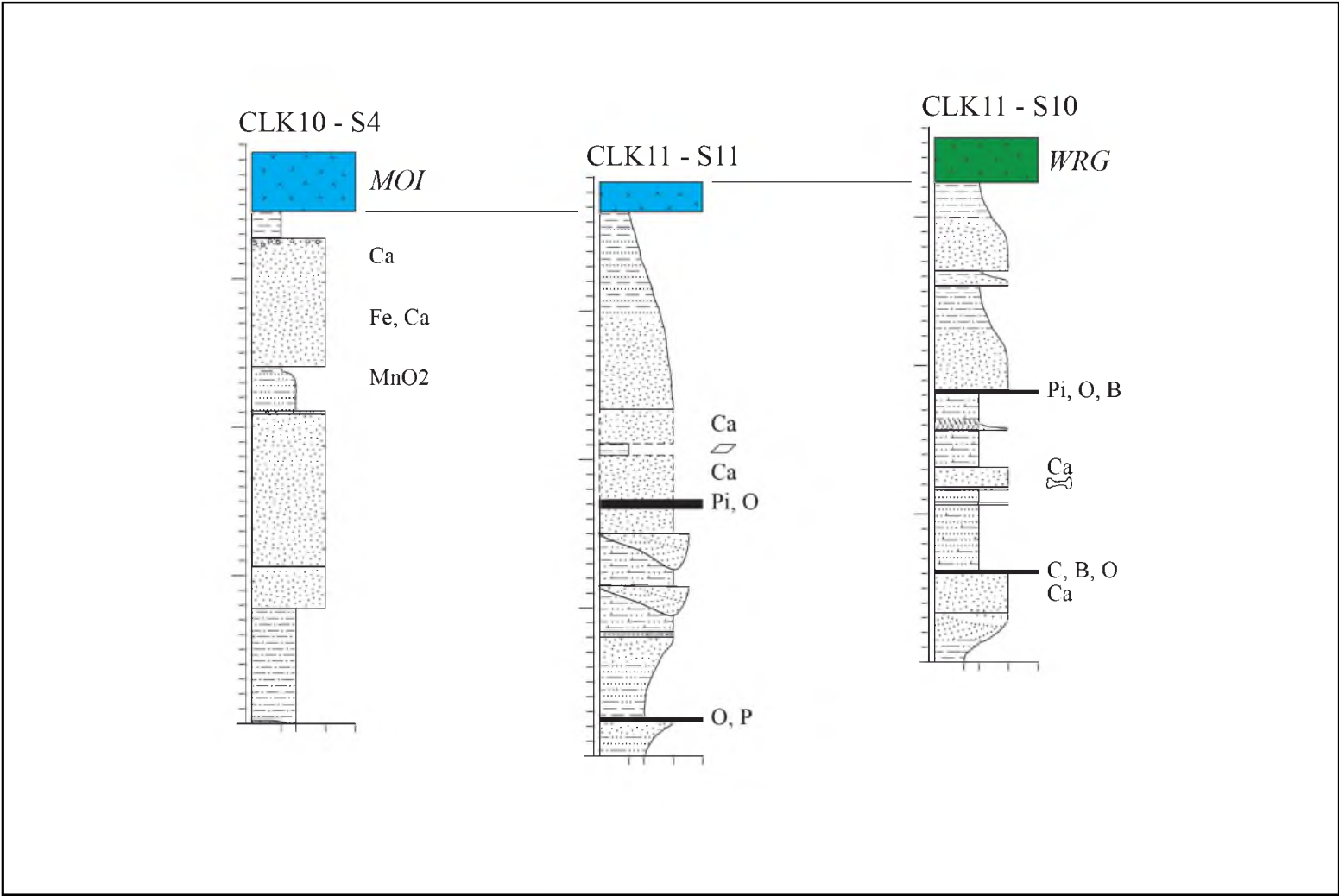
Figure 22. Stratigraphic sections of the upper interval of the Lonyumun Member, north of the confluence of Il Eriet with Il Dura.
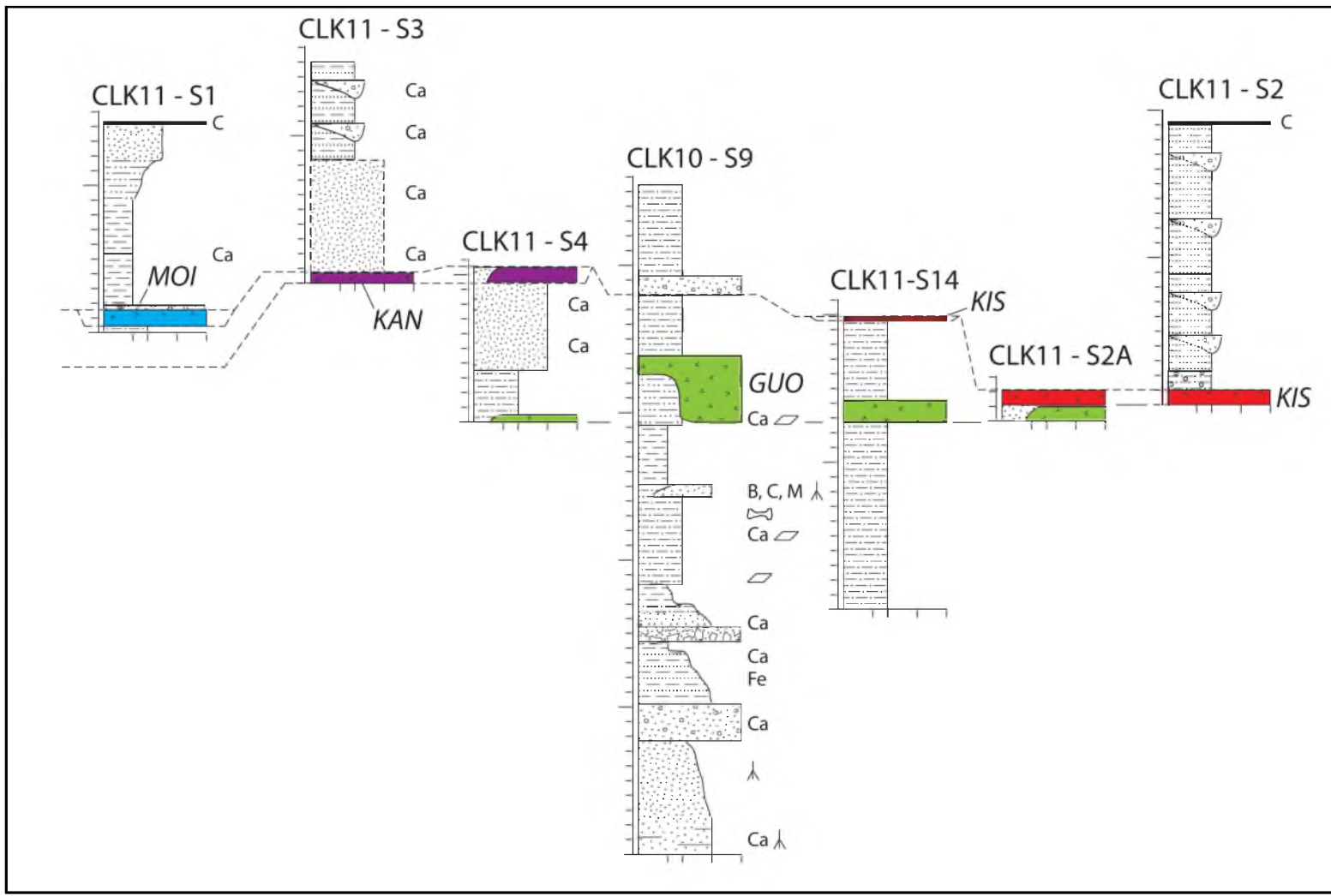
Figure 23. Stratigraphic sections of the upper interval of the Lonyumun Member in the Kisemei drainage.

Figure 24. Well-preserved crocodilian bone in muddy sandstones below the Guo Tuff (4.3830 N, 36.3706 E).

Figure 25. Cross-sectional view of soft-sediment deformation in a block of orange conglomeratic sandstone (4.42760 N, 36.37252 E).

Figure 26. Pumice gravel bar in the Moiti Tuff, Area 40 (4.40763 N, 36.35305 E).
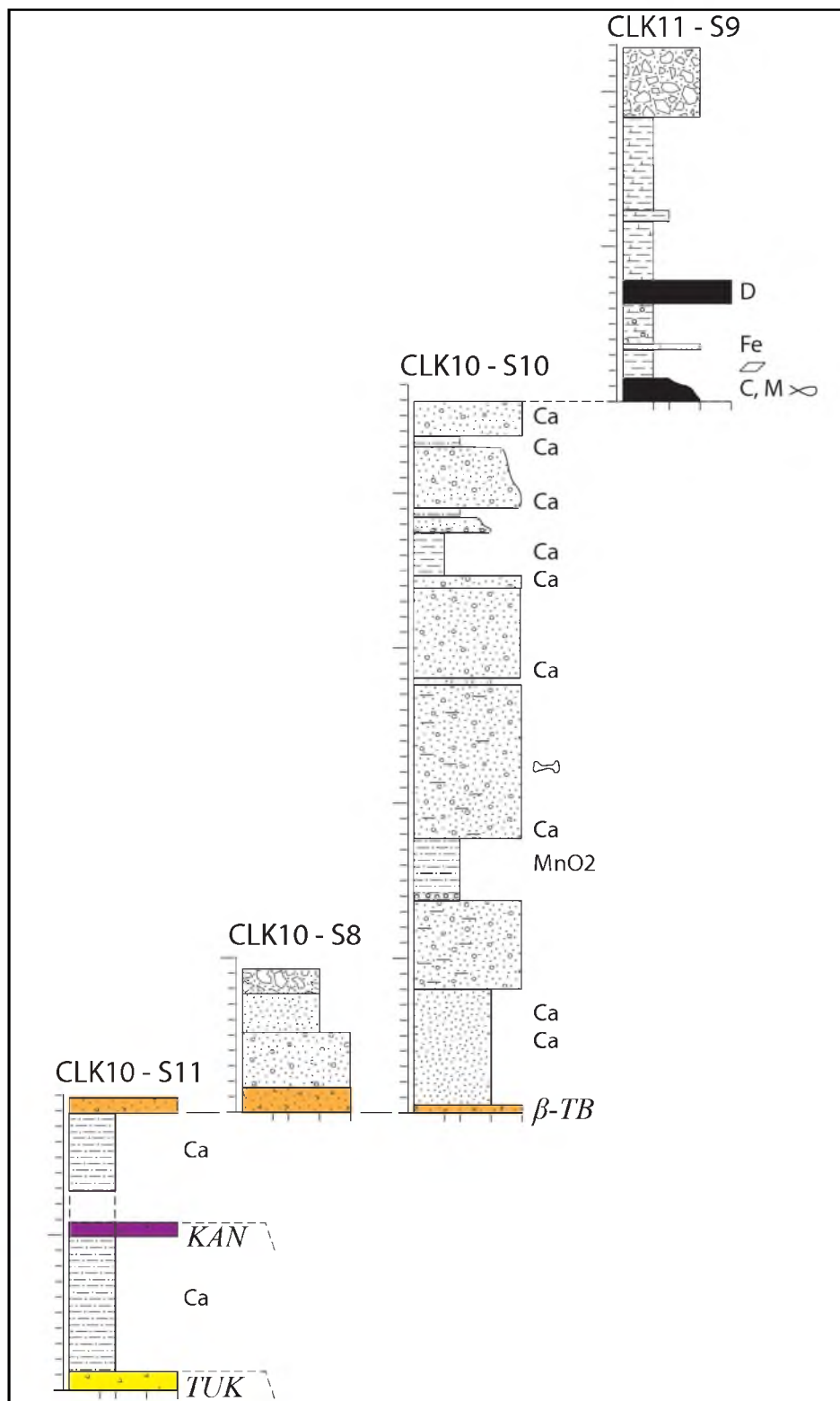
Figure 27. Stratigraphic sections of the Tulu Bor and upper Burgi members in the Namorotukunan area.

Figure 28. Possible extension of the Tulu Bor Member into Area 41, seen here cropping out in a cliff on the eastern bank of the Il Eriet in Area 41 (4.3911 N, 36.3522 E).

Figure 29. Gastropod packed sandstone near the disconformity between the Tulu Bor and upper Burgi members (4.3886 N, 36.3518 E)

Figure 30. Disconformity between the Tulu Bor and upper Burgi members at the western edge of Area 41. The disconformity is at the base of the laminated claystones (4.3824 N, 36.3479 E).

CHAPTER 6

AREAS 129, 130, 135, AND 139

At the beginning of the 2010 field season, the geology of Areas 129, 130, 135, and 139 (Figure 1) was investigated. This area needed geological interpretation because it is the type area of the Tulu Bor Tuff, and because underlying strata had not been assigned to members of the Koobi Fora Formation as defined by Brown and Feibel (1986). A number of observations and collections were made in these areas, some of which are important to interpretation of the stratigraphy in Areas 40 and 41, and others are significant to linkage with areas farther south. Amongst these are: 1) identification of the Aberegaiye Tuff, first discussed by Buchanan (2010) in Area 117; 2) recognition that initial deposition of the Tulu Bor Tuff lies lower in the section than the prominent tuff that is the name bearer; and 3) the clear absence of the Moiti and Lokochot Tuffs from these areas. Tuffs in Area 129 and 135 were collected and measured in a section that includes the KBS Tuff and the Brown Tuff, overlain by a suite of tuffs belonging to the Koobi Fora Tuff Complex in the Okote Member (Brown et al., 2006). Correlated columnar sections in Areas 129, 130 and 135 are shown in Figure 31 and their locations are shown in Figure 32. Lithologic symbols are the same used in the previous chapter (Figure 6).

6.1 Lonyumun Member

The Lonyumun Member in Area 129 consists of about ~ 45 m of section and is in contact with Asille Group volcanics on the southern margin of the Suregei Highlands (Figure 33). Strata in this member include lacustrine claystones, fluvial channel sandstones and gastropod packed sandy mudstones similar to sections CLK11-S6, S7 and S8 (Figure 18) in the middle interval of the Lonyumun Member in Areas 40 and 41. The Tulu Bor Tuff overlies the Lonyumun Member (Figure 34), but neither the Moiti Tuff, the Lokochot Tuff nor other minor tuffs associated with these have been identified in the region. Therefore it appears that a minimum of 600 ka is missing from the geological record in Area 129 between the top of the Lonyumun Member and the base of the Tulu Bor Member.

6.2 Tulu Bor Member

By definition, the Tulu Bor Member has its base at the base of the Tulu Bor Tuff (Brown and Feibel, 1986). The Tulu Bor Tuff forms a prominent cuesta in Area 129, dipping towards the southwest at less than 0.5°. It is noteworthy that the first appearance of the Tulu Bor Tuff in the section is not at the base of the prominent cliff formed by the thick part of the tuff, but instead at a tuffaceous sandstone containing shards of the α-Tulu Bor Tuff (sample CLK10-001; Table 1) that lies ~5 m below the base of the cliff-forming unit.

The Tulu Bor Tuff represents ≤10 m of section. It, and a very thin section with the Aberegaiye Tuff and an unnamed tuff, are the only representation of the Tulu Bor Member in Area 129. At the eastern margin of Area 129 the Tulu Bor pinches out

(Figure 35), into a volcaniclastic conglomerate that represents deposition of alluvium along the basin margin during the time of deposition of the Tulu Bor Tuff.

In the eastern part of Area 129, at approximately 4.21° N, 36.43° E, the Tulu Bor Tuff is faulted, yet this fault does not appear to affect overlying beds of the upper Burgi Member. It is reasonable to assume that deposits of the Tulu Bor Member were also affected by this fault, thus the faulting took place between 2.7 Ma and 2.0 Ma, and is likely related to tectonic movements that result in the disconformity at the base of the upper Burgi Member.

An anticline exposed in Area 139 may be related to the fault just described because the anticline also involves the Tulu Bor Tuff and underlying strata. This anticline is about 500 m across, with an axis oriented N37°E that plunges gently to the southwest. It is bounded on the west by a fault that may be part of a broad system of faults that strike northeast in Area 117 to the south that were mapped by Buchanan (2010).

In Area 130, a tuff overlies the Tulu Bor Tuff as a channel fill. Volcanic glass shards from this tuff are of a single composition that is indistinguishable from the composition of glass from the Aberegaiye Tuff in Area 116 (Buchanan, 2010). On this basis the two are correlated. In Area 130, this tuff locally contains large pumices the glass of which also corresponds compositionally to that of the Aberegaiye Tuff (CLK10-060; Table 3), and these pumices contain alkali feldspar phenocrysts. Buchanan (2010) tentatively placed this tuff below the Lokochot Tuff, and assigned it to the Moiti Member. Alkali feldspars from sample CLK10-060 were dated by the $^{40}Ar/^{39}Ar$ method at the University of Wisconsin–Madison, yielding an age of 2.70 Ma (Appendix C), which

places it instead in the Tulu Bor Member. A second tuff is exposed east of the Aberegaiye Tuff (CLK10-059; Table 4), and it too is known from the southern part of Area 116 (CLK11-122; Table 4), where it lies in the Tulu Bor Member below the Ninikaa Tuff (3.08 Ma). It therefore has an age of ~3.15 Ma, and provides evidence for deposition in Area 130 at this time. Prior to identification and dating of the Aberegaiye Tuff in Area 130, and correlation of the unnamed tuff to Area 116 there was little evidence for deposition during Tulu Bor Member time in Area 130, so these findings are of considerable importance to understanding regional stratigraphy.

6.3 Burgi Member

Above the anticline in Area 139, there is a tuff (CLK10-053) that lies disconformably above the Tulu Bor Tuff. A thorough search of over 2,900 average analyses of glasses from tuffs in the Omo-Turkana Basin, reveals only one possible correlate for this tuff. The possible correlate is a tuff in submember D-5 of the Shungura Formation that has an estimated age of 2.44 Ma. This tuff lies above Tuff D (2.52 Ma, a correlate to the Lokalalei Tuff in the Koobi Fora Formation) in the Shungura Formation, and is the highest unit hitherto known in the lower Burgi Member in the Koobi Fora Formation. If the correlation is correct, then this is the first indication of strata assignable to the lower Burgi Member north of Area 116, and also suggests that deposition continued (at least locally) in the Koobi Fora region between 2.5 and 2.0 Ma that was later removed by erosion. As this tuff lies disconformably on the Tulu Bor Tuff (and presumably on the Aberegaiye Tuff), it appears that there is a hiatus of 260,000 yr missing between the two.

A section was measured from the top of the Tulu Bor Tuff to the top of the outcrops in Area 135 (CLK-135.1). The lower 43 m and upper 24 m of strata are assigned to the upper Burgi and KBS members respectively. The base of the upper Burgi Member rests on the Tulu Bor Tuff in this area, and the KBS Tuff lies about 43 m above the base of the section, establishing the thickness of this unit. The lower 16 m of CLK-135.1 is muddy sandstone with lenses of medium sandstone that grade upward to sandstones packed with molluscs. This interval also includes a volcaniclastic conglomerate (~ 3 cm), probably derived in a way similar to that of the conglomerate described above on the eastern margin of Area 129. Muddy sandstones are overlain by ~ 27 m of very poorly exposed sandy section with lenses of volcaniclastic conglomerates. The KBS Tuff overlies this sandy section, its base marking the top of the upper Burgi member.

6.4 The KBS Member

By definition the KBS Member has its base at the base of the KBS Tuff (Brown and Feibel, 1986). In Area 135, the KBS Member is very thin, making up only ~12 m of section. It includes the KBS Tuff, and the Brown Tuff. The KBS Tuff (~ 3 m, 1.87 Ma) is directly overlain by two 1 meter intervals of the Brown Tuff, then ~ 6 m of volcanic clast absent conglomeratic sandstones with grains of quartz and feldspar. Laterally, stromatolites that form around basalt cobbles litter the surface in the northern part of Area 135 (Figure 36).

6.5 The Okote Member

The top 11 m of section in CLK-135.1 is all that is exposed of the Okote Member. The section includes a suite of tuffs which have compositions similar to those in the Koobi Fora and Okote Tuff Complexes. The top of is made up of a pumice rich tuffaceous sandstone (CLK10-109, -110), a tuffaceous sandstone (CLK10-112) and a vitric tuff (CLK10-111) with up to five different compositional modes. The polymodality of these tuffs may result from reworking of tuffs from elsewhere in this part of the basin. The Chari Tuff was not identified, so the thickness of 11 m for the Okote Member in this section is a minimum.

Table 3. Analyses of the Aberegaiye Tuff in Area 116, its correlate in Areas 139, an unnamed tuff in Area 139, and its possible correlate in the Shungura Formation.

Name/sample	M,N	No	SiO_2	TiO_2	ZrO_2	Al_2O_3	Fe_2O_3	MnO	MgO	CaO	Na_2O	K_2O	F	Cl	Sum	less O	H_2O	Total
Aberegaiye Tuff with comparative analyses (MB08-45, MB08-47) from Buchanan (2010)																		
CLK10-032	1,1	16	76.5	0.15	0.06	12.0	2.15	0.08	0.01	0.30	3.69	4.79	0.10	0.12	100.0	0.07	2.04	102.0
CLK10-049	1,1	18	74.2	0.14	0.07	11.6	2.29	0.08	0.01	0.32	3.53	4.08	0.15	0.13	96.6	0.09	4.53	101.1
CLK10-049A	1,1	11	73.3	0.15	0.09	11.5	2.34	0.08	0.01	0.30	3.87	3.82	0.13	0.13	95.7	0.08	5.67	101.3
CLK10-049B	1,1	14	73.6	0.17	0.06	11.5	2.29	0.08	0.00	0.30	4.08	4.51	0.10	0.13	96.8	0.07	4.24	101.0
CLK10-060	1,1	15	73.3	0.13	0.06	11.7	2.23	0.08	0.01	0.29	3.46	4.25	0.14	0.13	95.8	0.09	4.70	100.4
CLK10-060C	1,1	15	73.6	0.14	0.07	11.6	2.17	0.07	0.01	0.27	4.01	4.26	0.09	0.13	96.4	0.07	4.60	100.9
MB08-45	1,1	21	74.9	0.13	0.10	11.9	2.16	0.07	0.01	0.28	4.10	2.62	0.21	0.14	96.6	0.14	4.33	100.8
MB08-77	1,1	17	73.6	0.13	0.09	11.7	1.96	0.07	0.01	0.26	4.09	2.24	0.22	0.14	94.6	0.14	6.13	100.6
Unnamed tuff in Area 139 (CLK10-053, K11-745), and a possible correlate in submember D-5 of the Shungura Formation (ETH08-250)																		
CLK10-053	1,1	15	71.1	0.28	0.18	9.93	4.51	0.19	0.07	0.19	1.13	1.28	0.11	0.18	89.2	0.09	9.33	98.4
K11-745	1,1	13	72.4	0.26	0.20	9.83	4.66	0.20	0.08	0.17	1.44	1.45	0.12	0.18	91.0	0.09	8.66	99.5
ETH08-250	1,1	19	73.0	0.28	0.21	9.83	4.73	0.20	0.07	0.13	1.69	2.21	0.04	0.14	92.7	0.10	7.36	99.9

Table 4. Analyses of the Unnamed Tuff in Area 130 and its correlate in Area 116

Name/sample	M,N	No	SiO_2	TiO_2	ZrO_2	Al_2O_3	Fe_2O_3	MnO	MgO	CaO	Na_2O	K_2O	F	Cl	Sum	less O	H_2O	Total
Unnamed Tuff in Area 130 and its correlate in Area 116 in the Tulu Bor Member below the Ninikaa Tuff																		
CLK10-059	1,1	13	70.12	0.38	0.12	11.87	2.72	0.20	0.18	0.19	2.26	3.98	0.20	0.17	92.38	0.12	9.17	101.43
CLK11-122	1,1	16	71.39	0.37	0.15	11.91	2.79	0.19	0.18	0.18	2.41	2.68	0.12	0.16	92.54	0.09	7.34	99.78
K80- 187	1,1	15	69.78	0.39	0.14	11.88	2.79	0.21	0.17	0.18	2.86	2.81	0.10	0.15	91.46	0.08	9.30	100.68
K80- 187	1,1	31	70.89	0.36	0.13	11.49	2.69	0.21	0.17	0.17	2.27	2.76	0.00	0.16	91.37	0.06	8.06	99.37
K80- 187GAv	1,1	46	70.53	0.37	0.13	11.62	2.72	0.21	0.17	0.18	2.46	2.78	0.03	0.15	91.40	0.07	8.46	99.79
MB08-67	2,2	1	70.87	0.24	0.27	9.37	4.15	0.17	0.01	0.16	2.43	2.55	0.03	0.12	90.37	0.04	8.14	98.47
K80- 213GAv	2,2	3	72.76	0.12	0.11	10.86	2.46	0.07	0.02	0.19	3.52	4.31	0.16	0.12	94.69	0.09	6.73	101.33
MB08-67	2,2	10	73.81	0.15	0.15	10.94	2.39	0.08	0.03	0.17	4.37	4.05	0.22	0.12	96.52	0.13	3.56	99.94
K80- 213	1,2	14	69.77	0.39	0.13	11.88	2.78	0.19	0.18	0.18	3.02	3.98	0.17	0.16	92.82	0.11	8.74	101.46
K80- 213GAv	1,2	50	70.02	0.38	0.14	11.83	2.78	0.20	0.17	0.18	3.29	4.24	0.15	0.16	93.56	0.11	7.71	101.16
K80- 213II	1,1	19	70.34	0.36	0.12	11.72	2.76	0.20	0.17	0.17	3.38	4.39	0.10	0.15	93.95	0.10	6.11	99.95
K80- 213II	1,1	18	69.87	0.39	0.15	11.91	2.80	0.20	0.17	0.18	3.31	4.24	0.19	0.17	93.58	0.12	8.62	102.08
K81- 496	2,2	5	72.08	0.27	0.29	10.41	4.43	0.21	0.10	0.23	2.76	1.99	0.30	0.13	93.20	0.15	7.06	100.10
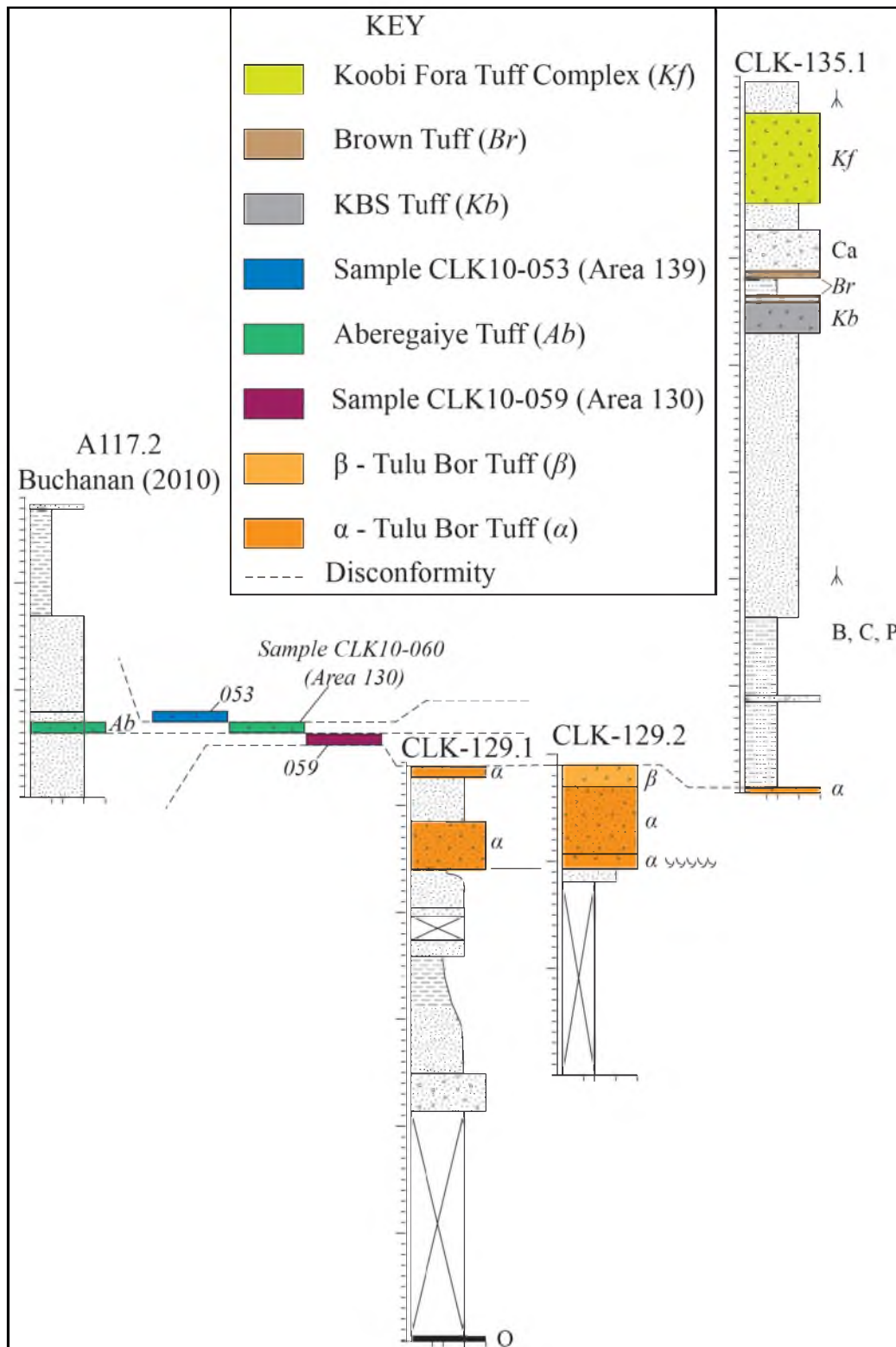
Figure 31. Correlated stratigraphic sections of the Koobi Fora Formation in Areas 117, 129, and 135
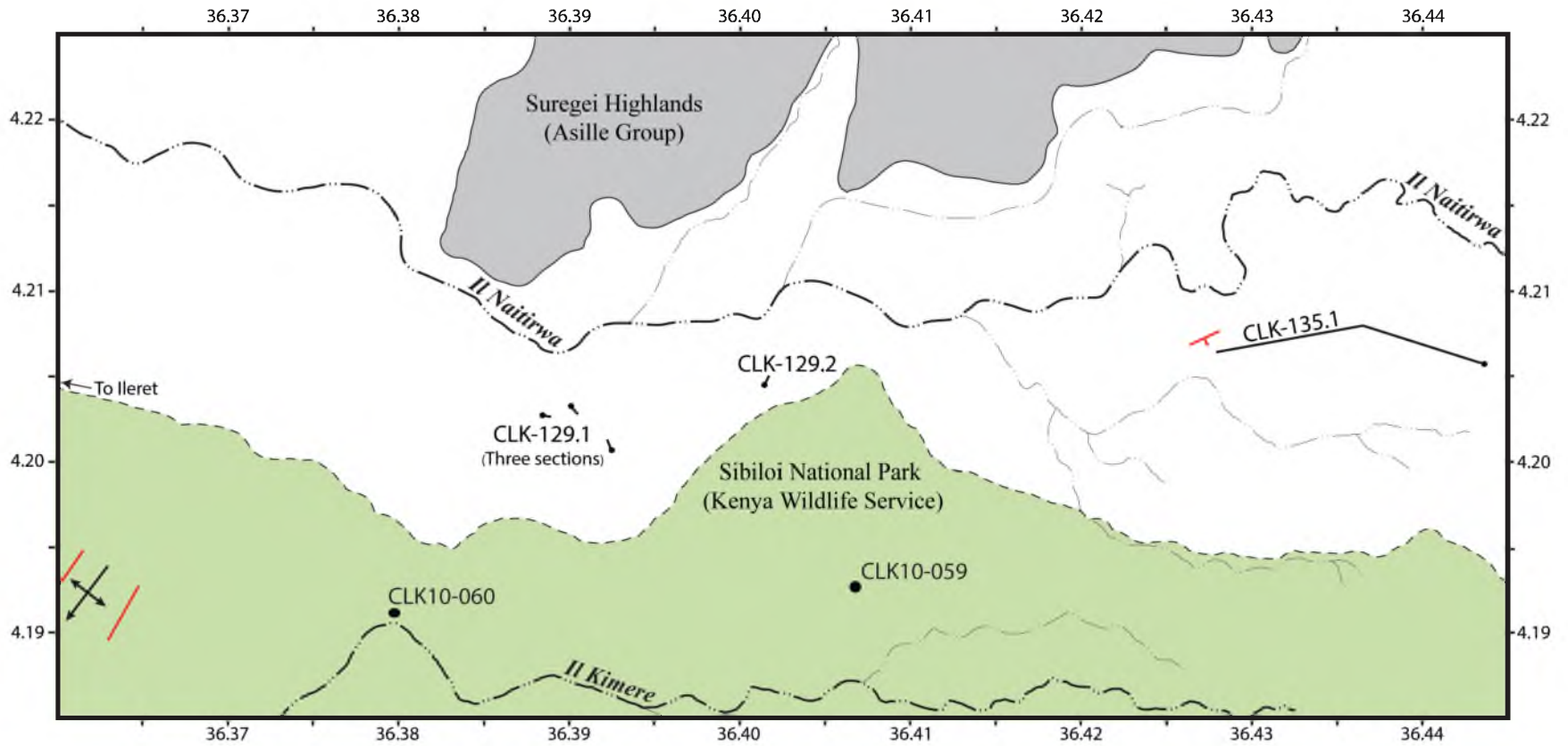
Figure 32. Locations of stratigraphic columns of the Koobi Fora Formation in Areas 129, 130, 135, and 139.

Figure 33. The basin margin in Area 139, showing colluvium developed on the Asille Group (4.2123 N, 36.3826 E).

Figure 34. Contact between the Lonyumun Member and the overlying Tulu Bor Tuff in Area 129 (4.2136 N, 36.4224 E).

Figure 35. View of the eastern termination of the Tulu Bor Tuff in Area 129, where it pinches out into a volcaniclastic conglomerate (4.2193 N, 36.4234 E).

Figure 36. Stromatolites that have formed around basalt cobbles in northern Area 135 (4.2285 N, 36.4458 E).

CHAPTER 7

MAGNETOSTRATIGRAPHY

Paleomagnetic samples were collected from the base of the Lonyumun Member to the Tulu Bor Tuff through measured lithologic sections including section PNG-41.2 of Gathogo (2003). Sampling was done in PNG-41.2 with the intention to link strata in the Lonyumun Member from Areas 40 and 41 to southern areas along the basin margin.

The need to collect samples for paleomagnetic measurement became apparent during the 2010 field season from the paucity of tuffs and other extensive marker beds in the Lonyumun Member. Paleomagnetic measurements had already been done on the Moiti Tuff (3.97 Ma) and Tulu Bor Tuff (3.43 Ma) which were deposited late in the Gilbert Chron (4.18–3.59 Ma) and early in the Gauss Chron (3.59–3.33 Ma), respectively (Hillhouse et al., 1986). With this knowledge it was hypothesized that paleomagnetic study would place tighter age constraints on the strata, fossils, and tuffs in the Lonyumun Member.

Results are compared to the Global Paleomagnetic Time Scale (GPTS), using ages of Gradstein, Ogg, and Smith (2004). Strata in each of the sections are assigned to appropriate subchrons using their polarity, and the known ages of the Moiti, Tulu Bor, and Kisemei tuffs. In doing so, correlations further constrained the ages of strata below the Tulu Bor Tuff including the fossil site in Area 40.

All tuffs were sampled in the study area except the β-Tulu Bor Tuff, because the

β-Tulu Bor Tuff is known to be of normal polarity everywhere it has been measured and

it has been assigned to the early Gauss Chron (3.59–3.33 Ma) (Brown et al., 1978;

Hillhouse et al., 1986; Shuey et al., 1974). The Guo Tuff was sampled at three localities

in the Kisemei drainage area and also in Area 15. At every site it yielded clear normal

polarity, and as it lies between overlying and underlying reversed section, it is assigned to

the Cochiti Subchron of the Gilbert Chron. The Tukunan Tuff is also of normal polarity

and assigned to the Cochiti Subchron. The Kanyeris and Kisemei tuffs were sampled at

all outcrops in the study area, and both are of reversed polarity on which basis they are

placed in the late Gilbert Chron (4.18–3.59 Ma). The Moiti Tuff was sampled in Area 41,

found to be of reversed polarity in agreement with measurements by Hillhouse et al.

(1986), and is assigned to the late Gilbert Chron, in accordance with its age of 3.97 ±

0.03 Ma (McDougall and Brown, 2008).

Strata are assigned to two magnetozones of normal polarity and two

magnetozones of reversed polarity within the composite section of the Koobi Fora

Formation in Areas 40 and 41 (Figure 38). These are discussed below from oldest to

youngest. All results from measured samples are listed in Appendix D.

7.1 Reverse Polarity (4.49–4.29 Ma)

The boundary between the early Gilbert Chron and the Cochiti Subchron (4.29–

4.18 Ma) is taken as the base of the Tukunan Tuff (CLK10-S11), however no strata were

measured below the Tukunan Tuff because it there is no exposure. A disconformity is

placed at the top of sections CLK11-S6, -S7 and CLK10-S7 in Area 40, and CLK10-S4a

in Area 41 where strata are continually reversed up to the bases of the Kanyeris and Moiti

Tuffs. To account for the absence of strata that record the Cochiti event (110 ka duration) the disconformity separates the youngest reversed magnetozone from the oldest. In the Kisemei drainage area (Area 41) strata below the Guo Tuff reveal reverse polarity down to the base of the Lonyumun Member and are also assigned to the early Gilbert Chron (4.49–4.29 Ma).

Section PNG-41.2 of Gathogo (2003) was sampled during the 2011 field season to confirm correlation to the Lonyumun Member in the study area. Results reveal reverse polarity throughout PNG-41.2, a section that is confidently correlated with lithologic sections in the study area. The strata of PNG-41.2 are therefore also assigned to the early Gilbert Chron (4.49–4.29 Ma).

The magnetozone described above may correlate to Area 129 where Hillhouse et al. (1977) sampled an 80 m interval from the contact with Asille Group volcanics of the Suregei Highland to the base of the α-Tulu Bor Tuff (3.43 Ma). Hillhouse et al. (1977) established normal polarity strata to a level ~ 36 m below the base of the α-Tulu Bor Tuff preceded by 36 m of reversed strata. Correlation from the study area to strata beneath the α-Tulu Bor in Area 129 is possible using magnetostratigraphy, however there are two possible ways in which the reversed strata in Area 129 may be accommodated by the GPTS. These are discussed below.

With an age of 3.4 Ma the α-Tulu Bor Tuff fits nicely within the early Gauss Chron. The ~ 36 m of normal polarity strata below the α-Tulu Bor must then lie between the Gilbert/Gauss epoch boundary (3.59 Ma) and 3.4 Ma. Were disconformities not a problem, strata below the Gilbert/Gauss boundary would be assigned to the late Gilbert Epoch (4.18–3.59 Ma). With the absence of the reverse polarity, Lokochot (3.6

Ma) and Moiti (4.0 Ma) tuffs, correlation to the later part of the Gilbert Chron in the

study area cannot be made with confidence. It is more likely that reversed strata under

the α-Tulu Bor Tuff belong to the reversed part of the Gilbert Chron between 4.49–4.29

Ma because related strata are mappable from Area 129 to Area 15 in the upper reaches of

Kolom Mega, where they rest directly on colluvium developed on the Asille volcanic

rocks, and where there are prominent diatomites near the base of the section. If this

placement is correct, it means that the Cochiti event (4.29–4.18 Ma) and the reversed

upper part of Gilbert Chron (4.18–3.59 Ma) are missing, signifying at least 700,000 years

missing from the geological record in Area 129 at the boundary between these

magnetozones.

7.2 Normal Polarity (4.29–4.18 Ma)

The Guo Tuff overlies strata assigned to the Gilbert Chron (4.49–4.29 Ma) in

CLK10-S9, is of normal polarity, and is older than the Kisemei Tuff (4.06 ± 0.03 Ma),

for these reasons the Guo Tuff is assigned to the Cochiti Subchron (4.29–4.18 Ma) in the

Gilbert Chron. The Tukunan Tuff also yielded normal polarity, and it can be assigned to

the Cochiti Subchron because it overlies the Guo Tuff in the Kisemei drainage (CLK10-

S9), and in Area 40 it is overlain by reverse strata assigned to the Gilbert Chron (4.18–

3.59 Ma) associated with the Kanyeris Tuff.

7.3 Reverse Polarity (4.18–3.59 Ma)

In Area 40, strata between the top of the Tukunan Tuff and the top of the

Kanyeris Tuff in CLK10-S11 are assigned to the late Gilbert Chron (4.18–3.59 Ma).

Farther east, strata below the Kanyeris Tuff in sections CLK10-S10 and CLK11-S13

(Figure 38) are also assigned to the late Gilbert Chron (4.18–3.59 Ma). In Areas 40 and

41 strata below and including the Moiti Tuff in CLK11-S15 and CLK10-S4, respectively

are also assigned to the late Gilbert Chron (4.18–3.59 Ma). The measured age of the

Moiti Tuff (3.97 ± 0.03 Ma) requires its placement in this interval. In the Kisemei

drainage the late Gilbert Chron (4.18–3.59 Ma) is limited to the Moiti, Kisemei, and

Kanyeris tuffs, because the boundary between the late Gilbert Chron and the Cochiti

Subchron was not found in sections containing these tuffs. No measurements were made

in strata above the Guo Tuff in CLK11-S4 or CLK10-S9 below the Kanyeris and Kisemei

tuffs, respectively, but these must belong to either the Cochiti Subchron (4.29–4.18 Ma)

or the Gilbert Chron (4.18–3.59 Ma). Further, the Kanyeris Tuff must be older than 4.06

± 0.02 Ma because of the measured date on the Kisemei Tuff, therefore an age of 4.12 ±

0.06 Ma can be estimated for the Kanyeris Tuff.

A disconformity marks the boundary between the magnetozone assigned to the

Cochiti Subchron (4.29–4.18 Ma) and the magnetozone assigned to the late Gilbert Chron

(4.18–3.59 Ma) in the Namorotukunan and Kisemei drainage areas. The boundary

appears to lie at the top of the Tukunan Tuff in Area 40 and at the base of the Kanyeris

and Kisemei Tuffs in Area 41.

7.4 Normal Polarity (3.59–3.33)

This magnetozone is only recorded in the Namorotukunan area and possibly at

Kisemei in strata above the late Gilbert Chron (4.18–3.59 Ma). Three samples were

collected 6 m above the Kanyeris Tuff in strata assigned to the undifferentiated

Lokochot/Tulu Bor members and all are of normal polarity. For these reasons strata

between the top of the Kanyeris Tuff in the Namorotukunan area can confidently be assigned to the early Gauss Chron (3.59–3.33)

A disconformity is placed above the Kanyeris, Moiti and Kisemei Tuffs in the Namorotukunan area and the Kisemei drainage area, where strata assigned to the normal early Gauss Chron (3.59–3.33 Ma) are in contact with the Kanyeris Tuff. Using the age estimate of 4.12 ± 0.06 Ma given above for the Kanyeris Tuff, the disconformity would represent 530,000 years of time, and the minimum amount of time missing from the geological record in this area is ~ 470,000 years.

Figure 37. Pits excavated to expose fresh rock for paleomagnetic sampling (4.4083 N, 36.3300 E).
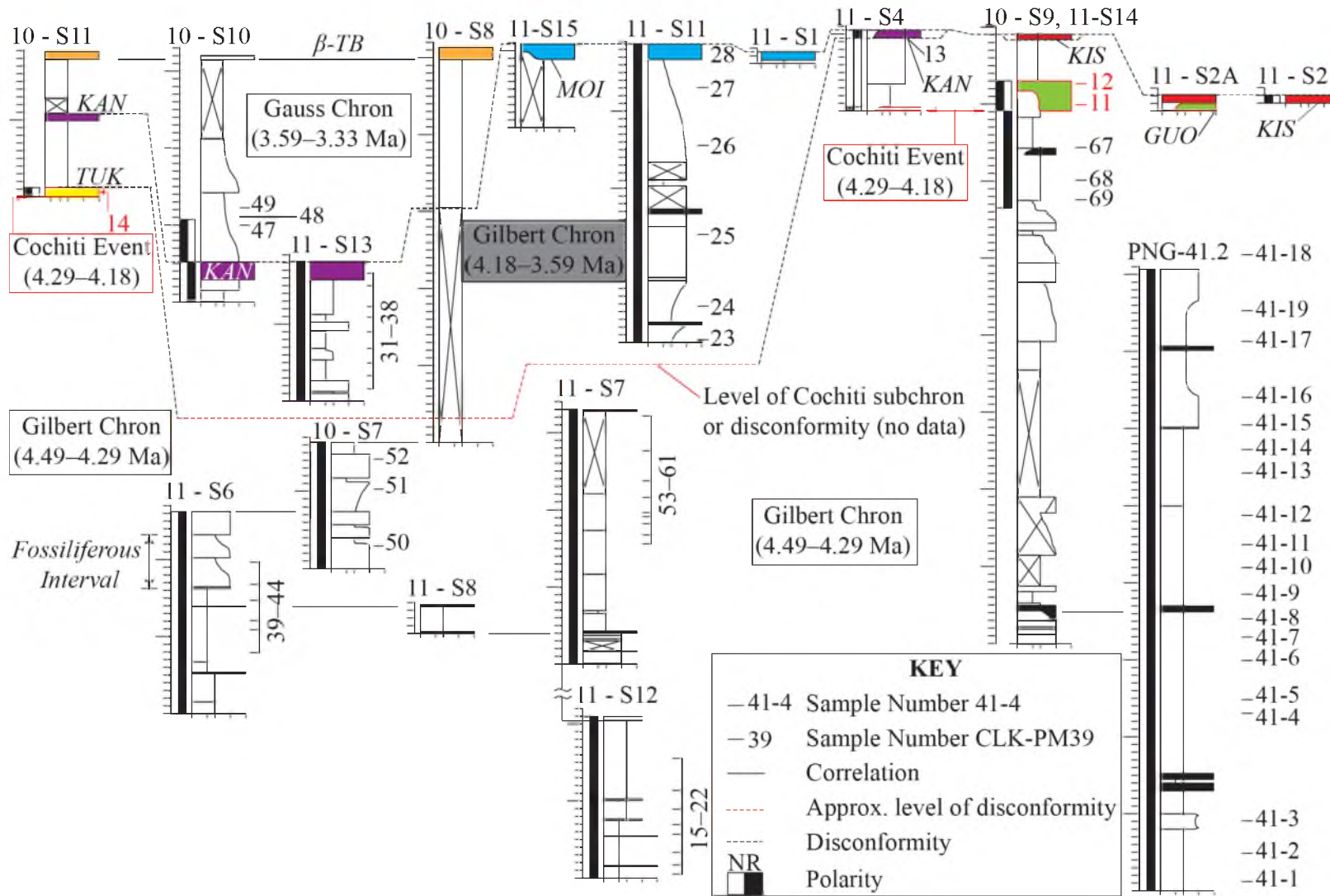
Figure 38. Correlated magnetozones between sections in which strata were sampled for paleomagnetic measurements.

CHAPTER 8

GEOLOGY OF FOSSIL OCCURRENCES

8.1 Vertebrate Fossils

The Koobi Fora Formation is well known for its abundance of vertebrate fossils, however until recently work was limited to the region south of Areas 40 and 41. Paleontological work that has been done in Area 41 is confined to the upper Burgi Member (Braun et al., 2007). The reason for this is that vertebrate fossils were thought to be few or non-existent in these areas because fossils were not found on a reconnaissance visit by Richard and Meave Leakey by camel (personal communication, Meave Leakey). Later, work in the area north of Il Eriet was discouraged for reasons of personal safety.

Initially, very few vertebrate fossils were recovered from Areas 40 and 41 and included only *Crocodylidae* and *Tragelaphini*, although fish bones, molluscs, plant, and diatom fossils were abundant. The 2011 summer field season revealed a wealth of mammalian fossils at one set of related localities in Area 40 (GPS coordinates in Appendix A).

The fossil assemblage lies at the bottom of the upper interval within the Lonyumun Member in magnetically reversed strata. Strata are characterized by deltaic front and lake margin lithofacies. Reconnaissance of this area continued to the end of the 2011 field season by the paleontology team headed by Dr. Meave Leakey, and continued into 2012. The paleontology team recovered a vertebrate fossil assemblage believed to

be similar to that of the Apak Member of the Nachukui Formation at Lothagam (Leakey and Harris, 2003). The implications of this fossil assemblage to the age of the Apak Member at Lothagam are discussed in Chapter 10.

8.2 Invertebrates, Plants, and Diatoms

Molluscs (Classes: Gastropoda and Bivalvia), ostracods, plants, and diatom fossils are plentiful in the Lonyumun Member and upper Burgi Member in Areas 40 and 41. Layers rich in invertebrates and diatoms are important marker beds for correlation between sections where tuffs were not present or were not widespread. Also, they are supplemental indicators of paleoenvironments as some of these organisms only thrive under particular conditions. Fossil molluscs occur near the base of the Lonyumun Member, and also in the middle and upper intervals described above. They are associated with lake margin, delta front, and distributary channel environments. Molluscs occur packed in fine to very fine sandstones, and gastropods dominate, with only a few beds being packed with bivalves. The most common gastropods are *Bellamya* sp. (Figure 39), *Cleopatra* sp., and *Melanoides* sp. (Figure 40). In the middle interval of the Lonyumun Member an extensive bivalve-packed sandstone used to correlate sections between Area 40 and 41 is dominated by *Pseudobovaria* sp. (Figure 41). North of Il Dura in Area 41, below the Moiti Tuff, an ostracod layer also contains sparse large bivalves that have been identified as *Pleiodon ovata* by Dr. Bert Bocxlaer (University of Gent, Belgium).

Ostracods also occur in the middle and upper intervals of the Lonyumun Member. In most instances the ostracod-rich layers have a matrix of fine to very fine quartz sand. Laterally the same layers may also contain bivalves, gastropods, and fish bone.

Well-preserved fossil wood (Figure 42) is abundant between Lala and the Il Eriet, where it occurs stratigraphically below the *Pseudobovaria* sp. layer in Area 41. Preservation is principally as small pieces of wood (<50 cm length x <10 cm breadth) the original material being replaced by calcite, seemingly impregnated with limonite, so that the fossil wood is pale orange. This is similar to fossil wood described by Gathogo (2003) and Gathogo and Brown (2006) in section PNG-41.2 in the middle part of the Lonyumun Member in lake margin lithofacies. Here the same interpretation holds as the wood fragments are found in a fish bone bearing interval of alternating silt and fine sand containing much limonite.

Diatomites are by far the most widespread, laterally continuous marker beds. Two distinct layers are seen at the bottom of the Lonyumun Member in Area 41, where they extend southward along the basin margin into Area 15, and northward across the Ethiopian border. The lowest diatomite layer in sections CLK10-S2 and CLK11-S5, S12 is used to correlate to the lower diatomite of section PNG-41.2 (Gathogo, 2003). Another thin diatomaceous siltstone overlain by the main *Pseudobovaria* sp. layer in Area 40 provides the primary correlation between sections CLK11-S6 and CLK11-S7.
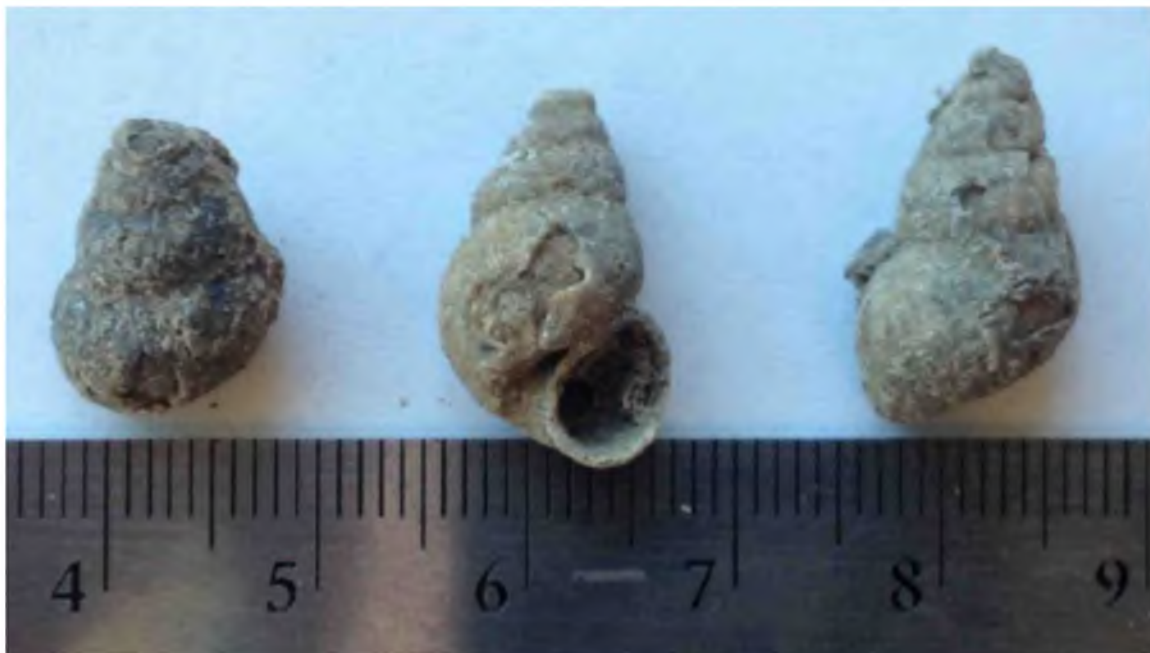
Figure 39. *Bellamya* sp. gastropods from the main *Pseudobovaria* sp. marker bed in Areas 40 and Area 41. Scale is in cm.

Figure 40. *Melanoides* sp. gastropods from the main *Pseudobovaria* sp. marker bed in Areas 40 and Area 41. Scale is in cm.

Figure 41. *Pseudobovaria* sp. bivalves from the main *Pseudobovaria* sp. marker bed in Areas 40 and Area 41
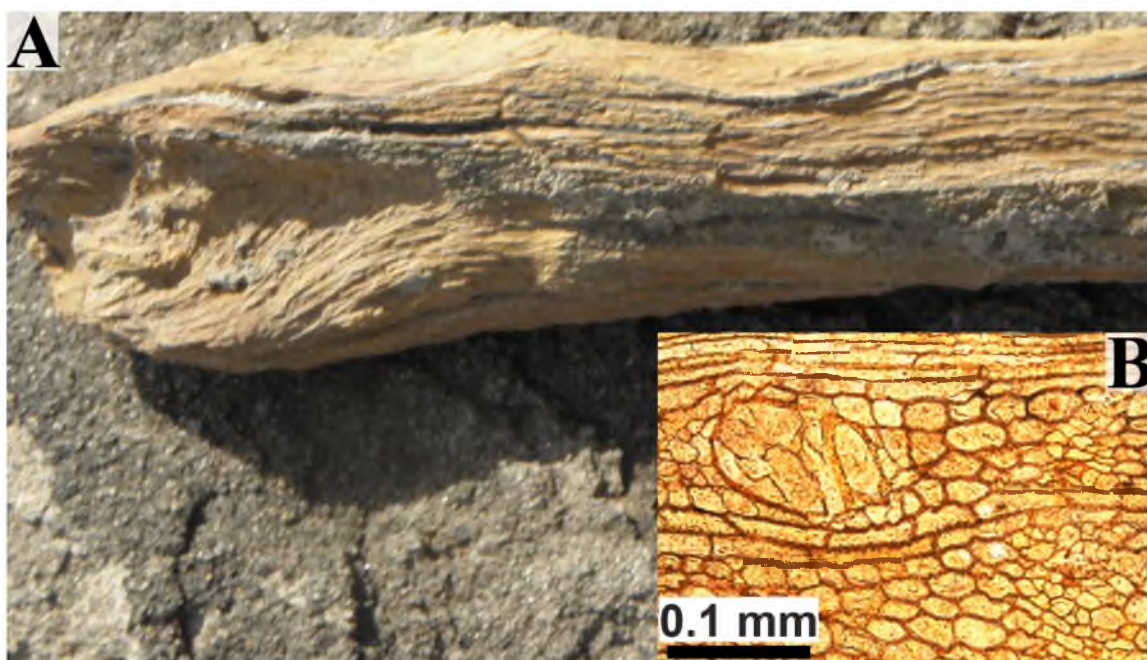
Figure 42. A) Fossilized wood in the middle interval of the Lonyumun Member below the main *Pseudobovaria* sp. bed in Area 41 (4.4125 N, 36.3679 E). Similar to those in the upper interval in PNG-41.2 described by Gathogo (2003). B) Photomicrograph of a thin section of the petrified wood showing excellent preservation.

CHAPTER 9

GEOLOGIC STRUCTURES

The study area is located on the eastern flank of the northern Kenyan Rift, which

runs N-S beneath and flanking Lake Turkana, and also includes the Kinu Sogo Fault

Zone east of the Koobi Fora region. All structures are associated with activity along this

divergent boundary. Large- and small-scale normal faults in the study area all have

general NNW-SSE trends.

Trending N-S along the western extent of the study area is a large normal fault

that can be traced north (Figure 43) to south (Figure 44) from the Ethiopian border to the

Il Eriet (~ 4.365 N). The fault was first recognized and mapped by Gathogo and Brown

(2006), however they do not discuss it in their publication. Here the fault is named the

North Gele Fault after Il Gele an ephemeral stream along which the fault is exposed near

the Ethiopian Border. Strata are dropped down to the west along this fault, so that along

the southern part of the fault the KBS and upper Burgi Members are in contact. To the

north the upper Burgi and Lonyumun members are in contact west and east of the fault,

respectively. The northern part of this fault is mapped with some uncertainty from

Namorotukunan to Il Gele because both upper Burgi and Lonyumun Members have

similar lithologies. The fault does extend as far north as the Il Gele, where it is well

exposed on the north side of the stream at (4.4459 N, 36.3234 E).

In Area 41 two normal faults trend NNW–SSE on either side of a synclinal structure involving the upper part of the Lonyumun Member. Strata on the east and west limbs dip from ~ 12–30 degrees, the steepest occurring in the middle portion of the faults (Figure 45). Dips decrease to ~ 2 degrees on the northern and southern ends of the syncline. The Moiti Tuff caps the syncline with ~ 13 m of a fining upward sequence diping at 16 and 8 degrees near the bottom and top respectively. In this locality the Moiti Tuff contains fluvial ripple marks representing fluvial deposition. Bedding planes of the Moiti Tuff appear to be horizontal, indicating that the syncline had formed before deposition of the tuff, thus placing formation of the syncline before 3.97 Ma.

Deformation also occurs on the eastern basin margin just southeast of the Na'uko Plateau, where an orange gastropod sandstone dips away from the Suregei Highlands forming an anticline (Gathogo, 2003). Similar fault boundaries may exist at 4.3645 N 36.4110 E along the contact with the Asille volcanic rocks in the upper part of the Kolom Ain Borana Drainage, and also at the easternmost extent of the Koobi Fora Formation along Il Dura.

Figure 43. Northernmost exposure of the North Gele Fault in Area 40, north of Il Gele
(4.4460 N, 36.3233 E).

Figure 44. Southern exposure of the North Gele Fault in Area 40 near an outcrop of the
KBS Tuff (4.3929 N, 36.3289 E).

Figure 45. Steeply dipping strata along the eastern normal fault bounding the syncline capped by the Moiti Tuff, Area 41 (4.4197 N, 36.3754 E).

CHAPTER 10

DISCUSSION

The center of the Turkana Basin has been in its current position under Lake

Turkana throughout the Pliocene and Pleistocene Epochs, (Haileab et al., 2004).

Sedimentation began in the basin with capture of the Omo River about 4.5 Ma, which

created the Lonyumun Lake, a water body with about 3 times the area of current Lake

Turkana (Brown and Feibel, 1991; Bruhn et al., 2011).

Diatomites and pelagic sediments resting on Miocene aged Asille Group volcanic

rocks record this large lake along the basin margin from the Ethiopian border in Area 41

to sections of Gathogo (2003) in Area 14 and to section CLK10-S1 in Area 15. Higher in

the section conglomeratic sandstones derived from southern Ethiopia and gastropods in

marginal lacustrine facies show that the lake was retreating toward the basin center, so

the marginal streams extended further west.

Lake regression, or deltaic infilling recorded by laminated layers of alternating

fine sand and siltstone with abundant limonite further, brought the Omo Delta into the

study area. At this time animals on the delta were preserved as fossils in Area 40 and

Pseudobovaria sp. inhabited fresh water channels of the Omo delta, being prevalent in

Areas 40 and 41.

Between 4.29 and 4.18 Ma (the Cochiti subchron), the Omo delta moved farther

south and the Omo River flowed through the study area bringing in the Guo and Tukunan

Tuffs. However deposition apparently did not occur north of Il Dura or Namorotukunan, because normal polarity strata of the Cochiti subchron do not occur at those localities

Sometime between 4.18 and 4.06 Ma the Kanyeris Tuff was deposited near Namorotukunan in the Kisemei drainage area, and as far south as Il Warata in Area 13, the type area of this unit. After deposition of the Kanyeris Tuff, but before 4.06 Ma, the Kisemei Tuff, along with its pumices, is deposited in the Kisemei drainage area, and incorporates some glass shards with compositions of the Kanyeris, Tukunan, and Guo tuffs showing that those units were already being eroded at that time.

By the time the Moiti Tuff was deposited at 3.97 Ma the synclinal structure containing the Moiti had formed and the Omo River continued to flow through the study area. The Moiti Tuff was either deposited across a floodplain of ~ 3 km width, or alternatively in two separate channels separated by ~ 2.3 km. The river may have been forced to turn westward by basalt outcrops at the western end of the Na'uko Plateau, and indeed, this basalt outcrop may have shielded the section containing the Guo Tuff from erosion by the Omo River.

The Wargolo Tuff is deposited on the Moiti Tuff and is the only record of sedimentation in this region, between 3.97 and 3.43 Ma. The next higher unit that can be identified with certainty is the β-Tulu Bor Tuff (3.43 Ma). The Gauss Chron is recorded by strata assigned to the undifferentiated Lokochot/Tulu Bor Members, derived from the Omo River and deposited sometime between 3.59 and 3.4 Ma, when the Omo River brings volcanic glass of the β-Tulu Bor Tuff to the Namorotukunan area. Sediments must have filled the basin to the west by this time because the β-Tulu Bor Tuff lies at the same elevation as the Moiti Tuff.

The unconformity at the base of the upper Burgi Member is recognizable over much of the Koobi Fora region, so that strata between 2.5 Ma and 2.0 Ma are not known from the Koobi Fora region, except perhaps for the tuff described earlier in Area 139. Deposition resumes with formation of the Lorenyang lake ~ 2.0 Ma ago. Its shores reached Area 40 as seen on the geographically high Namorotukunan Hill (487 m) that contains fish bone and gastropods in a beach environment, but does not appear to have extended much farther east. The lake margin reaches the area south of Il Dura where ephemeral streams entered the lake and locally deposited sands with abundant *Cleopatra* sp. that are found at elevations of ~520 m.

Beyond the North Gele Fault on the western boundary of the study area the KBS Member is exposed. The normal fault has brought the KBS Member down to the level of the upper Burgi Member in the south and the upper Burgi Member to the level of the Lonyumun Member in the north. The KBS Member must have been deposited in the study area, however after faulting occurred, subsequent erosion removed KBS member strata east of the North Gele Fault.

CHAPTER 11

CONCLUSIONS

This study used various geological techniques to assign strata in Areas 40 and 41 to members of the Koobi Fora Formation and to assign dates to intervals of strata within these members. This study was able to constrain ages on strata within the field area within a temporal range of 4.49–2.0 Ma.

Seven tephra layers were identified in the study area: the Guo Tuff, the Tukunan Tuff, the Kanyeris Tuff, the Kisemei Tuff, the Wargolo Tuff, the Moiti Tuff, and the β-Tulu Bor Tuff. Pliocene strata correlate southward along the eastern basin margin to sections of Gathogo (2003) in Areas 41 and 14, section CLK10-S1 in Area 15, and to sections in Areas 129 and 135 where strata overlain by the Tulu Bor Tuff are similar to those in the study area.

Two main structures are identified in the study area: a large normal fault named the North Gele Fault, and a synclinal structure capped by a plateau of Moiti Tuff. The normal fault was mapped by Gathogo and Brown (2006), and was extended to the Ethiopian border in the present study. Minimum ages are proposed for the formation of the synclinal structure (4 Ma) and for the North Gele Fault (<1.8 Ma).

11.1 Stratigraphy

Strata are assigned to six members of the Koobi Fora Formation in the study area:
the Lonyumun Member, Moiti Member, undifferentiated Lokochot/Tulu Bor Member,
Tulu Bor Member, and the upper Burgi Member. Twenty-seven stratigraphic sections
were measured to provide information on age of sediments and depositional
environments. Sections in related areas farther south (Area 129, etc) provide important
links between strata in Areas 40 and 41 and in other parts of the greater Koobi Fora
region.

In Area 129 the base of the Lonyumun Member is in contact with Asille Group
Volcanics where sandstones wrap around a "nose" of the Suregei Highlands, suggesting
that that elevated region actively rose after deposition of the sandstones. Wherever
exposed, the Pliocene strata dip away from the Suregei Highlands (Figures 8 and 12).
The Lonyumun Member is overlain by the upper part of the Lokochot Member followed
by the Tulu Bor Tuff, but neither the Moiti Tuff nor the Lokochot Tuff are present. The
Tulu Bor Tuff continues south into Sibiloi National Park in Area 130, where it is overlain
by the Aberegaiye Tuff (2.70 Ma), and Tuff D-5-2 of the Shungura Formation (2.44 Ma).

11.2 Magnetostratigraphy

Four magnetozones recorded in strata of the Koobi Fora Formation were assigned
to the Gilbert Chron between the Cochiti subchron and the Nunivak subchron (4.49–4.29
Ma), the Cochiti subchron (4.29–4.18 Ma), the Gilbert Chron above the Cochiti subchron
(4.18–3.59 Ma), and the Gauss Chron below the Mammoth subchron (3.59–3.33 Ma).
Results suggest that initiation of Pliocene sedimentation in the Turkana Basin does not

predate 4.5 Ma as suggested by earlier workers (e.g., Brown and Feibel, 1991; Bruhn et al., 2011).

In Area 129, Hillhouse *et al.* (1977) measured 36 m of strata of normal polarity overlying 36 m of reversed polarity strata below the Tulu Bor Tuff. Because the Lokochot, Moiti, Kanyeris, Tukunan, and Guo tuffs are not present in Area 129, it is most likely that the reversed polarity section belongs to the Gilbert Chron between the Cochiti and Nunivak subchrons (4.49–4.29 Ma) and therefore correlates to strata in the Lonyumun Member in Area 41 assigned to the same interval. This is consistent with the presence of a *Pseudobovaria* packed sandstone in Area 129. Normal strata overlying the Lonyumun Member, but below the α-Tulu Bor Tuff in Area 129 can only belong to the base of the Gauss Chron (3.59–3.33 Ma) in the upper Lokochot Member.

11.3 Ages of Volcanic Tephra

Four tuffs in the Lonyumun Member have been dated either directly or indirectly through $^{40}Ar/^{39}Ar$ dating techniques or magnetostratigraphy. The Kisemei Tuff contains pumices dated to 4.06 ± 0.02 Ma, and includes volcanic glass with composition of the Kanyeris and Tukunan tuffs. The Kanyeris Tuff is of reversed polarity, and lies below the Kisemei Tuff and above the Cochiti subchron, so it must be between 4.06 and 4.18 Ma, placing a minimum age on the Kanyeris of 4.06 ± 0.03 Ma. The Guo and Tukunan tuffs have been given an age constraint of 4.29–4.18 Ma on the basis of magnetostratigraphy. The Kanyeris and Kisemei Tuffs have also been given an age constraint of 4.18–4.06 ± 0.03 Ma on the basis of magnetostratigraphy and $^{40}Ar/^{39}Ar$ dates on the Kisemei Tuff. The Tukunan Tuff has a composition that may be related to that of the Kanyeris Tuff, however it has lower CaO content.

In Area 129 the Aberegaiye Tuff lies above the Tulu Bor Tuff, and contains pumices dated at 2.70 ± 0.02 Ma by $^{40}Ar/^{39}Ar$, showing that the stratigraphic placement in the Lonyumun Member (Buchanan, 2010) is incorrect; rather, the tuff lies within the Tulu Bor Member.

11.4 Disconformities

Disconformities are prominent features of the geology of Areas 40 and 41, representing vast periods of time missing from the geological record (Figure 46). In the Lonyumun Member a disconformity above the Guo and Tukunan Tuffs corresponds to ~110,000 years of either removal or nondeposition of strata during the time of the Cochiti Subchron in the northern areas of the study area. No strata have yet been identified elsewhere in the Koobi Fora region that record the Cochiti Subchron. Another disconformable surface marks the top of the Lonyumun Member, where the Moiti Tuff is absent, and must represent ~460,000 years, because the Lokochot Tuff is also absent from the study area. The Wargolo Tuff represents deposition during this interval where it overlies the Moiti Tuff and the Lonyumun or Moiti Member strata north of Namorotukunan.

In Areas 129 and 139, the disconformity between the Lonyumun and Lokochot member strata must represent loss of record corresponding to ~ 690,000 years of time, while at least two disconformable surfaces above the Tulu Bor Tuff must be invoked to separate a tuff ~3.15 Ma in age (CLK10-053) from the Aberegaiye Tuff (2.70 Ma), and the latter from a tuff that is probably ~2.44 Ma old. Time lost on these surfaces amounts to~ 300,000 years, 445,000 years, and 260,000 years, respectively. Above these surfaces there is a regional disconformity that represents about a half-million years of time lost

before deposition of the upper Burgi Member strata. The existence of tuffs that can be assigned ages with reasonable confidence is important in demonstrating that sedimentation continued in the area between 3.3 and 2.0 Ma, but that the record is now a palimpsest, having been removed by erosion multiple times.

11.5 Fossil Assemblage in Area 40

The fossil assemblage in Area 40 is said to be similar to that of the Apak Member of the Nachukui Formation at Lothagam site southwest of Lake Turkana (personal communication, Dr. Meave Leakey). McDougall and Feibel (2003) give an age range of 5.23–4.20 Ma for fossils of the Apak Member, but the age assigned to the fossils in Area 40 on the basis of their position with respect to the Kanyeris Tuff, and their magnetostratigraphy is 4.49–4.29 Ma.

This finding has implications for the age assigned to fauna from the Apak Member. As the lower part of the Apak Member is of normal polarity, it is likely that it lies within the Cochiti Event (4.18–4.29 Ma), and therefore the fauna from the lower Apak member at Lothagam is <4.29 Ma in age, a much closer constraint than that given by McDougall & Feibel (2003). Even if there is a disconformity in the lower Apak Member (for which no evidence has been adduced), the fauna is most likely younger than 4.63 Ma (the estimated age of the base of the Nunivak Event), and even this is a closer estimate than that given in McDougall and Feibel (2003).

11.6 Structures

Normal faults and a synclinal fold and normal faults are found in the study area. The N-S trending North Gele Fault makes up the western boundary of the study area.

The west side has dropped down bringing the KBS Member in contact with the upper

Burgi member in the southern extent of the fault. In the northern extent lacustrine strata

of the upper Burgi Member are in contact with similar strata of the Lonyumun Member

making mapping difficult. Faulting occurred after deposition of the KBS Tuff, that is

sometime less than 1.87 Ma ago. Displacement on the North Gele Fault is estimated to

be ~ 72 m, accounting for the thickness from the Kanyeris Tuff to the top of

Namorotukunan hill where upper Burgi strata cap the hill.

The synclinal structure containing the Moiti Tuff deforms strata above the lower

interval of the Lonyumun Member to ~ 14 m below the Moiti Tuff. Two minor normal

faults bound the syncline on the east and west with a NNW–SSE trend. The undeformed

strata under the Moiti Tuff were deposited by the ancestral Omo River, which flowed

from the north through the syncline, then meandered west depositing the Moiti Tuff at its

current position in Area 40. The undeformed floodplain and fluvial channel deposits

associated with the Moiti suggest that the syncline had formed before deposition of the

Moiti Tuff, and that the Omo River followed the axis of the syncline. Thus the syncline

formed between 4.5 Ma and 3.97 Ma. Displacement on the normal fault is ~ 23 m

accounting for the thickness of strata between the top of the orange sandstone

conglomerate the base of undeformed strata below the Moiti Tuff

These structures in the study area may be part of a SW–NE trending 0.5–1 km

diagonal fault zone that extends from the southeastern edge of Area 138 into Area 41

(Gathogo, 2003). Deformation along the basin margin, the syncline involving the Moiti

Tuff and the normal faults bounding that syncline, and the North Gele Fault may be

related to longitudinal normal faults that Gathogo (2003) describes elsewhere in the Ileret

Area.

In the eastern part of Area 129 the Tulu Bor is faulted with undeformed overlying

beds of the upper Burgi member, placing the timing of the between 2.7 Ma and 2.0 Ma

An exposed anticline with an axis oriented N37°E and plunging gently to the southwest is

exposed in Area 139, also involving the Tulu Bor Tuff and underlying strata. It is

bounded on the west by a fault that may be part of a broad system of faults mapped by

Buchanan (2010) in Area 117 to the south. Tuff D-5-2 in the Shungura Formation

appears undeformed, and overlies the eastern limb of the anticline placing its formation

sometime before 2.44 Ma.

11.7 Future Work

Future work in the study area could focus on paleomagnetic sampling at tighter

intervals throughout the exposures in Area 40 and 41. Although an effort was made to

sample at meter intervals, this was not possible through all sections, and in addition some

samples provided indeterminate directions. With denser sampling the positions of

magnetostratigraphic boundaries should be located more closely in the sections.

Further sampling in Areas 14, 15 and strata in Area 129 beneath the Tulu Bor

Tuff will either bolster or negate correlations made to those areas. Particular sections of

interest include: PNG-14.1, -14.2 (Area 14) and PNG-13.1 (Area 13), CLK10-S1 (Area

15), and CLK-129.1, -129.2, -130.1 (Areas 129 and 130).

Attention could also be focused on the orange conglomeratic sandstone interval at

the top of the lower interval of the Lonyumun Member. Here the sandstone has been

described as a slump deposit triggered by seismic activity or mass loading of sediment in

a deltaic environment. Much work needs to be focused on trend measurements and internal structures of the folds in this interval to interpret the true nature of formation.

Reconnaissance of the strata described by Davidson (1983) farther up the Ileret in Ethiopia should be considered. Davidson (1983) notes that in a low-gullied terrain there are exposures of light colored, well bedded sediments that include gravels, sands, silts, clays, and tuffs. He also notes that they appear to be younger than the Harr Basalt. Davidson correlates these strata to the Ileret sediments of (Vondra and Bowen, 1976). This thesis postulates that they belong to the Lonyumun Member, which is older than the Harr and related Gombe Basalts, however without field work in the area this cannot be confirmed. Work there may reveal tuffs that correlate with tuffs of known composition in the Turkana Basin, thus allowing direct correlation with the Koobi Fora Formation.
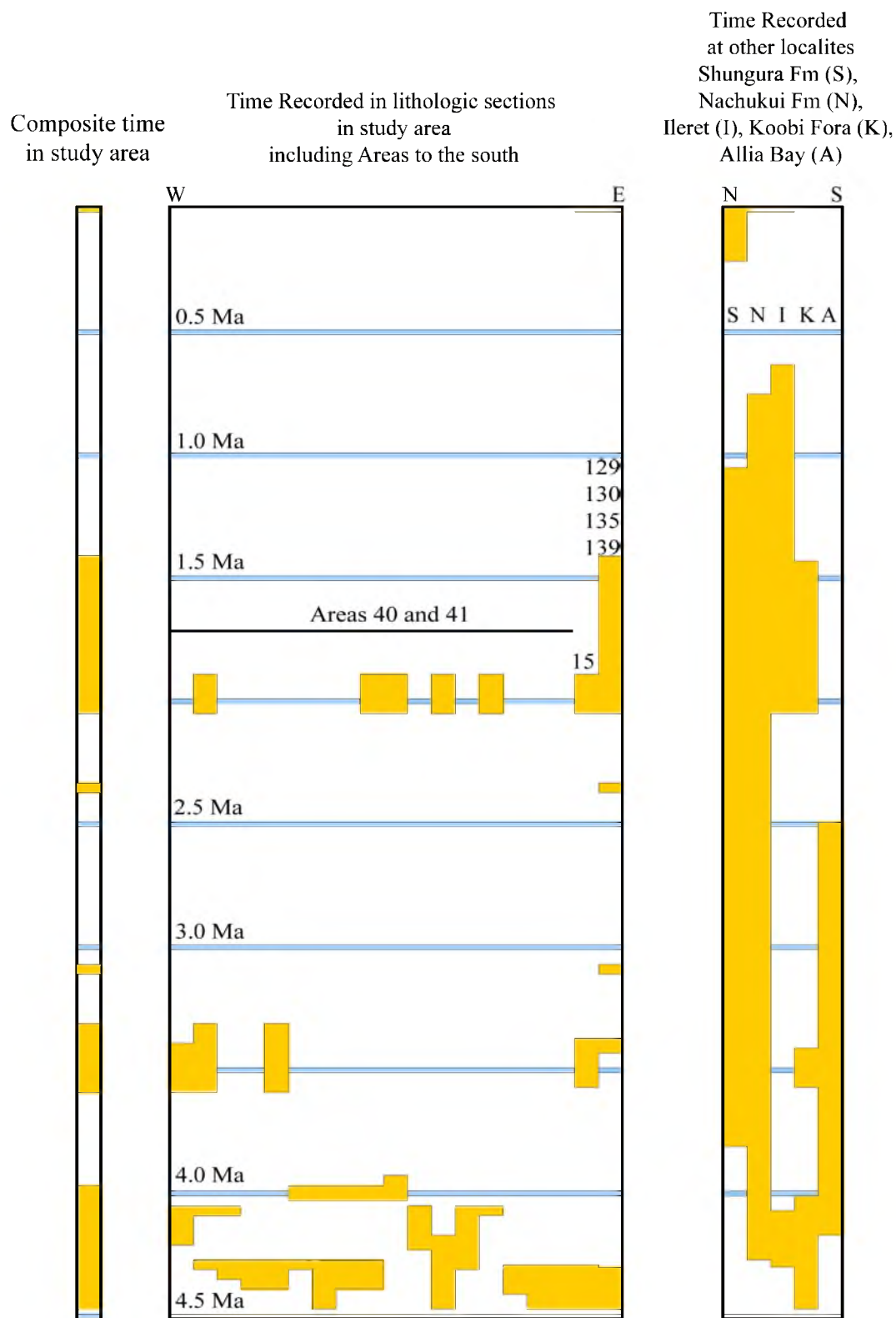
Figure 46. Time recorded in lithologic sections in the study area including Areas 15 and 129.

APPENDIX A

GEOLOGIC MAP

Geologic Map of Areas 40 and 41
Lake Turkana, Kenya

Casey L. Kidney
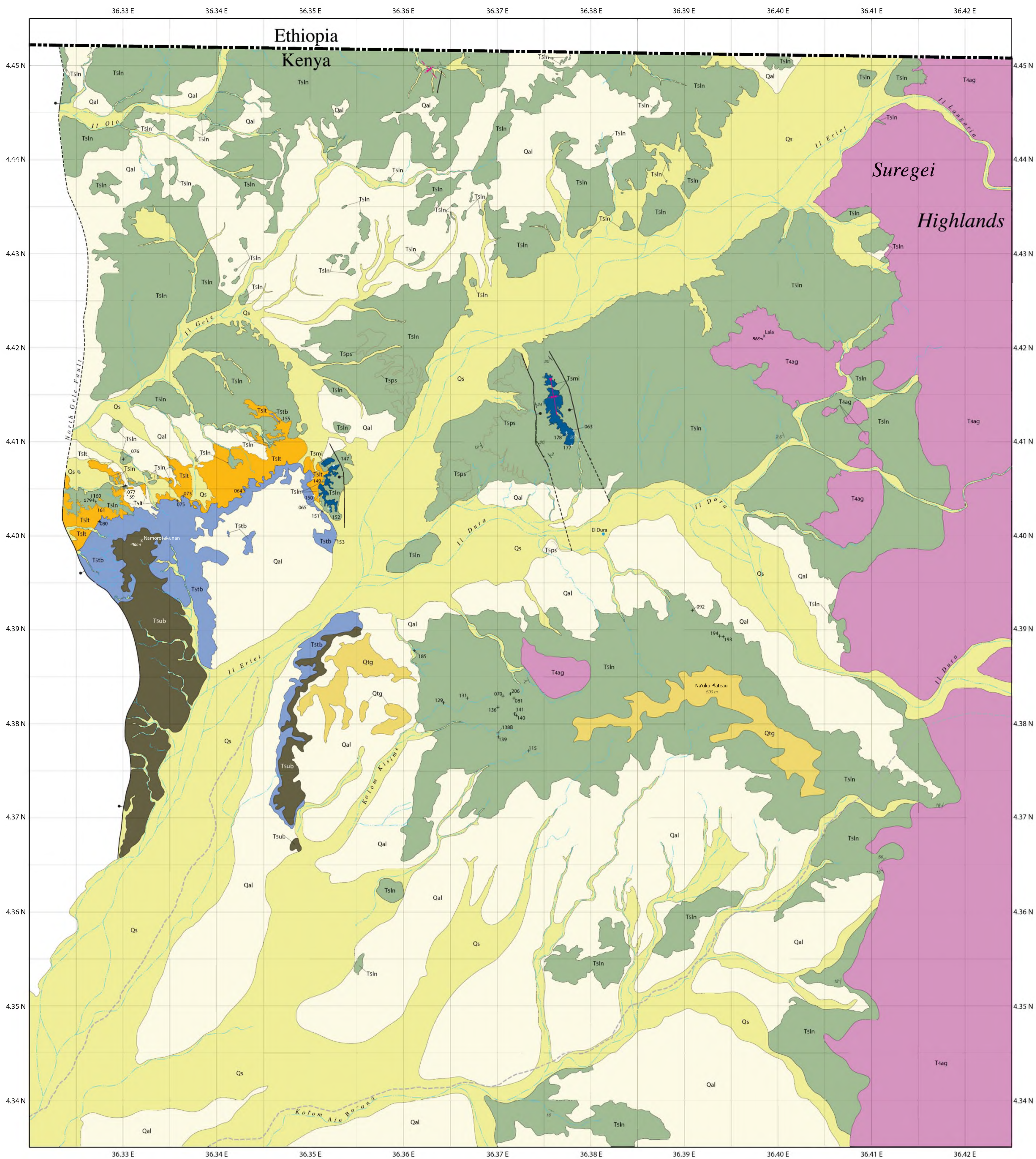
Syncline. Plunging in direction of large arrowhead. Solid where identity, existence and location is certain. Dashed where identity and existence is certain, location inferred.

Geologic contact with map-unit label. Solid where identity, existence and location is certain. Dashed where identity and existence is certain, location inferred.
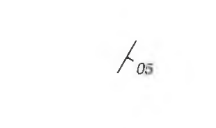
Attitude of bedding. Barb indicating dip, number indicating dip angle.

Normal fault. Barb and ball on downthrown block. Solid where identity, existence and location is certain. Dashed where identity, existence and location is certain, location inferred.

4WD Road

Ephemeral sand streams (laga in Gabra). Large streams are called Il and small streams are call Kolom in the Dasanetch language.

Sample locations. Marked by crosshair. Labeled as sample number without CLK-10- or CLK-11- prefix.

10-115

Water Well

Kenyan / Ethiopian Border

Holocene

Unstudied - Areas that were not studied in detail enough to map.

Qal Cover (Holocene) - Deposits of mainly fine- to coarse-grained sand, and eroded surficial Asille Group volcanic rocks.

Qs Stream deposits (Holocene) - Deposits of ephemeral sand streams, mainly quartz sand and eroded Asille Group volcanic rocks.

Qtg Terrace gravels - Older than Qal deposits that include large pebbles of basalt, quartz, feldspar, stone tools, minor obsidian and chalcedony.

Pliocene

T5ub upper Burgi Member(~2 Ma) - Marked by laminated claystones rich in fish bones. Strata of the upper Burgi member make up the top of Namorotukunan. Thickness: ~ 20 m.

T5tb Tulu Bor Member (Pliocene, ~2.64 - 3.43 Ma) - Includes all strata from the base of the Tulu Bor-β Tuff to the disconformity at the base of the upper Burgi member. Strata are mainly coarse to medium grained sandstones with intervals of muddy sandstones. Type locality: Area 202 and Area 204. Type thickness: 86.2 m.

T5lt Undifferentiated Lokochot/Tulu Bor Members (Pliocene, ~3.43 - 3.60 Ma) - These members are combined due to the absence of the Lokochot and Tulu Bor-α tuffs. The base of this interval is a disconformable surface which overlies the Lonyumun or Moiti members. The top is taken as the base of the Tulu Bor-β Tuff

T5mi Moiti Member (Pliocene, ~3.43 - 3.97 Ma) - Is defined by the Moiti Tuff in Areas 40 and 41. It includes the Moiti and Wargolo tuffs, in places overlain by a coarse quartzo-feldspathic sandstone. Total thickness of ~ 2–4 m. Type locality: northeastern flanks of Jarigole. Type thickness: 59.9 m.

T5ps Pseudobovaria sp. packed sandstone (Pliocene, ~4.30 Ma) - Occurs in Areas 40 and 41 where it caps strata of the middle interval of the Lonyumun Member. Pseudobovaria sp. bivalves in medium sandstone at ~ 0.2 m thick.

T5ln Lonyumun Member (Pliocene, ~3.97 - 4.49 Ma) - Strata below the Moiti Tuff or the disconformity at the top of the member. In contact with Asille Group volcanic rocks at its eastern extent. Composite thickness of ~ 120 m. Type Locality: Area 260. Type Thickness: 36.8 m.

T4ag Asille Group Volcanic Rocks (Miocene > 5.33 Ma) - Volcanic rocks of the Suregei Highlands.

References

Brown, F. H., and Feibel, C. S., 1986, Revision of lithostratigraphic nomenclature in the Koobi Fora region, Kenya: Journal of the Geological Society of London, v. 143, no. 2, p. 297–310.

Buchanan, M. J., 2010, Stratigraphic and structural geology of Area 117, Koobi Fora Region, northern Kenya [M.S. 1476646]: The University of Utah, 153 p.

Federal Geographic Data Committee (prepared for the Federal Geographic Data Committee by the U.S. Geological Survey), 2006, FGDC Digital Cartographic Standard for Geologic Map Symbolization: Reston, VA., Federal Geographic Data Committee Document Number FGDC-STD-013-2006, 290 p.

SCALE 1:25 000

1 MILE
1 KILOMETER

TRUE NORTH
MAGNETIC NORTH
1°16'
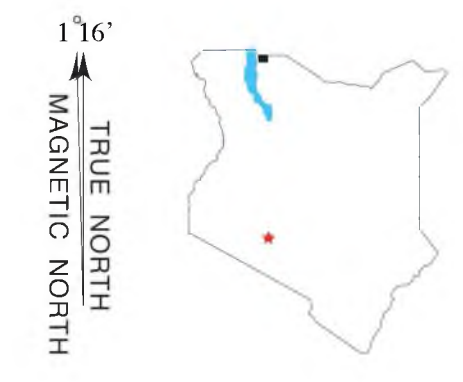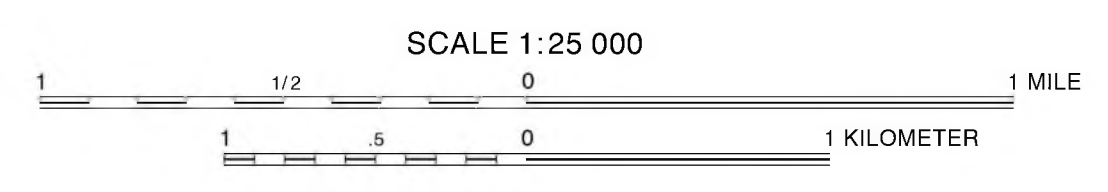
Derived from Google Earth Images obtained in 2010. Photoinspected from imagery taken in 1970 by the Hunting Survey (series HSL KEN 70).

World Geodetic System of 1984 (WGS84).

Suregei Highlands

Ethiopia
Kenya

APPENDIX B

SAMPLE LOCATIONS

Table 5. Locations of samples pertinent to this study

Sample	Type	Member/Tuff	Latitude	Longitude
CLK-10-001	Tuff	α-Tulu Bor	4.2065	36.4157
CLK-10-002	Tuff	α-Tulu Bor	4.2065	36.4157
CLK-10-003	Tuff	α-Tulu Bor	4.2102	36.4277
CLK-10-004	Tuff	α-Tulu Bor	4.2191	36.4235
CLK-10-005	Tuff	α-Tulu Bor	4.2212	36.4202
CLK-10-006	Tuff	α-Tulu Bor	4.2210	36.4199
CLK-10-009	Tuff	α-Tulu Bor	4.2121	36.4136
CLK-10-010	Tuff	α-Tulu Bor	4.2130	36.4097
CLK-10-014	Tuff	α-Tulu Bor	4.2089	36.4194
CLK-10-019	Tuff	α-Tulu Bor	4.2051	36.4017
CLK-10-020	Tuff	α-Tulu Bor	4.2006	36.3954
CLK-10-023	Tuff	α-Tulu Bor	4.1943	36.3754
CLK-10-024	Tuff	α-Tulu Bor	4.1939	36.3757
CLK-10-029	Tuff	α-Tulu Bor	4.1908	36.3718
CLK-10-039	Tuff	α-Tulu Bor	4.1940	36.3834
CLK-10-041	Tuff	α-Tulu Bor	4.1900	36.4080
CLK-10-044	Tuff	α-Tulu Bor	4.2055	36.4043
CLK-10-045	Molluscs	Lonyumun Member	4.2053	36.3832
CLK-10-046	Molluscs	Lonyumun Member	4.2053	36.3832
CLK-10-048	Tuff	β-Tulu Bor	4.1908	36.3721
CLK-10-049	Tuff	Aberegaiye	4.1921	36.3804
CLK-10-049A	Pumice	Aberegaiye	4.1921	36.3804
CLK-10-049B	Pumice	Aberegaiye	4.1921	36.3804
CLK-10-051	Tuff	α-Tulu Bor	4.1898	36.3699
CLK-10-052	Tuff	Submember D-5	4.1906	36.3647
CLK-10-053	Tuff	Submember D-5	4.1906	36.3647
CLK-10-054	Tuff	α-Tulu Bor	4.2008	36.3924
CLK-10-055	Tuff	α-Tulu Bor	4.2008	36.3924
CLK-10-056	Tuff	Kanyeris	4.2405	36.3208
CLK-10-057	Tuff	α-Tulu Bor	4.2367	36.3185
CLK-10-058	Tuff	β-Tulu Bor	4.2367	36.3185
CLK-10-059	Tuff	Tulu Bor Member	4.1964	36.4074
CLK-10-060	Tuff	Aberegaiye	4.1918	36.3803
CLK-10-060C	Pumice	Aberegaiye	4.1918	36.3803
CLK-10-061	Tuff	Aberegaiye	4.1941	36.3757
CLK-10-063	Tuff	Moiti	4.4110	36.3783
CLK-10-064	Tuff	β-Tulu Bor	4.4050	36.3430
CLK-10-065	Tuff	Moiti	4.4042	36.3509
CLK-10-070	Tuff	Guo	4.3830	36.3706

Table 5. continued

Sample	Type	Member/Tuff	Latitude	Longitude
CLK-10-073	Tuff	β-Tulu Bor	4.4043	36.3365
CLK-10-075	Tuff	Kanyeris	4.4058	36.3337
CLK-10-076	Tuff	Kanyeris	4.4082	36.3304
CLK-10-077	Tuff	Kanyeris	4.4053	36.3303
CLK-10-078	Tuff	Tukunan	4.4043	36.3269
CLK-10-079	Tuff	Kanyeris	4.4038	36.3272
CLK-10-080	Tuff	β-Tulu Bor	4.4017	36.3276
CLK-10-081	Tuff	Guo	4.3829	36.3667
CLK-10-087	Tuff	KBS	4.2110	36.4483
CLK-10-088	Tuff	KBS	4.2120	36.4483
CLK-10-089	Tuff	Okote Member	4.2210	36.4443
CLK-10-090	Pumice	Okote Member	4.2210	36.4443
CLK-10-091	Tuff	KBS	4.2213	36.4481
CLK-10-092	Tuff	Okote Member	4.2213	36.4481
CLK-10-093	Tuff	Okote Member	4.2213	36.4481
CLK-10-094	Tuff	Okote Member	4.2285	36.4458
CLK-10-096	Molluscs	–	4.2182	36.4428
CLK-10-097	Tuff	KBS	4.2092	36.4475
CLK-10-098	Tuff	α-Tulu Bor	4.2051	36.4017
CLK-10-099	Tuff	β-Tulu Bor	4.2073	36.4272
CLK-10-100	Tuff	α-Tulu Bor	4.2073	36.4272
CLK-10-101	Tuff	α-Tulu Bor	4.2094	36.4265
CLK-10-102	Tuff	Brown	4.2079	36.4366
CLK-10-103	Tuff	KBS	4.2079	36.4366
CLK-10-106	Tuff	KBS	4.2091	36.4430
CLK-10-107	Tuff	KBS	–	–
CLK-10-108	Tuff	Brown	–	–
CLK-10-109	Tuff	Okote Member	4.2070	36.4433
CLK-10-110A	Tuff	Okote Member	4.2070	36.4433
CLK-10-110B	Tuff	Okote Member	4.2070	36.4433
CLK-10-111	Tuff	Okote Member	4.2062	36.4432
CLK-10-113	Tuff	Okote Member	4.2056	36.4445
CLK-10-115	Tuff	Moiti	4.3771	36.3733
CLK-11-119	Tuff	KBS	4.2735	36.3476
CLK-11-120	Tuff	α-Tulu Bor	4.2719	36.3468
CLK-11-121	Tuff	Ninikaa	4.0292	36.3405
CLK-11-122	Tuff	Sub Ninikaa	4.0309	36.3453
CLK-11-123	Tuff	Ninikaa	4.0340	36.3448
CLK-11-124	Pumice	Ninikaa	4.0340	36.3448

Table 5. continued

Sample	Type	Member/Tuff	Latitude	Longitude
CLK-11-125	Tuff	Sub Ninikaa	4.0327	36.3441
CLK-11-126	Pumice	Sub Ninikaa	4.0327	36.3441
CLK-11-127	Tuff	Sub Ninikaa	4.0324	36.3453
CLK-11-128	Tuff	Sub Ninikaa	4.0298	36.3465
CLK-11-129	Tuff	Kanyeris	4.3824	36.3642
CLK-11-131	Tuff	Guo	4.3829	36.3667
CLK-11-136	Tuff	Guo	4.3819	36.3700
CLK-11-137A	Pumice	Guo	4.3821	36.3699
CLK-11-138A(2)	Pumice	Kisemei	4.3792	36.3700
CLK-11-138A(3)	Pumice	Kisemei	4.3792	36.3700
CLK-11-138B	Tuff	Kisemei	4.3792	36.3700
CLK-11-139	Tuff	Kisemei	4.3787	36.3700
CLK-11-140	Tuff	Kisemei	4.3811	36.3720
CLK-11-141	Tuff	Guo	4.3812	36.3718
CLK-11-149	Tuff	β-Tulu Bor	4.4064	36.3505
CLK-11-150	Tuff	β-Tulu Bor	4.4043	36.3505
CLK-11-151	Tuff	β-Tulu Bor	4.4028	36.3513
CLK-11-152	Tuff	Wargolo	4.4030	36.3520
CLK-11-153	Tuff	β-Tulu Bor	4.3998	36.3530
CLK-11-155	Tuff	β-Tulu Bor	4.4123	36.3467
CLK-11-159	Tuff	Kanyeris	4.4053	36.3303
CLK-11-160	Tuff	Tukunan	4.4043	36.3269
CLK-11-161	Tuff	Kanyeris	4.4038	36.3272
CLK-11-169	Diatomite	Lonyumun Member	4.4225	36.3609
CLK-11-173	Molluscs	Lonyumun Member	4.4132	36.3734
CLK-11-175	Molluscs	Lonyumun Member	4.4075	36.3706
CLK-11-177	Tuff	Wargolo	4.4096	36.3780
CLK-11-178	Tuff	Wargolo	4.4110	36.3774
CLK-11-179	Molluscs	Lonyumun Member	4.2053	36.3833
CLK-11-180	Ostracodite	Lonyumun Member	4.2057	36.3849
CLK-11-181	Molluscs	Lonyumun Member	4.2061	36.3838
CLK-11-182	Molluscs	–	4.1987	36.3771
CLK-11-185	Tuff	Kanyeris	4.3880	36.3611
CLK-11-187	Tuff	Kanyeris	4.3879	36.3618
CLK-11-188	Ostracodite	Lonyumun Member	4.4159	36.3374
CLK-11-191	Shells	Lonyumun Member	4.3882	36.3727
CLK-11-193	Tuff	Wargolo	4.3894	36.3940
CLK-11-194	Tuff	Wargolo	4.3895	36.3937
CLK-11-196	Tuff	Wargolo	4.3895	36.3937

Table 5. continued

Sample	Type	Member/Tuff	Latitude	Longitude
CLK-11-197	Molluscs	Lonyumun Member	4.3885	36.4014
CLK-11-198	Pumice	Moiti	4.4084	36.3522
CLK-11-206	Tuff	Kisemei	4.3834	36.3713
CLK-11-206A	Tuff	Kisemei	4.3834	36.3713
CLK-11-206B	Tuff	Kisemei	4.3834	36.3713
CLK-11-206C	Tuff	Kisemei	4.3834	36.3713

APPENDIX C

FELDSPAR 40Ar/39Ar DATING RESULTS

Table 6. Summary of $^{40}Ar/^{39}Ar$ laser fusion ages

Sample Number	Tuff	n	Arithmetic Mean Age (Ma ± lSD)	Weighted Mean Age (Ma ± ISD)	Isochron Age (Ma ± ISD)	MSWD	$^{40}Ar/^{36}Ar$	K/Ca ± ISD
CLK11-138A(3)	Kisemei	18 of 18	4.08±0.07	4.07±0.03	4.08±0.02	0.35	289.7±7.6	36.4±4.2
CLK11-138A(2)	Kisemei	14 of 14	4.03±0.10	4.05±0.02	4.01±0.03	0.75	326.7±24.1	25.4±5.2
CLK11-138A (All)	Kisemei	32 of 32	4.06±0.07	4.06±0.02	4.05±0.01	0.58	297.3±7.0	28.7±3.7
CLK10-49B	Aberegaiye	15 of 15	2.68±0.03	2.68±0.01	2.68±0.01	0.78	295.2±1.2	22.9±3.4
CLK11-060C	Aberegaiye	12 of 12	2.70±0.04	2.71±0.02	2.68±0.02	0.82	321.1±14.9	33.6±1.3
CLK11-192	Miocene Tuff	17 of 17	15.73±0.03	15.74±0.03	15.74±0.02	0.32	293.9±1.9	

Samples are single crystal sanidine feldspars from the Kisemei Tuff and Miocene Tuff, and anorthoclase feldspars from the Aberegaiye Tuff. Ages calculated relative to 28.201 Ma for the Fish Canyon sanidine (Kuiper et. al., 2008) using decay constants of Min et. al. (2001). Irradiation was done for 1 hour in the CLICIT facility, TRIGA reactor, at Oregon State University. For samples CLK10-49B, -60C, irradiation UW94, J=0.00103190 ± 0.00000062. For samples CLK11-138A(2), -138A(3), -192, irradiation UW96, J=0.00131160 ± 0.00000092. Decay constants used: λ_{40_K} = 5.463 (± 0.11) x 10^{-10} a^{-1}; $\lambda_{39_{Ar}}$ = 2.94 (± 0.03) x 10^{-7} h^{-1}; $\lambda_{37_{Ar}}$ = 8.23 (± 0.08) x 10^{-4} h^{-1}. Sample CLK11-192 was done on an altered tuff containing feldspars (4.3922 N 36.3907 E), but not used in this study.

APPENDIX D

PALEOMAGNETIC MEASUREMENTS

Table 7. Declination, inclination, and intensity data on paleomagnetic samples used in the study

Sample	Demag field (°C)	Run	Dec.	Inc.	Intensity (emu/cc)	I/I$_o$	Run	Dec.	Inc.	Intensity (emu/cc)	I/I$_o$
CLK11-PM8	0	1	11.2	-21.2	8.40E-06	1.00	2	–	–	–	–
	100	1	17.5	-28.4	5.02E-06	0.60	2	–	–	–	–
	150	1	19.3	-27.4	4.37E-06	0.52	2	–	–	–	–
	200	1	21.1	-24.1	3.75E-06	0.45	2	–	–	–	–
	250	1	17.0	-28.8	3.27E-06	0.39	2	–	–	–	–
	300	1	9.4	-24.7	2.65E-06	0.32	2	–	–	–	–
	350	1	4.1	-19.8	2.16E-06	0.26	2	–	–	–	–
	380	1	11.3	-17.6	2.26E-06	0.27	2	–	–	–	–
	400	1	–	–	–	–	2	–	–	–	–
	420	1	7.8	-39.7	2.00E-06	0.24	2	–	–	–	–
	450	1	0.3	-12.1	1.61E-06	0.19	2	–	–	–	–
	480	1	17.7	-33.8	7.54E-07	0.47	2	–	–	–	–
	500	1	195.0	-30.9	4.98E-06	0.59	2	–	–	–	–
	520	1	7.9	22.7	9.80E-07	0.12	2	–	–	–	–
	550	1	30.3	-17.4	5.78E-07	0.07	2	–	–	–	–
	580	1	9.9	60.5	1.06E-06	0.13	2	–	–	–	–
	600	1	307.4	-6.6	1.26E-06	0.15	2	–	–	–	–
	620	1	89.8	25.4	5.68E-07	0.07	2	–	–	–	–
	650	1	187.6	6.6	6.29E-07	0.07	2	–	–	–	–
	680	1	182.8	-41.4	1.17E-06	0.14	2	–	–	–	–
CLK11-PM9	0	1	28.1	-15.0	4.67E-06	1.00	2	–	–	–	–
	100	1	28.6	-18.5	2.58E-06	0.55	2	–	–	–	–
	150	1	25.2	-16.7	2.38E-06	0.51	2	–	–	–	–
	200	1	28.4	-17.4	2.14E-06	0.46	2	–	–	–	–
	250	1	23.0	-15.5	2.01E-06	0.43	2	–	–	–	–
	300	1	20.7	-20.1	1.57E-06	0.34	2	–	–	–	–
	350	1	13.3	-20.9	1.25E-06	0.27	2	–	–	–	–
	380	1	25.5	-38.5	1.37E-06	0.29	2	–	–	–	–
	400	1	–	–	–	–	2	–	–	–	–
	420	1	23.4	-17.6	1.32E-06	0.28	2	–	–	–	–
	450	1	22.2	-49.5	5.96E-07	0.13	2	–	–	–	–
	480	1	51.8	-48.3	7.03E-07	0.15	2	–	–	–	–
	500	1	26.9	16.1	1.39E-05	2.97	2	–	–	–	–
	520	1	14.0	33.3	7.46E-07	0.16	2	–	–	–	–
	550	1	359.7	4.3	7.01E-07	0.15	2	–	–	–	–
	580	1	212.7	83.3	1.54E-06	0.33	2	–	–	–	–
	600	1	200.8	-4.5	3.07E-06	0.66	2	–	–	–	–
	620	1	296.1	80.0	7.14E-07	0.15	2	–	–	–	–
	650	1	262.2	58.9	1.11E-07	0.02	2	–	–	–	–
	680	1	326.2	-15.3	2.51E-06	0.54	2	–	–	–	–
CLK11-PM10	0	1	339.4	40.4	7.17E-05	1.00	2	244.1	-15.6	5.46E-04	1.00
	100	1	334.4	40.6	5.15E-05	0.72	2	239.4	-16.5	5.00E-04	0.91
	150	1	335.0	39.1	4.31E-05	0.60	2	240.5	-13.8	4.65E-04	0.85
	200	1	342.3	36.0	3.18E-05	0.44	2	241.0	-14.2	4.03E-04	0.74
	250	1	341.4	31.1	2.67E-05	0.37	2	241.1	-15.4	3.89E-04	0.71
	300	1	345.2	23.5	1.63E-05	0.23	2	241.9	-16.8	2.71E-04	0.50
	350	1	357.4	14.3	9.60E-06	0.13	2	243.8	-18.1	2.05E-04	0.38
	380	1	5.3	7.0	8.25E-06	0.12	2	240.3	-14.6	2.09E-04	0.38
	400	1	–	–	–	–	2	–	–	–	–
	420	1	5.1	-8.2	4.52E-06	0.06	2	247.9	-22.4	1.16E-05	0.02
	450	1	3.7	-4.9	3.85E-06	0.05	2	246.6	-22.2	6.61E-06	0.01
	480	1	2.9	11.3	3.49E-06	0.05	2	313.8	4.2	2.90E-06	0.01
	500	1	328.8	-23.0	5.54E-06	0.08	2	261.5	9.8	5.19E-06	0.01
	520	1	8.7	-17.4	3.71E-06	0.05	2	246.2	15.7	3.68E-06	0.01
	550	1	350.9	-14.4	3.98E-06	0.06	2	241.5	2.5	5.04E-06	0.01
	580	1	14.3	-9.5	2.41E-06	0.03	2	274.8	-25.1	5.30E-06	0.01
	600	1	334.6	-13.5	2.70E-06	0.04	2	289.0	-11.6	8.01E-06	0.01
	620	1	17.8	9.9	9.90E-07	0.01	2	338.8	-8.7	2.09E-06	0.00
	650	1	355.8	17.6	3.72E-07	0.01	2	136.2	-49.1	2.06E-06	0.00
	680	1	263.0	67.1	5.50E-07	0.01	2	304.0	54.3	4.62E-06	0.01

Table 7. continued

Sample	Demag field (°C)	Run	Dec.	Inc.	Intensity (emu/cc)	I/I$_o$	Run	Dec.	Inc.	Intensity (emu/cc)	I/I$_o$
CLK11-PM11	0	1	244.1	-15.6	5.46E-04	1.00	2	253.3	-8.3	7.45E-05	1.00
	100	1	239.4	-16.5	5.00E-04	0.92	2	251.7	-6.4	7.03E-05	0.94
	150	1	240.5	-13.8	4.65E-04	0.85	2	251.9	-6.4	6.67E-05	0.89
	200	1	241.0	-14.2	4.03E-04	0.74	2	251.1	-8.3	6.34E-05	0.85
	250	1	241.1	-15.4	3.89E-04	0.71	2	251.4	-7.5	5.68E-05	0.76
	300	1	241.9	-16.8	2.71E-04	0.50	2	252.2	-7.1	5.40E-05	0.72
	350	1	243.8	-18.1	2.05E-04	0.38	2	254.0	-7.5	3.88E-05	0.52
	380	1	240.3	-14.6	2.09E-04	0.38	2	–	–	–	–
	400	1	–	–	–	–	2	253.0	-6.6	2.99E-05	0.40
	420	1	247.9	-22.4	1.16E-05	0.02	2	253.0	-8.5	2.14E-05	0.29
	450	1	246.6	-22.2	6.61E-06	0.01	2	249.8	-13.4	8.59E-06	0.12
	480	1	313.8	4.2	2.90E-06	0.01	2	249.9	-16.2	5.50E-06	0.07
	500	1	261.5	9.8	5.19E-06	0.01	2	–	–	–	–
	520	1	246.2	15.7	3.68E-06	0.01	2	206.1	-26.3	1.83E-06	0.02
	550	1	241.5	2.5	5.04E-06	0.01	2	142.3	-24.2	8.61E-07	0.01
	580	1	274.8	-25.1	5.30E-06	0.01	2	–	–	–	–
	600	1	289.0	-11.6	8.01E-06	0.01	2	120.6	-19.6	6.07E-07	0.01
	620	1	338.8	-8.7	2.09E-06	0.00	2	–	–	–	–
	650	1	136.2	-49.1	2.06E-06	0.00	2	–	–	–	–
	680	1	304.0	54.3	4.62E-06	0.01	2	–	–	–	–
CLK11-PM12	0	1	36.0	-9.6	1.03E-04	1.00	2	40.3	-10.6	9.46E-05	1.00
	100	1	36.8	-10.8	9.53E-05	0.93	2	44.8	-10.9	8.81E-05	0.93
	150	1	35.3	-9.3	8.80E-05	0.86	2	42.5	-10.3	8.57E-05	0.91
	200	1	35.1	-9.0	7.98E-05	0.78	2	43.9	-10.6	7.58E-05	0.80
	250	1	37.7	-8.7	7.81E-05	0.76	2	43.5	-10.8	7.00E-05	0.74
	300	1	35.7	-8.9	6.87E-05	0.67	2	44.0	-11.4	5.50E-05	0.58
	350	1	28.9	-9.7	3.88E-05	0.38	2	40.2	-11.0	5.53E-05	0.58
	380	1	15.5	-15.6	2.63E-05	0.26	2	–	–	–	–
	400	1	–	–	–	–	2	23.7	-15.9	2.26E-05	0.24
	420	1	5.8	-14.6	1.32E-05	0.13	2	–	–	–	–
	450	1	4.5	-12.3	1.23E-05	0.12	2	29.7	-13.4	2.21E-05	0.23
	480	1	10.8	-5.0	1.26E-05	0.12	2	22.4	-17.4	2.29E-05	0.24
	500	1	24.5	-19.3	1.42E-05	0.14	2	–	–	–	–
	520	1	9.5	-24.3	1.37E-05	0.13	2	9.4	-22.5	9.54E-06	0.10
	550	1	16.5	-26.4	1.43E-05	0.14	2	13.0	-13.7	1.02E-05	0.11
	580	1	14.2	-8.5	1.39E-05	0.14	2	–	–	–	–
	600	1	23.2	-26.0	5.69E-06	0.06	2	23.8	-20.2	3.36E-06	0.04
	620	1	13.7	-14.8	6.17E-06	0.06	2	–	–	–	–
	650	1	8.2	-17.7	4.72E-06	0.05	2	–	–	–	–
	680	1	351.6	-63.5	1.70E-06	0.02	2	–	–	–	–
CLK11-PM13	0	1	187.9	3.4	2.39E-04	1.00	2	181.6	6.5	1.88E-04	1.00
	100	1	185.3	2.0	2.38E-04	0.99	2	180.6	8.5	1.93E-04	1.03
	150	1	187.6	4.3	2.30E-04	0.96	2	180.5	7.9	1.92E-04	1.02
	200	1	188.6	4.2	2.06E-04	0.86	2	182.1	4.5	1.65E-04	0.88
	250	1	186.9	2.7	1.60E-04	0.67	2	183.3	7.8	1.59E-04	0.84
	300	1	187.1	3.4	1.33E-04	0.56	2	181.1	9.7	1.05E-04	0.56
	350	1	184.2	5.4	1.01E-04	0.42	2	184.3	5.5	1.05E-04	0.56
	380	1	188.8	2.0	9.88E-05	0.41	2	–	–	–	–
	400	1	–	–	–	–	2	179.8	5.7	6.83E-05	0.36
	420	1	184.2	3.6	6.27E-05	0.26	2	182.6	6.7	6.87E-05	0.37
	450	1	185.7	6.9	6.28E-05	0.26	2	181.2	7.9	5.68E-05	0.30
	480	1	181.9	5.1	6.14E-05	0.26	2	176.4	5.3	5.52E-05	0.29
	500	1	183.5	6.9	6.52E-05	0.27	2	–	–	–	–
	520	1	193.2	7.4	6.48E-05	0.27	2	180.8	4.0	4.08E-05	0.22
	550	1	190.0	2.7	7.51E-05	0.31	2	174.5	4.2	3.66E-05	0.19
	580	1	184.0	12.9	6.81E-05	0.28	2	–	–	–	–
	600	1	191.1	8.2	6.51E-05	0.27	2	173.2	4.5	3.61E-05	0.19
	620	1	184.7	9.4	5.94E-05	0.25	2	–	–	–	–
	650	1	187.2	5.6	5.98E-05	0.25	2	–	–	–	–
	680	1	186.0	2.2	5.15E-05	0.22	2	–	–	–	–

Table 7. continued

Sample	Demag field (°C)	Run	Dec.	Inc.	Intensity (emu/cc)	I/I$_o$	Run	Dec.	Inc.	Intensity (emu/cc)	I/I$_o$
CLK11-PM14	0	1	6.6	-6.0	1.99E-05	1.00	2	2.5	-5.5	3.76E-05	1.00
	100	1	5.1	-7.2	1.71E-05	0.86	2	357.4	-5.7	3.49E-05	0.93
	150	1	6.3	-7.3	1.56E-05	0.78	2	0.6	-6.9	3.44E-05	0.91
	200	1	10.0	-8.5	1.40E-05	0.71	2	0.3	-5.0	3.16E-05	0.84
	250	1	8.4	-7.4	1.26E-05	0.63	2	0.1	-7.3	3.03E-05	0.81
	300	1	7.2	-8.0	1.07E-05	0.54	2	2.4	-4.8	2.37E-05	0.63
	350	1	1.8	-9.5	6.26E-06	0.32	2	8.2	-6.8	2.35E-05	0.63
	380	1	359.5	-14.8	4.61E-06	0.23	2	–	–	–	–
	400	1	–	–	–	–	2	4.0	-8.8	1.50E-05	0.40
	420	1	345.4	-17.5	3.08E-06	0.15	2	358.6	-7.3	1.06E-05	0.28
	450	1	356.3	-13.2	2.59E-06	0.13	2	4.1	-7.3	1.11E-05	0.29
	480	1	22.4	18.7	1.76E-06	0.09	2	0.5	-6.1	7.96E-06	0.21
	500	1	23.7	9.2	2.00E-06	0.10	2	–	–	–	–
	520	1	359.5	3.8	1.94E-06	0.10	2	3.1	-6.8	7.20E-06	0.19
	550	1	24.8	4.3	1.68E-06	0.08	2	7.3	-11.4	5.05E-06	0.13
	580	1	179.1	32.5	1.96E-06	0.10	2	–	–	–	–
	600	1	10.5	45.2	8.83E-07	0.04	2	4.8	-9.1	3.17E-06	0.08
	620	1	302.4	81.4	8.07E-07	0.04	2	–	–	–	–
	650	1	155.5	43.7	5.20E-07	0.03	2	–	–	–	–
	680	1	229.7	59.0	2.30E-07	0.01	2	–	–	–	–
CLK11-PM15	0	1	190.9	-51.4	6.65E-04	1.00	2	177.7	-65.8	8.76E-04	1.00
	100	1	197.9	-40.7	7.11E-04	1.07	2	186.0	-49.9	8.38E-04	0.96
	150	1	199.4	-23.0	7.25E-04	1.09	2	190.8	-33.5	8.68E-04	0.99
	200	1	207.1	-6.0	7.27E-04	1.09	2	189.5	-30.2	8.61E-04	0.98
	250	1	200.6	-1.5	6.25E-04	0.94	2	193.3	-11.1	7.36E-04	0.84
	300	1	204.5	-2.9	4.97E-04	0.75	2	197.6	-12.5	7.15E-04	0.82
	350	1	203.4	-3.7	3.52E-04	0.53	2	191.8	-13.9	3.69E-04	0.42
	380	1	–	–	–	–	2	–	–	–	–
	400	1	204.9	6.7	1.50E-04	0.22	2	193.4	-12.5	3.27E-04	0.37
	420	1	199.2	1.6	1.33E-04	0.20	2	192.2	-9.3	2.50E-04	0.28
	450	1	201.7	6.0	1.04E-04	0.16	2	183.2	-7.2	2.24E-04	0.26
	480	1	268.0	-23.4	6.10E-05	0.09	2	186.5	-7.4	1.37E-04	0.16
	500	1	–	–	–	–	2	–	–	–	–
	520	1	200.2	3.4	8.17E-05	0.12	2	201.9	-22.6	1.97E-04	0.23
	550	1	219.4	-0.1	4.92E-05	0.07	2	–	–	–	–
	580	1	189.6	4.4	5.32E-05	0.08	2	–	–	–	–
	600	1	219.0	-16.0	2.41E-05	0.04	2	–	–	–	–
	620	1	–	–	–	–	2	–	–	–	–
	650	1	–	–	–	–	2	–	–	–	–
	680	1	–	–	–	–	2	–	–	–	–
CLK11-PM16	0	1	12.1	-35.3	5.83E-06	1.00	2	345.4	4.2	8.26E-06	1.00
	100	1	1.2	-26.0	1.04E-06	0.18	2	326.8	-4.2	1.63E-06	0.20
	150	1	129.5	-64.8	1.75E-05	3.01	2	216.1	-24.4	1.68E-06	0.20
	200	1	180.6	-7.3	2.77E-06	0.48	2	195.8	-21.0	3.38E-06	0.41
	250	1	175.7	-11.7	3.08E-06	0.53	2	200.0	-13.4	2.04E-06	0.25
	300	1	180.2	-5.1	1.31E-06	0.22	2	228.7	-6.8	2.92E-06	0.35
	350	1	154.1	-23.6	7.81E-07	0.13	2	195.7	-13.6	1.48E-06	0.18
	380	1	134.7	-64.3	2.94E-07	0.05	2	–	–	–	–
	400	1	–	–	–	–	2	237.0	-49.6	1.79E-06	0.22
	420	1	9.6	-56.7	3.74E-07	0.06	2	–	–	–	–
	450	1	112.1	-70.8	3.76E-07	0.06	2	232.4	-51.1	2.02E-06	0.24
	480	1	288.1	2.7	7.24E-07	0.12	2	244.4	-47.5	1.49E-06	0.18
	500	1	110.0	32.3	8.60E-07	0.15	2	–	–	–	–
	520	1	211.4	43.9	9.53E-07	0.16	2	214.0	-18.0	8.53E-07	0.10
	550	1	251.0	-50.9	8.04E-07	0.14	2	151.1	-55.3	1.68E-06	0.20
	580	1	133.3	29.7	7.66E-07	0.13	2	–	–	–	–
	600	1	239.4	-11.1	1.95E-06	0.33	2	111.0	-40.0	7.41E-07	0.09
	620	1	300.5	62.4	1.45E-06	0.25	2	–	–	–	–
	650	1	223.1	47.1	6.07E-07	0.10	2	–	–	–	–
	680	1	138.3	-24.9	1.34E-06	0.23	2	–	–	–	–

Table 7. continued

Sample	Demag field (°C)	Run	Dec.	Inc.	Intensity (emu/cc)	I/I$_o$	Run	Dec.	Inc.	Intensity (emu/cc)	I/I$_o$
CLK11-PM17	0	1	26.2	-31.0	4.10E-05	1.00	2	87.2	-27.2	1.97E-05	1.00
	100	1	41.5	-55.5	1.74E-05	0.42	2	136.4	-31.8	3.38E-05	1.71
	150	1	130.9	-64.4	1.77E-05	0.43	2	151.5	-28.0	4.93E-05	2.50
	200	1	165.1	-46.3	2.24E-05	0.55	2	162.8	-22.9	6.78E-05	3.44
	250	1	174.8	-38.0	2.82E-05	0.69	2	171.4	-18.0	8.68E-05	4.41
	300	1	181.1	-28.5	2.76E-05	0.67	2	174.3	-16.8	8.60E-05	4.36
	350	1	179.8	-28.0	2.39E-05	0.58	2	171.2	-16.3	9.19E-05	4.66
	380	1	179.7	-27.3	2.21E-05	0.54	2	–	–	–	–
	400	1	–	–	–	–	2	172.4	-15.4	8.12E-05	4.12
	420	1	179.1	-23.8	1.97E-05	0.48	2	–	–	–	–
	450	1	180.6	-22.9	1.98E-05	0.48	2	149.7	-8.1	6.42E-05	3.26
	480	1	184.0	-22.1	1.80E-05	0.44	2	173.6	-16.3	6.03E-05	3.06
	500	1	185.1	-17.9	1.43E-05	0.35	2	–	–	–	–
	520	1	175.4	-11.6	1.87E-05	0.46	2	170.8	-14.0	5.00E-05	2.54
	550	1	190.3	-20.1	1.52E-05	0.37	2	168.2	-18.3	4.56E-05	2.32
	580	1	179.7	-8.3	1.53E-05	0.37	2	–	–	–	–
	600	1	127.7	-26.3	1.09E-05	0.27	2	171.1	-14.4	2.28E-05	1.16
	620	1	158.3	-53.9	2.97E-06	0.07	2	–	–	–	–
	650	1	164.5	-1.1	3.00E-06	0.07	2	–	–	–	–
	680	1	9.6	55.7	1.69E-06	0.04	2	–	–	–	–
CLK11-PM18	0	1	44.2	-0.6	4.08E-06	1.00	2	351.0	1.1	8.02E-06	1.00
	100	1	162.7	18.1	4.40E-06	1.08	2	183.0	42.9	2.24E-06	0.28
	150	1	166.9	17.3	6.15E-06	1.51	2	175.5	22.4	4.27E-06	0.53
	200	1	170.0	14.8	7.03E-06	1.72	2	176.8	17.5	5.28E-06	0.66
	250	1	168.9	15.9	6.85E-06	1.68	2	171.5	15.5	5.76E-06	0.72
	300	1	174.4	12.9	5.34E-06	1.31	2	177.8	15.7	6.02E-06	0.75
	350	1	177.5	16.6	4.34E-06	1.06	2	167.6	9.1	3.32E-06	0.41
	380	1	177.8	13.3	3.16E-06	0.77	2	–	–	–	–
	400	1	–	–	–	–	2	176.5	20.9	3.61E-06	0.45
	420	1	175.6	11.3	3.41E-06	0.84	2	–	–	–	–
	450	1	149.3	65.8	2.28E-06	0.56	2	218.0	23.0	1.47E-05	1.83
	480	1	23.8	19.0	1.73E-06	0.42	2	151.9	15.7	1.76E-06	0.22
	500	1	197.2	18.9	2.07E-06	0.51	2	–	–	–	–
	520	1	223.2	20.4	3.42E-06	0.84	2	154.9	18.3	2.15E-06	0.27
	550	1	201.0	22.4	1.81E-06	0.44	2	166.4	-13.7	2.19E-06	0.27
	580	1	137.3	-12.6	4.98E-05	12.21	2	–	–	–	–
	600	1	143.4	56.1	1.95E-06	0.48	2	85.0	0.1	4.30E-06	0.54
	620	1	124.4	30.7	1.87E-06	0.46	2	–	–	–	–
	650	1	118.3	73.0	1.21E-06	0.30	2	–	–	–	–
	680	1	225.7	0.4	4.37E-07	0.11	2	–	–	–	–
CLK11-PM19	0	1	201.5	-69.5	6.15E-06	1.00	2	143.5	-46.2	8.57E-06	1.00
	100	1	170.2	-9.2	1.17E-05	1.90	2	161.4	-18.7	1.38E-05	1.61
	150	1	168.5	-2.8	1.31E-05	2.14	2	163.8	-18.2	1.39E-05	1.62
	200	1	168.3	1.4	1.36E-05	2.21	2	163.2	-15.2	1.52E-05	1.77
	250	1	167.6	0.8	1.25E-05	2.04	2	162.9	-14.9	1.42E-05	1.66
	300	1	173.0	2.8	9.17E-06	1.49	2	164.1	-12.1	1.35E-05	1.57
	350	1	177.1	-3.3	1.21E-05	1.97	2	172.0	-15.5	1.17E-05	1.37
	380	1	184.7	-2.0	8.32E-06	1.35	2	–	–	–	–
	400	1	–	–	–	–	2	165.1	-14.5	1.16E-05	1.35
	420	1	169.8	-2.1	6.80E-06	1.11	2	163.6	-13.7	9.60E-06	1.12
	450	1	156.2	11.0	9.12E-06	1.48	2	164.7	-12.0	8.66E-06	1.01
	480	1	179.0	16.5	5.61E-06	0.91	2	165.2	-13.2	9.23E-06	1.08
	500	1	164.4	3.1	6.56E-06	1.07	2	–	–	–	–
	520	1	200.0	5.8	5.10E-06	0.83	2	171.2	-16.4	9.31E-06	1.09
	550	1	170.7	15.3	3.93E-06	0.64	2	163.7	-12.9	7.30E-06	0.85
	580	1	174.1	0.7	4.84E-06	0.79	2	–	–	–	–
	600	1	163.7	13.7	5.06E-06	0.82	2	185.9	-43.9	6.90E-06	0.80
	620	1	179.2	11.1	4.31E-06	0.70	2	–	–	–	–
	650	1	38.5	21.8	1.84E-05	3.00	2	182.7	-6.4	6.86E-06	0.80
	680	1	204.6	-16.7	1.45E-05	2.35	2	–	–	–	–

Table 7. continued

Sample	Demag field (°C)	Run	Dec.	Inc.	Intensity (emu/cc)	I/I$_o$	Run	Dec.	Inc.	Intensity (emu/cc)	I/I$_o$
CLK11-PM20	0	1	352.9	-23.0	1.12E-05	1.00	2	349.2	14.9	1.32E-05	1.00
	100	1	347.4	-36.6	2.52E-06	0.22	2	339.1	5.8	3.19E-06	0.24
	150	1	323.5	-43.7	1.36E-06	0.12	2	306.1	12.4	1.34E-06	0.10
	200	1	277.7	-47.3	6.80E-07	0.06	2	217.3	10.7	9.42E-07	0.07
	250	1	289.2	-8.4	4.90E-07	0.04	2	237.5	-2.4	8.59E-07	0.07
	300	1	305.4	-14.6	9.95E-07	0.09	2	243.2	19.9	1.29E-06	0.10
	350	1	245.4	-31.3	2.25E-06	0.20	2	260.5	24.9	1.15E-06	0.09
	380	1	346.1	-11.5	8.38E-07	0.07	2	–	–	–	–
	400	1	–	–	–	–	2	268.5	19.8	8.94E-07	0.07
	420	1	354.2	10.6	2.84E-06	0.25	2	–	–	–	–
	450	1	278.6	-63.6	1.94E-06	0.17	2	232.3	-25.7	3.77E-06	0.29
	480	1	217.4	-46.0	6.48E-06	0.58	2	282.5	-31.5	6.73E-06	0.51
	500	1	140.3	-30.8	7.37E-06	0.66	2	–	–	–	–
	520	1	28.6	-22.0	1.08E-05	0.96	2	23.4	26.4	2.96E-07	0.02
	550	1	266.3	-34.2	5.03E-06	0.45	2	27.4	21.8	1.77E-05	1.35
	580	1	–	–	–	–	2	–	–	–	–
	600	1	75.3	-9.3	1.68E-06	0.15	2	56.1	-51.4	1.85E-05	1.40
	620	1	–	–	–	–	2	–	–	–	–
	650	1	297.1	-6.4	2.46E-06	0.22	2	–	–	–	–
	680	1	–	–	–	–	2	–	–	–	–
CLK11-PM21	0	1	0.5	-5.3	5.91E-06	1.00	2	9.6	9.7	3.85E-06	1.00
	100	1	31.1	4.9	1.80E-06	0.30	2	9.4	-2.6	1.50E-06	0.39
	150	1	81.3	7.2	9.99E-07	0.17	2	165.7	-25.0	6.76E-07	0.18
	200	1	114.6	11.1	1.05E-06	0.18	2	183.3	-37.3	1.24E-06	0.32
	250	1	104.9	19.8	6.30E-07	0.11	2	160.2	-26.6	8.98E-07	0.23
	300	1	91.0	-10.3	3.74E-07	0.06	2	143.0	-13.3	1.07E-06	0.28
	350	1	74.3	0.6	9.79E-07	0.17	2	243.8	-12.7	4.05E-07	0.11
	380	1	65.9	-32.0	1.20E-06	0.20	2	–	–	–	–
	400	1	–	–	–	–	2	156.3	-69.7	3.13E-07	0.08
	420	1	71.8	22.2	8.53E-07	0.14	2	–	–	–	–
	450	1	24.9	-3.9	2.95E-06	0.50	2	211.0	-53.6	9.67E-07	0.25
	480	1	163.4	27.1	2.77E-06	0.47	2	61.0	27.3	2.19E-06	0.57
	500	1	13.5	-5.9	1.63E-06	0.28	2	–	–	–	–
	520	1	169.7	1.6	7.63E-06	1.29	2	316.6	-27.3	6.94E-07	0.18
	550	1	21.9	15.7	8.63E-07	0.15	2	145.2	-44.7	3.21E-06	0.83
	580	1	315.8	-9.7	1.70E-06	0.29	2	–	–	–	–
	600	1	178.3	-8.0	1.09E-05	1.83	2	154.3	-47.9	2.84E-06	0.74
	620	1	247.4	48.6	8.13E-07	0.14	2	–	–	–	–
	650	1	243.1	-11.2	6.95E-06	1.18	2	–	–	–	–
	680	1	105.7	-7.2	1.31E-06	0.22	2	–	–	–	–
CLK11-PM22	0	1	340.8	2.0	3.79E-05	1.00	2	352.4	8.7	3.64E-05	1.00
	100	1	347.1	3.8	2.41E-05	0.63	2	354.4	5.3	2.55E-05	0.70
	150	1	348.6	5.2	1.59E-05	0.42	2	351.9	5.4	2.37E-05	0.65
	200	1	348.4	4.0	1.09E-05	0.29	2	347.9	5.1	1.20E-05	0.33
	250	1	346.2	3.8	8.17E-06	0.22	2	346.8	3.4	1.04E-05	0.28
	300	1	351.2	16.0	7.17E-06	0.19	2	348.7	5.5	9.32E-06	0.26
	350	1	347.2	2.0	5.63E-06	0.15	2	4.5	21.9	8.63E-06	0.24
	380	1	6.4	-13.9	5.66E-06	0.15	2	–	–	–	–
	400	1	–	–	–	–	2	6.9	8.9	3.91E-06	0.11
	420	1	11.4	-5.4	3.60E-06	0.09	2	–	–	–	–
	450	1	340.0	-19.8	1.34E-05	0.35	2	275.6	3.9	1.51E-05	0.41
	480	1	263.4	48.6	1.42E-05	0.37	2	352.8	-2.7	6.29E-06	0.17
	500	1	66.0	-7.4	1.14E-05	0.30	2	–	–	–	–
	520	1	106.2	-4.7	7.46E-05	1.97	2	25.4	11.7	4.00E-06	0.11
	550	1	22.8	-4.7	1.23E-05	0.33	2	345.6	-12.8	1.06E-05	0.29
	580	1	346.4	-18.6	6.88E-06	0.18	2	–	–	–	–
	600	1	329.7	-23.8	6.90E-05	1.82	2	167.4	-45.3	3.08E-05	0.85
	620	1	359.1	6.4	2.03E-05	0.54	2	–	–	–	–
	650	1	139.1	-74.3	2.36E-05	0.62	2	–	–	–	–
	680	1	208.1	-42.6	1.43E-05	0.38	2	–	–	–	–

Table 7. continued

Sample	Demag field (°C)	Run	Dec.	Inc.	Intensity (emu/cc)	I/I$_o$	Run	Dec.	Inc.	Intensity (emu/cc)	I/I$_o$
CLK11-PM23	0	1	197.1	2.2	1.61E-05	1.00	2	192.2	-11.8	1.91E-05	1.00
	100	1	194.5	-11.1	2.60E-05	1.62	2	193.3	-5.9	2.51E-05	1.32
	150	1	192.2	-12.1	2.75E-05	1.71	2	191.5	-4.9	2.67E-05	1.40
	200	1	192.0	-10.4	2.78E-05	1.73	2	193.4	-4.7	2.73E-05	1.43
	250	1	192.3	-11.4	2.21E-05	1.37	2	192.0	-7.1	2.50E-05	1.31
	300	1	190.3	-9.2	1.73E-05	1.08	2	188.8	-5.9	2.48E-05	1.30
	350	1	189.9	-13.4	1.54E-05	0.96	2	191.5	-11.9	1.87E-05	0.98
	380	1	203.1	-21.8	1.46E-05	0.91	2	–	–	–	–
	400	1	–	–	–	–	2	186.1	-5.2	2.00E-05	1.05
	420	1	184.4	-14.7	9.22E-06	0.57	2	198.8	-7.1	2.04E-05	1.07
	450	1	200.4	0.1	1.18E-05	0.73	2	192.5	-6.4	1.73E-05	0.91
	480	1	171.9	-15.0	9.77E-06	0.61	2	189.5	-4.9	1.63E-05	0.86
	500	1	188.5	-3.3	1.03E-05	0.64	2	–	–	–	–
	520	1	144.5	-30.4	5.89E-06	0.37	2	195.5	-3.8	1.08E-05	0.57
	550	1	194.4	-5.8	1.10E-05	0.68	2	195.6	-4.9	1.17E-05	0.62
	580	1	196.5	-11.8	9.40E-06	0.58	2	–	–	–	–
	600	1	183.4	0.9	5.45E-05	3.39	2	194.7	-7.7	7.02E-06	0.37
	620	1	172.6	-2.5	9.59E-06	0.60	2	–	–	–	–
	650	1	102.6	-74.1	3.52E-05	2.19	2	–	–	–	–
	680	1	316.9	-19.7	2.61E-05	1.62	2	–	–	–	–
CLK11-PM24	0	1	165.7	7.1	1.80E-04	1.00	2	150.1	15.1	2.05E-04	1.00
	100	1	171.3	4.4	2.02E-04	1.12	2	157.5	7.7	2.22E-04	1.08
	150	1	172.3	1.8	2.22E-04	1.23	2	161.1	7.0	2.39E-04	1.16
	200	1	177.2	-4.0	2.33E-04	1.30	2	162.0	5.5	2.48E-04	1.21
	250	1	167.2	-4.4	1.85E-04	1.03	2	161.3	5.3	2.22E-04	1.08
	300	1	184.9	-5.3	1.80E-04	1.00	2	160.8	4.4	1.99E-04	0.97
	350	1	176.3	-8.6	1.72E-04	0.96	2	165.1	4.2	1.74E-04	0.85
	380	1	179.8	-13.8	1.25E-04	0.69	2	–	–	–	–
	400	1	–	–	–	–	2	164.9	1.8	1.51E-04	0.73
	420	1	181.0	-8.1	1.11E-04	0.62	2	170.1	1.5	1.49E-04	0.73
	450	1	180.5	-13.9	1.02E-04	0.57	2	167.7	-0.2	1.18E-04	0.58
	480	1	176.3	-11.4	1.16E-04	0.65	2	169.2	-1.9	1.16E-04	0.57
	500	1	151.9	-5.7	1.14E-04	0.63	2	–	–	–	–
	520	1	150.4	-1.6	1.28E-04	0.71	2	168.4	1.9	1.19E-04	0.58
	550	1	171.6	-7.2	1.24E-04	0.69	2	175.0	-0.6	1.20E-04	0.58
	580	1	169.2	-4.3	1.07E-04	0.60	2	–	–	–	–
	600	1	190.2	-8.3	8.91E-05	0.49	2	172.7	3.3	1.06E-04	0.52
	620	1	176.8	-7.8	1.17E-04	0.65	2	–	–	–	–
	650	1	240.4	33.0	2.24E-04	1.24	2	–	–	–	–
	680	1	123.1	-22.8	1.32E-04	0.73	2	–	–	–	–
CLK11-PM25	0	1	192.3	69.0	5.29E-04	1.00	2	138.3	46.6	8.39E-05	1.00
	100	1	177.8	54.2	4.92E-04	0.93	2	160.8	35.6	1.04E-04	1.24
	150	1	172.8	34.5	5.04E-04	0.95	2	172.5	20.2	1.59E-04	1.90
	200	1	174.4	24.8	4.93E-04	0.93	2	179.1	8.1	2.96E-04	3.53
	250	1	169.6	26.8	3.30E-04	0.62	2	181.8	7.3	2.97E-04	3.54
	300	1	176.4	22.6	2.10E-04	0.40	2	178.3	7.0	1.75E-04	2.09
	350	1	180.3	18.9	1.30E-04	0.25	2	175.1	5.8	1.80E-04	2.14
	380	1	184.9	25.2	7.92E-05	0.15	2	–	–	–	–
	400	1	–	–	–	–	2	168.8	1.6	7.80E-05	0.93
	420	1	177.6	11.2	5.75E-05	0.11	2	161.1	0.2	7.98E-05	0.95
	450	1	162.2	43.2	8.13E-05	0.15	2	201.4	-4.1	4.40E-05	0.52
	480	1	181.8	-6.7	8.00E-05	0.15	2	163.5	-13.2	2.24E-05	0.27
	500	1	199.4	17.5	3.77E-05	0.07	2	–	–	–	–
	520	1	249.8	4.6	8.85E-05	0.17	2	176.4	-15.0	3.60E-05	0.43
	550	1	338.4	2.9	6.71E-05	0.13	2	197.3	-27.8	3.11E-05	0.37
	580	1	151.4	4.2	1.21E-04	0.23	2	–	–	–	–
	600	1	54.8	-17.1	5.19E-05	0.10	2	237.8	-67.3	2.27E-05	0.27
	620	1	339.8	-67.6	6.90E-05	0.13	2	–	–	–	–
	650	1	150.1	3.6	5.05E-05	0.10	2	–	–	–	–
	680	1	335.8	-35.7	2.84E-05	0.05	2	–	–	–	–

Table 7. continued

Sample	Demag field (°C)	Run	Dec.	Inc.	Intensity (emu/cc)	I/I_o	Run	Dec.	Inc.	Intensity (emu/cc)	I/I_o
CLK11-PM26	0	1	10.4	-3.3	7.18E-04	1.00	2	350.2	9.7	8.83E-04	1.00
	100	1	11.2	-7.4	4.84E-04	0.67	2	347.6	19.6	3.86E-04	0.44
	150	1	38.6	1.5	1.69E-04	0.24	2	348.5	27.9	2.48E-04	0.28
	200	1	135.6	12.8	1.63E-04	0.23	2	178.0	14.0	2.32E-04	0.26
	250	1	153.9	6.0	1.48E-04	0.21	2	179.8	6.9	2.32E-04	0.26
	300	1	153.4	-1.1	1.45E-04	0.20	2	181.4	4.5	2.14E-04	0.24
	350	1	145.3	6.8	1.14E-04	0.16	2	179.8	9.4	2.09E-04	0.24
	380	1	161.3	4.8	1.04E-04	0.14	2	–	–	–	–
	400	1	–	–	–	–	2	176.1	1.6	2.01E-04	0.23
	420	1	164.7	18.1	7.44E-05	0.10	2	–	–	–	–
	450	1	138.2	11.2	1.02E-04	0.14	2	178.1	-17.2	2.05E-04	0.23
	480	1	188.8	67.0	1.23E-04	0.17	2	183.6	-39.2	1.28E-04	0.15
	500	1	192.7	56.1	1.41E-04	0.20	2	–	–	–	–
	520	1	242.9	17.3	5.24E-05	0.07	2	186.3	-2.1	6.66E-05	0.08
	550	1	197.9	-12.4	1.22E-04	0.17	2	158.2	-24.3	1.20E-04	0.14
	580	1	181.1	23.1	8.18E-05	0.11	2	–	–	–	–
	600	1	165.5	-50.9	6.68E-05	0.09	2	123.2	-15.7	2.86E-05	0.03
	620	1	165.5	17.6	1.58E-04	0.22	2	–	–	–	–
	650	1	110.6	9.8	6.62E-05	0.09	2	–	–	–	–
	680	1	155.0	-9.6	9.32E-05	0.13	2	–	–	–	–
CLK11-PM27	0	1	14.6	-18.0	6.84E-04	1.00	2	1.1	-7.9	5.28E-04	1.00
	100	1	17.8	-13.2	5.54E-04	0.81	2	3.1	-8.9	4.15E-04	0.79
	150	1	20.6	-20.2	3.04E-04	0.44	2	334.2	-17.9	5.99E-05	0.11
	200	1	79.8	-55.5	7.54E-05	0.11	2	218.2	-13.5	2.78E-05	0.05
	250	1	173.5	-24.7	1.17E-04	0.17	2	193.4	-0.7	6.46E-05	0.12
	300	1	179.8	-18.2	1.06E-04	0.15	2	197.4	-9.2	1.48E-04	0.28
	350	1	177.3	-16.6	1.18E-04	0.17	2	208.5	1.8	1.53E-04	0.29
	380	1	172.7	-20.2	9.98E-05	0.15	2	–	–	–	–
	400	1	–	–	–	–	2	204.2	-7.7	9.33E-05	0.18
	420	1	180.5	-19.5	8.91E-05	0.13	2	–	–	–	–
	450	1	205.4	-7.3	7.68E-05	0.11	2	184.9	3.9	2.24E-04	0.42
	480	1	178.6	27.0	7.09E-05	0.10	2	157.4	-6.4	9.64E-05	0.18
	500	1	145.4	-45.6	1.26E-04	0.18	2	–	–	–	–
	520	1	158.1	-59.3	7.32E-05	0.11	2	185.7	-2.9	4.13E-05	0.08
	550	1	183.7	-28.3	1.97E-04	0.29	2	174.6	-10.8	6.36E-05	0.12
	580	1	154.8	-47.2	1.17E-04	0.17	2	–	–	–	–
	600	1	164.3	5.0	1.76E-04	0.26	2	164.2	-20.4	8.74E-05	0.17
	620	1	49.3	-63.8	2.00E-04	0.29	2	–	–	–	–
	650	1	154.4	-20.8	9.31E-05	0.14	2	–	–	–	–
	680	1	143.2	-24.7	1.23E-04	0.18	2	–	–	–	–
CLK11-PM28	0	1	169.1	-10.1	3.04E-04	1.00	2	50.2	-63.2	3.94E-05	1.00
	100	1	167.0	-8.3	3.18E-04	1.05	2	149.1	-51.8	3.37E-05	0.86
	150	1	169.2	-4.3	3.18E-04	1.05	2	167.0	-30.4	4.32E-05	1.10
	200	1	166.1	-8.4	2.97E-04	0.98	2	174.1	-16.5	5.95E-05	1.51
	250	1	172.8	-8.0	2.68E-04	0.88	2	174.6	-12.8	6.09E-05	1.54
	300	1	171.4	-7.4	2.61E-04	0.86	2	172.3	-12.5	5.50E-05	1.39
	350	1	166.3	-7.5	2.42E-04	0.80	2	175.2	-10.5	5.62E-05	1.42
	380	1	169.4	-7.5	1.97E-04	0.65	2	–	–	–	–
	400	1	–	–	–	–	2	176.5	-8.7	5.67E-05	1.44
	420	1	169.5	-7.6	2.11E-04	0.69	2	174.8	-9.0	5.43E-05	1.38
	450	1	170.2	-8.9	1.80E-04	0.59	2	176.9	-5.9	5.71E-05	1.45
	480	1	168.7	-3.8	1.82E-04	0.60	2	175.1	-5.9	5.83E-05	1.48
	500	1	173.3	-10.4	1.34E-04	0.44	2	–	–	–	–
	520	1	169.7	-8.1	1.02E-04	0.34	2	176.4	-5.9	5.54E-05	1.41
	550	1	168.2	-6.2	8.17E-06	0.03	2	176.5	-2.6	3.18E-05	0.81
	580	1	–	–	–	–	2	–	–	–	–
	600	1	–	–	–	–	2	159.4	-6.1	1.28E-05	0.33
	620	1	–	–	–	–	2	–	–	–	–
	650	1	–	–	–	–	2	150.1	4.2	1.64E-05	0.42
	680	1	–	–	–	–	2	–	–	–	–

Table 7. continued

Sample	Demag field (°C)	Run	Dec.	Inc.	Intensity (emu/cc)	I/I$_o$	Run	Dec.	Inc.	Intensity (emu/cc)	I/I$_o$
CLK11-PM29	0	1	194.1	2.0	2.64E-05	1.00	2	358.1	-19.3	5.09E-05	1.00
	100	1	195.8	2.2	2.92E-05	1.11	2	356.7	-22.3	4.84E-05	0.95
	150	1	193.7	1.9	2.96E-05	1.12	2	356.7	-22.6	4.67E-05	0.92
	200	1	194.7	3.2	2.88E-05	1.09	2	356.8	-20.9	4.22E-05	0.83
	250	1	192.1	1.0	2.57E-05	0.97	2	356.9	-20.4	3.93E-05	0.77
	300	1	194.3	0.8	2.42E-05	0.92	2	358.1	-21.7	2.90E-05	0.57
	350	1	192.5	1.5	2.09E-05	0.79	2	0.8	-20.0	2.93E-05	0.58
	380	1	195.1	1.0	1.96E-05	0.74	2	–	–	–	–
	400	1	–	–	–	–	2	358.4	-23.1	2.17E-05	0.43
	420	1	189.7	3.0	1.80E-05	0.68	2	359.7	-23.6	2.17E-05	0.43
	450	1	191.1	-1.7	1.61E-05	0.61	2	353.2	-13.7	1.32E-05	0.26
	480	1	192.1	1.3	1.67E-05	0.63	2	358.9	-24.1	1.56E-05	0.31
	500	1	192.2	2.1	1.44E-05	0.54	2	–	–	–	–
	520	1	192.8	0.9	1.28E-05	0.48	2	359.0	-26.1	9.83E-06	0.19
	550	1	197.6	0.5	9.45E-06	0.36	2	2.5	-31.1	6.66E-06	0.13
	580	1	–	–	–	–	2	–	–	–	–
	600	1	198.9	2.4	5.06E-06	0.19	2	5.6	-53.1	5.93E-07	0.01
	620	1	–	–	–	–	2	–	–	–	–
	650	1	–	–	–	–	2	–	–	–	–
	680	1	–	–	–	–	2	–	–	–	–
CLK11-PM30	0	1	198.9	12.8	9.62E-04	1.00	2	201.8	25.6	4.22E-04	1.00
	100	1	188.5	10.5	9.41E-04	0.98	2	196.0	18.9	4.66E-04	1.10
	150	1	182.1	5.2	1.04E-03	1.08	2	186.1	5.8	6.63E-04	1.57
	200	1	178.6	4.1	1.10E-03	1.15	2	185.2	8.0	6.81E-04	1.61
	250	1	179.6	4.1	9.02E-04	0.94	2	182.2	1.8	7.11E-04	1.68
	300	1	178.5	3.5	6.92E-04	0.72	2	179.1	1.7	6.93E-04	1.64
	350	1	174.3	2.9	4.52E-04	0.47	2	185.7	-0.9	4.38E-04	1.04
	380	1	169.6	0.8	2.99E-04	0.31	2	–	–	–	–
	400	1	–	–	–	–	2	181.6	0.5	4.39E-04	1.04
	420	1	167.8	5.0	2.65E-04	0.28	2	176.6	7.5	4.14E-04	0.98
	450	1	182.5	-50.0	2.29E-04	0.24	2	179.0	-4.3	1.86E-04	0.44
	480	1	163.3	1.4	1.96E-04	0.20	2	163.1	-4.8	1.86E-04	0.44
	500	1	159.3	3.8	1.74E-04	0.18	2	–	–	–	–
	520	1	167.2	-2.0	1.99E-04	0.21	2	161.2	-1.1	1.64E-04	0.39
	550	1	181.9	-2.6	1.24E-04	0.13	2	186.3	-7.0	1.16E-04	0.27
	580	1	–	–	–	–	2	–	–	–	–
	600	1	175.9	8.0	1.05E-04	0.11	2	189.4	-1.8	9.78E-05	0.23
	620	1	–	–	–	–	2	–	–	–	–
	650	1	–	–	–	–	2	–	–	–	–
	680	1	–	–	–	–	2	–	–	–	–
CLK11-PM31	0	1	347.3	64.0	8.04E-04	1.00	2	345.5	18.5	2.23E-04	1.00
	100	1	338.0	62.6	5.80E-04	0.72	2	336.2	15.1	1.44E-04	0.65
	150	1	329.4	70.5	4.53E-04	0.56	2	189.5	-11.0	1.21E-04	0.54
	200	1	275.6	76.3	3.32E-04	0.41	2	195.6	-12.6	1.25E-04	0.56
	250	1	246.0	72.0	2.59E-04	0.32	2	185.3	-12.2	1.87E-04	0.84
	300	1	254.8	65.0	2.11E-04	0.26	2	181.0	-13.4	2.15E-04	0.96
	350	1	249.7	67.1	1.79E-04	0.22	2	181.4	-22.4	1.02E-04	0.46
	380	1	240.7	60.2	1.30E-04	0.16	2	–	–	–	–
	400	1	–	–	–	–	2	176.5	-25.9	1.20E-04	0.54
	420	1	272.5	63.8	1.26E-04	0.16	2	–	–	–	–
	450	1	230.7	-31.4	1.05E-04	0.13	2	189.9	-43.4	1.05E-04	0.47
	480	1	214.6	23.8	4.84E-05	0.06	2	204.7	-35.5	1.32E-04	0.59
	500	1	256.3	-4.6	2.06E-05	0.03	2	–	–	–	–
	520	1	191.9	17.1	6.26E-05	0.08	2	183.9	-25.7	7.45E-05	0.33
	550	1	195.5	-5.2	4.32E-05	0.05	2	233.8	-74.7	2.63E-05	0.12
	580	1	–	–	–	–	2	–	–	–	–
	600	1	106.0	38.8	3.02E-05	0.04	2	320.3	34.6	1.67E-05	0.07
	620	1	–	–	–	–	2	–	–	–	–
	650	1	348.9	6.1	2.90E-05	0.04	2	–	–	–	–
	680	1	–	–	–	–	2	–	–	–	–

Table 7. continued

Sample	Demag field (°C)	Run	Dec.	Inc.	Intensity (emu/cc)	I/I$_o$	Run	Dec.	Inc.	Intensity (emu/cc)	I/I$_o$
CLK11-PM32	0	1	320.6	41.8	8.25E-05	1.00	2	330.7	22.9	9.44E-05	1.00
	100	1	310.1	54.9	5.43E-05	0.66	2	325.9	25.2	6.14E-05	0.65
	150	1	306.3	57.8	4.38E-05	0.53	2	305.6	31.5	4.06E-05	0.43
	200	1	259.2	52.1	3.14E-05	0.38	2	276.5	28.4	2.67E-05	0.28
	250	1	240.0	37.9	2.75E-05	0.33	2	251.5	21.9	2.64E-05	0.28
	300	1	219.5	23.1	2.33E-05	0.28	2	258.9	24.3	2.59E-05	0.27
	350	1	236.8	35.5	1.91E-05	0.23	2	261.3	33.0	2.10E-05	0.22
	380	1	229.4	22.8	2.04E-05	0.25	2	–	–	–	–
	400	1	–	–	–	–	2	275.5	15.6	1.97E-05	0.21
	420	1	228.5	31.2	1.88E-05	0.23	2	–	–	–	–
	450	1	141.7	-26.5	1.71E-05	0.21	2	217.2	-41.4	1.31E-05	0.14
	480	1	225.5	-10.5	7.98E-06	0.10	2	227.9	-53.5	1.06E-05	0.11
	500	1	283.5	-39.6	1.21E-05	0.15	2	–	–	–	–
	520	1	181.2	-51.2	1.19E-05	0.14	2	276.7	39.9	4.10E-06	0.04
	550	1	197.8	-34.3	1.76E-05	0.21	2	153.5	-58.9	2.54E-05	0.27
	580	1	–	–	–	–	2				
	600	1	219.2	-9.8	7.88E-06	0.10	2	192.9	-38.7	2.86E-06	0.03
	620	1	–	–	–	–	2				
	650	1	168.6	-30.2	5.35E-05	0.65	2	–	–	–	–
	680	1	–	–	–	–	2	–	–	–	–
CLK11-PM33	0	1	267.1	26.1	1.17E-03	1.00	2	264.7	23.1	1.32E-03	1.00
	100	1	256.1	24.5	1.04E-03	0.89	2	247.0	21.4	1.15E-03	0.87
	150	1	257.1	25.7	9.85E-04	0.84	2	232.3	18.4	9.29E-04	0.70
	200	1	248.5	23.1	8.93E-04	0.76	2	223.4	15.3	8.51E-04	0.64
	250	1	239.6	23.1	8.35E-04	0.71	2	210.9	9.8	6.98E-04	0.53
	300	1	229.0	15.2	7.25E-04	0.62	2	216.5	7.9	5.35E-04	0.40
	350	1	222.7	12.9	6.36E-04	0.54	2	209.6	0.4	3.08E-04	0.23
	380	1	220.9	2.1	1.51E-04	0.13	2	–	–	–	–
	400	1	–	–	–	–	2	204.8	-1.0	2.46E-04	0.19
	420	1	206.7	-3.3	1.13E-04	0.10	2	–	–	–	–
	450	1	225.9	-55.2	9.56E-05	0.08	2	208.5	1.7	1.38E-04	0.10
	480	1	222.5	-15.8	6.24E-05	0.05	2	194.3	-13.5	1.83E-04	0.14
	500	1	212.3	-16.5	6.51E-05	0.06	2	–	–	–	–
	520	1	212.7	-16.5	7.58E-05	0.06	2	215.2	-4.7	8.51E-05	0.06
	550	1	255.1	-70.7	1.81E-05	0.02	2	147.9	3.3	1.06E-04	0.08
	580	1	–	–	–	–	2				
	600	1	156.6	-8.1	3.01E-05	0.03	2	218.6	11.1	1.38E-04	0.10
	620	1	–	–	–	–	2				
	650	1	90.3	-2.4	7.00E-05	0.06	2	–	–	–	–
	680	1	–	–	–	–	2	–	–	–	–
CLK11-PM34	0	1	328.2	22.2	4.31E-05	1.00	2	–	–	–	–
	100	1	309.5	17.3	2.00E-05	0.46	2	–	–	–	–
	150	1	265.4	18.6	1.53E-05	0.35	2	–	–	–	–
	200	1	259.5	12.9	1.18E-05	0.27	2	–	–	–	–
	250	1	249.7	-1.4	1.42E-05	0.33	2	–	–	–	–
	300	1	267.4	-0.9	1.14E-05	0.27	2	–	–	–	–
	350	1	252.0	2.1	8.64E-06	0.20	2	–	–	–	–
	380	1	264.9	3.9	1.26E-05	0.29	2	–	–	–	–
	400	1	–	–	–	–	2	–	–	–	–
	420	1	262.6	-2.4	1.06E-05	0.25	2	–	–	–	–
	450	1	267.1	5.3	1.06E-05	0.25	2	–	–	–	–
	480	1	240.3	0.0	5.23E-06	0.12	2	–	–	–	–
	500	1	–	–	–	–	2	–	–	–	–
	520	1	145.4	-12.0	6.84E-06	0.16	2	–	–	–	–
	550	1	201.0	-49.4	5.59E-06	0.13	2	–	–	–	–
	580	1	222.8	-29.1	5.14E-06	0.12	2	–	–	–	–
	600	1	261.3	-14.5	3.90E-06	0.09	2	–	–	–	–
	620	1	–	–	–	–	2	–	–	–	–
	650	1	185.4	-31.2	2.89E-05	0.67	2	–	–	–	–
	680	1	–	–	–	–	2	–	–	–	–

Table 7. continued

Sample	Demag field (°C)	Run	Dec.	Inc.	Intensity (emu/cc)	I/I$_o$	Run	Dec.	Inc.	Intensity (emu/cc)	I/I$_o$
CLK11-PM35	0	1	323.9	16.5	6.87E-03	1.00	2	251.6	44.5	4.22E-03	1.00
	100	1	284.2	42.9	4.68E-03	0.68	2	247.3	42.8	3.99E-03	0.95
	150	1	276.4	44.5	4.08E-03	0.59	2	246.3	41.4	3.43E-03	0.81
	200	1	275.0	43.8	3.18E-03	0.46	2	246.3	40.2	3.11E-03	0.74
	250	1	274.0	42.6	2.44E-03	0.36	2	240.3	39.1	2.49E-03	0.59
	300	1	270.9	42.5	1.69E-03	0.25	2	242.8	39.0	1.98E-03	0.47
	350	1	270.0	42.1	1.21E-03	0.18	2	242.8	38.7	1.57E-03	0.37
	380	1	270.8	49.3	7.99E-04	0.12	2	–	–	–	–
	400	1	–	–	–	–	2	236.4	35.7	1.05E-03	0.25
	420	1	272.8	43.4	5.52E-04	0.08	2	–	–	–	–
	450	1	258.4	35.3	2.57E-04	0.04	2	231.8	29.2	5.06E-04	0.12
	480	1	262.1	41.5	2.46E-04	0.04	2	228.1	30.0	3.72E-04	0.09
	500	1	262.5	46.8	2.01E-04	0.03	2	–	–	–	–
	520	1	267.9	52.2	1.29E-04	0.02	2	233.7	40.4	4.19E-04	0.10
	550	1	273.7	54.7	9.04E-05	0.01	2	211.3	12.0	9.58E-05	0.02
	580	1	–	–	–	–	2	–	–	–	–
	600	1	194.4	49.8	2.45E-05	0.00	2	212.4	10.7	6.66E-05	0.02
	620	1	–	–	–	–	2	–	–	–	–
	650	1	199.3	20.1	5.24E-05	0.01	2	–	–	–	–
	680	1	–	–	–	–	2	–	–	–	–
CLK11-PM36	0	1	323.9	16.4	6.88E-03	1.00	2	327.5	6.8	6.43E-03	1.00
	100	1	326.8	15.4	6.19E-03	0.90	2	327.4	7.6	5.80E-03	0.90
	150	1	325.4	15.3	5.63E-03	0.82	2	327.9	7.4	5.36E-03	0.83
	200	1	324.3	15.7	4.51E-03	0.66	2	326.0	6.5	4.27E-03	0.66
	250	1	319.5	15.0	3.64E-03	0.53	2	324.3	7.1	4.23E-03	0.66
	300	1	322.0	17.2	2.85E-03	0.41	2	326.3	8.7	3.76E-03	0.58
	350	1	317.4	16.3	2.39E-03	0.35	2	322.4	7.1	1.78E-03	0.28
	380	1	317.3	20.8	1.65E-03	0.24	2	–	–	–	–
	400	1	–	–	–	–	2	317.9	9.6	7.07E-04	0.11
	420	1	317.1	17.0	1.39E-03	0.20	2	–	–	–	–
	450	1	316.7	13.7	8.00E-04	0.12	2	318.7	13.8	6.63E-04	0.10
	480	1	313.2	21.2	4.02E-04	0.06	2	308.8	15.3	2.58E-04	0.04
	500	1	313.2	21.4	3.45E-04	0.05	2	–	–	–	–
	520	1	311.4	19.2	3.02E-04	0.04	2	303.8	16.7	2.55E-04	0.04
	550	1	293.6	25.1	1.05E-04	0.02	2	218.7	26.3	5.96E-05	0.01
	580	1	–	–	–	–	2	–	–	–	–
	600	1	233.8	38.3	5.52E-05	0.01	2	210.3	12.0	7.08E-05	0.01
	620	1	–	–	–	–	2	–	–	–	–
	650	1	238.5	3.3	8.59E-05	0.01	2	–	–	–	–
	680	1	–	–	–	–	2	–	–	–	–
CLK11-PM37	0	1	151.6	-2.9	1.63E-02	1.00	2	155.1	-1.7	1.35E-02	1.00
	100	1	151.7	-1.8	1.55E-02	0.95	2	154.8	-3.0	1.26E-02	0.93
	150	1	150.4	-3.6	1.49E-02	0.91	2	153.7	-0.9	1.17E-02	0.87
	200	1	153.8	-2.2	1.31E-02	0.80	2	155.9	-0.3	1.17E-02	0.87
	250	1	150.2	-2.0	1.03E-02	0.63	2	156.1	-3.2	7.73E-03	0.57
	300	1	151.4	-2.6	8.22E-03	0.50	2	153.6	-3.8	7.33E-03	0.54
	350	1	151.6	-1.8	6.83E-03	0.42	2	155.4	-2.8	4.84E-03	0.36
	380	1	149.4	-2.8	5.58E-03	0.34	2	–	–	–	–
	400	1	–	–	–	–	2	157.6	-2.2	4.71E-03	0.35
	420	1	154.8	-2.7	5.41E-03	0.33	2	156.3	-2.4	3.50E-03	0.26
	450	1	156.2	-2.9	4.43E-03	0.27	2	158.3	-1.5	3.29E-03	0.24
	480	1	150.4	-2.8	3.08E-03	0.19	2	155.8	0.7	1.39E-03	0.10
	500	1	146.0	-5.5	2.96E-03	0.18	2	–	–	–	–
	520	1	151.7	-3.8	2.89E-03	0.18	2	156.2	-2.0	1.31E-03	0.10
	550	1	149.6	0.5	1.23E-03	0.08	2	154.8	-3.1	3.75E-04	0.03
	580	1	–	–	–	–	2	–	–	–	–
	600	1	151.6	-0.9	1.10E-03	0.07	2	159.0	-3.1	2.75E-05	0.00
	620	1	–	–	–	–	2	–	–	–	–
	650	1	–	–	–	–	2	–	–	–	–
	680	1	–	–	–	–	2	–	–	–	–

Table 7. continued

Sample	Demag field (°C)	Run	Dec.	Inc.	Intensity (emu/cc)	I/I_o	Run	Dec.	Inc.	Intensity (emu/cc)	I/I_o
CLK11-PM38	0	1	–	–	–	–	2	–	–	–	–
	100	1	–	–	–	–	2	–	–	–	–
	150	1	–	–	–	–	2	–	–	–	–
	200	1	–	–	–	–	2	–	–	–	–
	250	1	–	–	–	–	2	–	–	–	–
	300	1	–	–	–	–	2	–	–	–	–
	350	1	–	–	–	–	2	–	–	–	–
	380	1	–	–	–	–	2	–	–	–	–
	400	1	–	–	–	–	2	–	–	–	–
	420	1	–	–	–	–	2	–	–	–	–
	450	1	–	–	–	–	2	–	–	–	–
	480	1	–	–	–	–	2	–	–	–	–
	500	1	–	–	–	–	2	–	–	–	–
	520	1	–	–	–	–	2	–	–	–	–
	550	1	–	–	–	–	2	–	–	–	–
	580	1	–	–	–	–	2	–	–	–	–
	600	1	–	–	–	–	2	–	–	–	–
	620	1	–	–	–	–	2	–	–	–	–
	650	1	–	–	–	–	2	–	–	–	–
	680	1	–	–	–	–	2	–	–	–	–
CLK11-PM39	0	1	24.4	5.9	1.16E-05	1.00	2	50.3	-3.3	1.40E-05	1.00
	100	1	126.6	-15.4	5.20E-06	0.45	2	100.5	-5.5	6.87E-06	0.49
	150	1	168.1	-5.4	1.30E-05	1.12	2	132.8	-1.8	8.21E-06	0.59
	200	1	175.9	-1.3	2.02E-05	1.73	2	165.0	-2.4	1.69E-05	1.21
	250	1	182.2	-9.6	2.38E-05	2.05	2	171.4	1.8	1.99E-05	1.43
	300	1	180.7	-6.8	2.45E-05	2.11	2	178.9	-4.0	2.23E-05	1.59
	350	1	184.2	-6.0	2.49E-05	2.14	2	177.3	-4.9	2.17E-05	1.56
	380	1	182.4	-6.2	2.51E-05	2.16	2	–	–	–	–
	400	1	–	–	–	–	2	178.4	-4.0	2.30E-05	1.64
	420	1	183.0	-7.8	2.61E-05	2.24	2	180.8	-2.2	2.28E-05	1.63
	450	1	183.3	-8.3	2.65E-05	2.28	2	184.2	1.5	2.18E-05	1.56
	480	1	187.9	-1.1	2.56E-05	2.20	2	181.5	1.3	2.33E-05	1.67
	500	1	–	–	–	–	2	–	–	–	–
	520	1	189.4	-1.8	1.45E-05	1.25	2	185.7	-2.0	2.03E-05	1.45
	550	1	183.4	-2.1	1.48E-05	1.27	2	182.1	0.4	2.04E-05	1.46
	580	1	178.7	-7.0	9.78E-06	0.84	2	–	–	–	–
	600	1	209.2	-4.5	5.87E-06	0.51	2	190.3	-1.4	1.55E-05	1.11
	620	1	–	–	–	–	2	–	–	–	–
	650	1	–	–	–	–	2	181.8	-5.1	1.50E-05	1.08
	680	1	–	–	–	–	2	–	–	–	–
CLK11-PM40	0	1	106.1	3.6	2.78E-04	1.00	2	143.6	-28.4	7.30E-05	1.00
	100	1	150.7	-1.9	2.19E-04	0.79	2	174.7	-13.0	1.77E-04	2.42
	150	1	158.9	-2.7	2.27E-04	0.82	2	176.3	-8.8	2.47E-04	3.38
	200	1	170.0	-3.0	2.82E-04	1.01	2	177.6	-6.5	2.98E-04	4.08
	250	1	175.7	-0.9	3.10E-04	1.11	2	184.1	-5.4	3.64E-04	4.98
	300	1	181.5	-4.2	3.84E-04	1.38	2	181.8	-5.6	3.50E-04	4.79
	350	1	180.2	-3.2	4.04E-04	1.45	2	183.5	-6.8	2.93E-04	4.02
	380	1	177.4	-8.8	3.14E-04	1.13	2	–	–	–	–
	400	1	–	–	–	–	2	181.7	-6.3	2.89E-04	3.96
	420	1	184.1	-4.1	3.71E-04	1.33	2	178.1	-6.6	2.52E-04	3.45
	450	1	181.0	-6.0	3.46E-04	1.24	2	182.8	-3.6	2.36E-04	3.23
	480	1	186.5	-6.3	2.89E-04	1.04	2	182.2	-5.9	1.77E-04	2.42
	500	1	183.2	-12.7	3.04E-04	1.09	2	–	–	–	–
	520	1	185.5	-9.4	2.98E-04	1.07	2	189.3	-8.5	1.86E-04	2.55
	550	1	192.6	-9.0	2.73E-04	0.98	2	177.5	-5.8	1.66E-04	2.27
	580	1	–	–	–	–	2	–	–	–	–
	600	1	186.1	-6.3	2.36E-04	0.85	2	193.2	-9.7	1.87E-04	2.56
	620	1	–	–	–	–	2	–	–	–	–
	650	1	–	–	–	–	2	250.9	-10.6	1.16E-05	0.16
	680	1	–	–	–	–	2	–	–	–	–

Table 7. continued

Sample	Demag field (°C)	Run	Dec.	Inc.	Intensity (emu/cc)	I/I$_o$	Run	Dec.	Inc.	Intensity (emu/cc)	I/I$_o$
CLK11-PM41	0	1	173.4	5.8	3.43E-04	1.00	2	183.5	4.3	6.57E-04	1.00
	100	1	177.4	6.7	5.12E-04	1.49	2	184.7	9.6	7.25E-04	1.10
	150	1	182.7	4.3	5.89E-04	1.72	2	180.4	8.9	7.61E-04	1.16
	200	1	175.7	6.5	6.24E-04	1.82	2	184.5	8.0	8.03E-04	1.22
	250	1	179.2	1.8	5.47E-04	1.60	2	180.2	8.5	7.03E-04	1.07
	300	1	176.6	7.2	4.43E-04	1.29	2	179.5	9.3	5.62E-04	0.86
	350	1	177.7	1.3	3.40E-04	0.99	2	180.9	8.6	5.08E-04	0.77
	380	1	173.5	5.1	3.39E-04	0.99	2	–	–	–	–
	400	1	–	–	–	–	2	178.4	6.8	4.14E-04	0.63
	420	1	182.0	9.2	2.72E-04	0.79	2	173.3	4.8	4.07E-04	0.62
	450	1	176.2	4.6	2.66E-04	0.78	2	176.1	7.5	3.18E-04	0.48
	480	1	177.9	-4.0	2.61E-04	0.76	2	176.4	6.7	3.07E-04	0.47
	500	1	172.3	1.8	2.52E-04	0.74	2	–	–	–	–
	520	1	174.7	5.3	2.68E-04	0.78	2	180.2	5.7	2.83E-04	0.43
	550	1	175.9	6.5	2.43E-04	0.71	2	176.1	6.9	1.83E-04	0.28
	580	1	–	–	–	–	2	–	–	–	–
	600	1	175.8	5.8	2.31E-04	0.67	2	183.0	3.4	7.65E-05	0.12
	620	1	–	–	–	–	2	–	–	–	–
	650	1	–	–	–	–	2	175.9	13.2	4.58E-05	0.07
	680	1	–	–	–	–	2	–	–	–	–
CLK11-PM42	0	1	186.9	1.4	4.21E-04	1.00	2	188.0	1.1	6.57E-04	1.00
	100	1	184.7	1.5	5.68E-04	1.35	2	185.2	0.2	6.51E-04	0.99
	150	1	188.3	-4.0	5.69E-04	1.35	2	184.3	0.6	6.41E-04	0.97
	200	1	185.1	6.0	5.67E-04	1.35	2	183.4	1.9	6.07E-04	0.92
	250	1	183.9	-1.2	5.01E-04	1.19	2	186.0	-0.6	5.52E-04	0.84
	300	1	186.7	-3.2	3.98E-04	0.95	2	176.9	1.0	3.69E-04	0.56
	350	1	176.7	-6.7	2.35E-04	0.56	2	179.0	2.6	3.20E-04	0.49
	380	1	179.1	6.8	2.09E-04	0.50	2	–	–	–	–
	400	1	–	–	–	–	2	177.1	2.6	1.62E-04	0.25
	420	1	173.9	14.0	2.06E-04	0.49	2	172.5	2.6	1.65E-04	0.25
	450	1	181.9	1.9	1.24E-04	0.29	2	183.1	1.4	1.15E-04	0.18
	480	1	178.1	-4.6	1.09E-04	0.26	2	172.6	-0.1	1.02E-04	0.16
	500	1	167.5	0.5	1.08E-04	0.26	2	–	–	–	–
	520	1	191.8	-6.8	1.38E-04	0.33	2	188.1	-9.1	1.28E-04	0.19
	550	1	160.9	0.6	1.05E-04	0.25	2	176.2	1.5	1.23E-04	0.19
	580	1	–	–	–	–	2	–	–	–	–
	600	1	195.5	0.1	6.62E-05	0.16	2	167.5	-0.5	1.25E-04	0.19
	620	1	–	–	–	–	2	–	–	–	–
	650	1	–	–	–	–	2	–	–	–	–
	680	1	–	–	–	–	2	–	–	–	–
CLK11-PM43	0	1	202.3	-2.8	4.34E-03	1.00	2	199.1	-0.5	3.63E-03	1.00
	100	1	200.1	-0.8	3.65E-03	0.84	2	199.6	0.8	3.15E-03	0.87
	150	1	201.8	-0.3	3.20E-03	0.74	2	199.5	3.5	2.77E-03	0.76
	200	1	201.1	-0.5	2.72E-03	0.63	2	197.9	3.3	2.28E-03	0.63
	250	1	197.2	-0.2	2.16E-03	0.50	2	200.1	4.4	1.65E-03	0.45
	300	1	200.3	-1.5	1.94E-03	0.45	2	195.7	1.1	1.13E-03	0.31
	350	1	198.2	-0.8	7.04E-04	0.16	2	194.6	-0.8	8.07E-04	0.22
	380	1	–	–	–	–	2	–	–	–	–
	400	1	195.0	0.2	4.40E-04	0.10	2	192.2	2.1	4.24E-04	0.12
	420	1	194.3	1.0	3.00E-04	0.07	2	191.4	2.1	3.73E-04	0.10
	450	1	190.9	0.1	2.40E-04	0.06	2	190.7	3.9	2.00E-04	0.05
	480	1	235.1	-10.2	1.86E-04	0.04	2	187.4	1.4	1.68E-04	0.05
	500	1	–	–	–	–	2	–	–	–	–
	520	1	187.4	0.5	1.45E-04	0.03	2	185.7	3.6	1.25E-04	0.03
	550	1	196.9	0.2	9.47E-05	0.02	2	192.8	3.4	1.28E-04	0.04
	580	1	231.0	3.9	3.44E-05	0.01	2	–	–	–	–
	600	1	167.3	-7.7	4.04E-05	0.01	2	212.4	-11.1	4.05E-05	0.01
	620	1	–	–	–	–	2	–	–	–	–
	650	1	–	–	–	–	2	–	–	–	–
	680	1	–	–	–	–	2	–	–	–	–

Table 7. continued

Sample	Demag field (°C)	Run	Dec.	Inc.	Intensity (emu/cc)	I/I_o	Run	Dec.	Inc.	Intensity (emu/cc)	I/I_o
CLK11-PM44	0	1	227.8	-2.9	1.33E-02	1.00	2	223.9	5.1	7.69E-03	1.00
	100	1	227.2	-3.8	1.15E-02	0.87	2	216.6	-0.4	6.68E-03	0.87
	150	1	225.0	-4.6	8.87E-03	0.67	2	218.7	-0.3	5.35E-03	0.70
	200	1	217.9	-3.3	7.88E-03	0.59	2	216.9	1.5	4.06E-03	0.53
	250	1	221.6	-4.3	7.09E-03	0.53	2	213.3	0.6	2.37E-03	0.31
	300	1	223.3	-4.7	2.14E-03	0.16	2	213.3	-0.7	1.66E-03	0.22
	350	1	217.0	-4.8	1.09E-03	0.08	2	213.2	0.8	7.50E-04	0.10
	380	1	–	–	–	–	2	–	–	–	–
	400	1	217.4	-4.7	6.34E-04	0.05	2	210.4	-4.6	4.43E-04	0.06
	420	1	212.9	-6.3	4.47E-04	0.03	2	207.4	-2.9	3.52E-04	0.05
	450	1	212.1	-4.7	3.11E-04	0.02	2	206.6	2.4	2.32E-04	0.03
	480	1	357.5	-30.8	4.03E-05	0.00	2	204.5	-0.9	1.77E-04	0.02
	500	1	–	–	–	–	2	–	–	–	–
	520	1	203.1	-4.5	1.97E-04	0.01	2	194.7	-1.6	8.84E-05	0.01
	550	1	201.3	-6.2	1.17E-04	0.01	2	206.4	-3.3	8.67E-05	0.01
	580	1	92.3	38.9	3.64E-05	0.00	2	–	–	–	–
	600	1	171.6	-10.4	7.36E-05	0.01	2	206.0	-10.1	2.92E-05	0.00
	620	1	–	–	–	–	2	–	–	–	–
	650	1	–	–	–	–	2	–	–	–	–
	680	1	–	–	–	–	2	–	–	–	–
CLK11-PM45	0	1	68.6	-39.8	1.62E-04	1.00	2	204.5	-10.7	1.29E-04	1.00
	100	1	117.5	-28.3	1.51E-04	0.93	2	194.7	-4.2	1.93E-04	1.51
	150	1	156.7	-6.1	2.25E-04	1.39	2	187.4	-4.6	2.41E-04	1.88
	200	1	166.7	-2.0	2.59E-04	1.61	2	188.1	-4.6	2.39E-04	1.86
	250	1	165.2	-0.7	2.05E-04	1.27	2	186.5	-6.3	1.89E-04	1.47
	300	1	168.6	-3.6	1.87E-04	1.16	2	185.4	-5.3	1.88E-04	1.46
	350	1	172.1	-11.6	1.44E-04	0.89	2	187.3	-9.6	8.82E-05	0.69
	380	1	169.5	-4.8	1.05E-04	0.65	2	–	–	–	–
	400	1	–	–	–	–	2	185.0	-5.5	9.08E-05	0.71
	420	1	153.9	-8.4	1.01E-04	0.62	2	178.6	-11.5	4.57E-05	0.36
	450	1	185.7	-12.2	8.73E-05	0.54	2	192.8	-1.3	4.46E-05	0.35
	480	1	169.5	-14.9	5.48E-05	0.34	2	208.8	1.8	3.83E-05	0.30
	500	1	174.0	-10.2	4.57E-05	0.28	2	–	–	–	–
	520	1	183.9	-22.1	5.47E-05	0.34	2	192.5	-13.4	3.29E-05	0.26
	550	1	163.2	-9.0	2.49E-05	0.15	2	174.9	-11.5	3.10E-05	0.24
	580	1	–	–	–	–	2	–	–	–	–
	600	1	168.7	-14.4	1.22E-05	0.08	2	144.3	-58.7	6.15E-06	0.05
	620	1	–	–	–	–	2	–	–	–	–
	650	1	–	–	–	–	2	–	–	–	–
	680	1	–	–	–	–	2	–	–	–	–
CLK11-PM46	0	1	3.8	-1.4	3.19E-04	1.00	2	8.5	-0.1	2.67E-04	1.00
	100	1	3.9	-1.7	4.18E-04	1.31	2	7.2	-1.9	2.37E-04	0.89
	150	1	3.0	-1.8	3.60E-04	1.13	2	7.6	0.8	2.18E-04	0.82
	200	1	2.6	-2.4	3.39E-04	1.06	2	9.1	-0.1	1.86E-04	0.70
	250	1	3.4	-2.6	2.57E-04	0.80	2	7.5	-1.1	1.49E-04	0.56
	300	1	0.4	-1.0	2.17E-04	0.68	2	8.7	-0.6	1.22E-04	0.46
	350	1	5.3	-2.5	1.31E-04	0.41	2	9.8	-3.5	1.17E-04	0.44
	380	1	3.1	-0.9	1.55E-04	0.48	2	–	–	–	–
	400	1	–	–	–	–	2	12.7	-1.3	9.05E-05	0.34
	420	1	4.6	-1.6	1.51E-04	0.47	2	7.9	-2.7	9.02E-05	0.34
	450	1	3.4	-3.3	1.18E-04	0.37	2	6.3	-2.2	6.87E-05	0.26
	480	1	5.9	-11.6	3.25E-05	0.10	2	16.7	-11.7	9.88E-06	0.04
	500	1	11.2	-21.8	2.01E-05	0.06	2	–	–	–	–
	520	1	357.2	-38.7	1.26E-05	0.04	2	10.2	-10.3	9.62E-06	0.04
	550	1	41.2	-53.9	4.09E-06	0.01	2	20.6	-18.7	4.38E-06	0.02
	580	1	–	–	–	–	2	–	–	–	–
	600	1	141.5	-50.5	3.00E-06	0.01	2	101.1	-45.1	1.91E-06	0.01
	620	1	–	–	–	–	2	–	–	–	–
	650	1	153.2	-7.8	8.43E-06	0.03	2	–	–	–	–
	680	1	–	–	–	–	2	–	–	–	–

Table 7. continued

Sample	Demag field (°C)	Run	Dec.	Inc.	Intensity (emu/cc)	I/I$_o$	Run	Dec.	Inc.	Intensity (emu/cc)	I/I$_o$
CLK11-PM47	0	1	26.3	-5.6	2.08E-04	1.00	2	28.5	2.7	2.77E-04	1.00
	100	1	20.6	-5.3	2.47E-04	1.19	2	28.9	2.2	2.49E-04	0.90
	150	1	19.5	-4.2	2.27E-04	1.09	2	23.8	2.7	2.22E-04	0.80
	200	1	19.9	-4.5	2.14E-04	1.03	2	27.3	3.2	1.87E-04	0.67
	250	1	22.8	-4.6	1.67E-04	0.80	2	28.7	2.2	1.51E-04	0.55
	300	1	24.1	-5.4	1.49E-04	0.72	2	22.9	5.3	1.00E-04	0.36
	350	1	23.0	-10.3	1.01E-04	0.49	2	24.0	3.1	1.34E-04	0.48
	380	1	25.6	-5.7	1.19E-04	0.57	2	–	–	–	–
	400	1	–	–	–	–	2	49.0	-7.4	8.73E-05	0.32
	420	1	29.0	-5.9	1.13E-04	0.54	2	23.0	1.8	9.95E-05	0.36
	450	1	23.5	-9.0	9.57E-05	0.46	2	24.5	1.1	6.23E-05	0.22
	480	1	15.7	-15.2	3.68E-05	0.18	2	21.9	0.7	6.30E-05	0.23
	500	1	19.5	-14.9	3.70E-05	0.18	2	–	–	–	–
	520	1	20.2	-14.4	3.43E-05	0.17	2	25.4	2.0	4.99E-05	0.18
	550	1	19.1	-14.4	2.64E-05	0.13	2	19.6	5.1	4.49E-05	0.16
	580	1	–	–	–	–	2	–	–	–	–
	600	1	32.8	-12.5	7.39E-06	0.04	2	12.6	-2.9	2.37E-05	0.09
	620	1	–	–	–	–	2	–	–	–	–
	650	1	40.9	-20.4	2.80E-05	0.14	2	–	–	–	–
	680	1	–	–	–	–	2	–	–	–	–
CLK11-PM48	0	1	15.5	0.3	2.68E-04	1.00	2	11.7	-10.3	2.75E-04	1.00
	100	1	18.4	1.6	3.05E-04	1.14	2	14.6	-8.0	2.50E-04	0.91
	150	1	20.2	2.6	2.51E-04	0.94	2	6.7	-8.7	2.35E-04	0.86
	200	1	22.0	4.9	2.08E-04	0.78	2	11.8	-8.4	1.66E-04	0.61
	250	1	17.4	4.9	1.57E-04	0.59	2	15.6	-7.4	1.62E-04	0.59
	300	1	22.5	5.2	1.25E-04	0.47	2	13.0	-6.6	1.28E-04	0.47
	350	1	18.5	1.6	7.19E-05	0.27	2	15.1	-6.9	1.21E-04	0.44
	380	1	23.7	4.3	8.84E-05	0.33	2	–	–	–	–
	400	1	–	–	–	–	2	14.7	-10.7	1.20E-04	0.44
	420	1	28.6	3.5	6.42E-05	0.24	2	16.5	-11.7	1.21E-04	0.44
	450	1	22.5	0.7	6.48E-05	0.24	2	17.0	-8.9	1.18E-04	0.43
	480	1	28.0	-14.8	5.51E-05	0.21	2	16.6	-7.2	6.16E-05	0.22
	500	1	26.0	-11.3	7.27E-05	0.27	2	–	–	–	–
	520	1	22.7	6.5	5.97E-05	0.22	2	15.9	-4.7	4.80E-05	0.17
	550	1	14.0	3.1	6.38E-05	0.24	2	15.1	-8.6	4.31E-05	0.16
	580	1	–	–	–	–	2	–	–	–	–
	600	1	10.1	-1.2	1.66E-05	0.06	2	21.7	-10.5	2.89E-05	0.11
	620	1	–	–	–	–	2	–	–	–	–
	650	1	62.2	29.0	2.11E-05	0.08	2	–	–	–	–
	680	1	–	–	–	–	2	–	–	–	–
CLK11-PM49	0	1	8.0	12.2	2.63E-04	1.00	2	349.9	9.3	3.06E-04	1.00
	100	1	8.5	12.6	3.11E-04	1.18	2	348.4	14.6	2.77E-04	0.91
	150	1	4.7	19.4	2.52E-04	0.96	2	348.2	19.8	2.06E-04	0.67
	200	1	4.7	20.4	2.21E-04	0.84	2	351.0	20.6	1.75E-04	0.57
	250	1	8.9	26.7	1.55E-04	0.59	2	349.6	19.6	1.69E-04	0.55
	300	1	6.4	31.8	1.27E-04	0.48	2	341.0	23.5	1.24E-04	0.41
	350	1	4.0	26.9	8.90E-05	0.34	2	341.0	23.9	1.08E-04	0.35
	380	1	6.9	25.1	8.35E-05	0.32	2	–	–	–	–
	400	1	–	–	–	–	2	340.7	26.7	1.07E-04	0.35
	420	1	339.6	27.3	6.53E-05	0.25	2	333.1	29.1	7.61E-05	0.25
	450	1	21.4	26.6	6.44E-05	0.24	2	337.5	29.2	8.35E-05	0.27
	480	1	13.0	19.5	6.41E-05	0.24	2	344.8	27.7	5.84E-05	0.19
	500	1	356.7	23.1	5.56E-05	0.21	2	–	–	–	–
	520	1	12.4	27.1	4.95E-05	0.19	2	339.9	31.9	6.66E-05	0.22
	550	1	19.6	19.0	6.07E-05	0.23	2	346.3	33.5	6.05E-05	0.20
	580	1	–	–	–	–	2	–	–	–	–
	600	1	355.9	15.5	1.91E-05	0.07	2	347.1	31.2	5.60E-05	0.18
	620	1	–	–	–	–	2	–	–	–	–
	650	1	95.4	34.8	3.22E-05	0.12	2	–	–	–	–
	680	1	–	–	–	–	2	–	–	–	–

Table 7. continued

Sample	Demag field (°C)	Run	Dec.	Inc.	Intensity (emu/cc)	I/I_o	Run	Dec.	Inc.	Intensity (emu/cc)	I/I_o
CLK11-PM50	0	1	141.1	-44.2	9.30E-05	1.00	2	87.1	-66.4	6.10E-05	1.00
	100	1	167.4	-22.1	1.46E-04	1.57	2	162.6	-22.5	1.10E-04	1.80
	150	1	167.2	-10.3	2.10E-04	2.26	2	166.7	-12.3	1.68E-04	2.76
	200	1	173.1	-3.8	2.54E-04	2.73	2	171.4	-9.8	1.88E-04	3.08
	250	1	175.6	-2.5	2.81E-04	3.02	2	172.1	-7.2	2.15E-04	3.52
	300	1	175.4	-0.8	2.40E-04	2.58	2	165.4	-3.9	2.23E-04	3.66
	350	1	164.9	4.6	1.47E-04	1.58	2	168.1	-3.7	1.58E-04	2.58
	380	1	176.3	-2.5	1.95E-04	2.10	2	–	–	–	–
	400	1	–	–	–	–	2	165.9	-2.7	1.15E-04	1.88
	420	1	158.3	4.1	1.52E-04	1.64	2	171.3	1.3	1.23E-04	2.02
	450	1	179.4	-3.7	1.42E-04	1.52	2	165.0	2.6	9.74E-05	1.60
	480	1	181.8	-2.5	1.32E-04	1.42	2	157.6	7.4	1.16E-04	1.89
	500	1	184.1	-3.5	1.11E-04	1.19	2	–	–	–	–
	520	1	175.6	-2.1	1.59E-04	1.70	2	168.2	20.6	9.80E-05	1.61
	550	1	179.0	0.6	1.17E-04	1.25	2	157.0	2.9	9.90E-05	1.62
	580	1	–	–	–	–	2	–	–	–	–
	600	1	178.2	0.4	4.04E-05	0.43	2	181.3	11.1	1.03E-04	1.70
	620	1	–	–	–	–	2	–	–	–	–
	650	1	–	–	–	–	2	170.0	-4.4	1.04E-04	1.70
	680	1	–	–	–	–	2	–	–	–	–
CLK11-PM51	0	1	1.8	0.0	7.44E-05	1.00	2	72.2	-32.3	8.03E-06	1.00
	100	1	358.4	7.8	4.85E-05	0.65	2	160.2	-12.1	3.20E-05	3.98
	150	1	358.3	11.6	3.13E-05	0.42	2	165.2	-6.8	5.66E-05	7.05
	200	1	1.5	26.9	2.28E-05	0.31	2	165.6	-10.5	5.97E-05	7.44
	250	1	54.2	68.0	9.95E-06	0.13	2	170.7	-10.6	6.87E-05	8.56
	300	1	24.5	78.2	7.96E-06	0.11	2	165.4	-8.4	6.00E-05	7.47
	350	1	1.1	-38.3	9.65E-06	0.13	2	170.9	-4.1	3.12E-05	3.89
	380	1	106.8	6.4	8.45E-06	0.11	2	–	–	–	–
	400	1	–	–	–	–	2	175.0	-13.7	3.63E-05	4.52
	420	1	271.7	-18.1	1.41E-05	0.19	2	–	–	–	–
	450	1	297.0	-15.8	5.30E-06	0.07	2	166.7	-5.3	5.63E-05	7.02
	480	1	266.9	-42.7	4.63E-06	0.06	2	185.0	-46.7	3.58E-05	4.46
	500	1	241.9	-28.1	6.34E-06	0.09	2	–	–	–	–
	520	1	357.8	-26.6	2.35E-05	0.32	2	151.5	-12.2	2.78E-05	3.46
	550	1	209.9	-40.6	6.64E-06	0.09	2	160.5	-27.4	2.26E-05	2.81
	580	1	–	–	–	–	2	–	–	–	–
	600	1	113.3	-16.6	2.77E-06	0.04	2	150.8	-17.3	3.99E-05	4.97
	620	1	–	–	–	–	2	–	–	–	–
	650	1	144.7	-11.1	1.95E-05	0.26	2	–	–	–	–
	680	1	–	–	–	–	2	–	–	–	–
CLK11-PM52	0	1	102.9	42.0	6.59E-04	1.00	2	101.1	32.6	8.72E-04	1.00
	100	1	110.9	28.8	8.22E-04	1.25	2	109.0	30.6	8.96E-04	1.03
	150	1	112.7	27.7	8.32E-04	1.26	2	117.9	28.3	8.88E-04	1.02
	200	1	118.2	25.4	8.36E-04	1.27	2	127.3	21.5	7.33E-04	0.84
	250	1	134.7	21.3	7.33E-04	1.11	2	128.7	23.5	6.11E-04	0.70
	300	1	135.7	19.7	6.47E-04	0.98	2	124.1	21.0	3.57E-04	0.41
	350	1	124.5	23.5	4.34E-04	0.66	2	132.3	14.5	2.60E-04	0.30
	380	1	130.9	7.0	3.09E-04	0.47	2	–	–	–	–
	400	1	–	–	–	–	2	134.5	14.0	8.76E-05	0.10
	420	1	122.8	18.0	3.52E-04	0.53	2	144.7	13.2	9.63E-05	0.11
	450	1	134.2	1.1	2.51E-04	0.38	2	154.9	16.4	6.90E-05	0.08
	480	1	132.9	6.3	4.16E-05	0.06	2	121.3	17.6	6.01E-05	0.07
	500	1	162.1	3.8	4.28E-05	0.06	2	–	–	–	–
	520	1	140.1	4.4	3.09E-05	0.05	2	144.1	33.4	4.74E-05	0.05
	550	1	157.7	-15.9	1.10E-05	0.02	2	95.7	25.4	3.03E-05	0.03
	580	1	–	–	–	–	2	–	–	–	–
	600	1	121.1	8.9	3.08E-05	0.05	2	164.0	20.4	6.25E-05	0.07
	620	1	–	–	–	–	2	–	–	–	–
	650	1	–	–	–	–	2	–	–	–	–
	680	1	–	–	–	–	2	–	–	–	–

Table 7. continued

Sample	Demag field (°C)	Run	Dec.	Inc.	Intensity (emu/cc)	I/I$_o$	Run	Dec.	Inc.	Intensity (emu/cc)	I/I$_o$
CLK11-PM53	0	1	11.2	-3.1	6.37E-04	1.00	2	–	–	–	–
	100	1	10.9	-2.8	4.36E-04	0.68	2	–	–	–	–
	150	1	15.0	-2.3	2.43E-04	0.38	2	–	–	–	–
	200	1	17.3	0.0	2.07E-04	0.33	2	–	–	–	–
	250	1	42.4	-5.8	3.79E-05	0.06	2	–	–	–	–
	300	1	59.9	-10.0	2.23E-05	0.04	2	–	–	–	–
	350	1	136.4	-26.5	1.81E-05	0.03	2	–	–	–	–
	380	1	–	–	–	–	2	–	–	–	–
	400	1	166.1	-2.4	2.05E-05	0.03	2	–	–	–	–
	420	1	150.6	3.8	2.63E-05	0.04	2	–	–	–	–
	450	1	162.9	-10.9	2.91E-05	0.05	2	–	–	–	–
	480	1	48.3	8.4	8.33E-05	0.13	2	–	–	–	–
	500	1	–	–	–	–	2	–	–	–	–
	520	1	190.2	-3.5	2.17E-05	0.03	2	–	–	–	–
	550	1	191.7	-20.8	6.77E-06	0.01	2	–	–	–	–
	580	1	120.7	30.7	2.19E-05	0.03	2	–	–	–	–
	600	1	213.6	-13.7	1.18E-05	0.02	2	–	–	–	–
	620	1	–	–	–	–	2	–	–	–	–
	650	1	–	–	–	–	2	–	–	–	–
	680	1	–	–	–	–	2	–	–	–	–
CLK11-PM54	0	1	16.5	14.4	5.92E-04	1.00	2	15.5	7.3	5.70E-04	1.00
	100	1	15.5	24.8	3.79E-04	0.64	2	14.8	9.6	4.87E-04	0.85
	150	1	28.1	42.5	1.99E-04	0.34	2	36.4	29.8	1.38E-04	0.24
	200	1	143.3	53.8	1.29E-04	0.22	2	38.9	34.5	1.22E-04	0.21
	250	1	166.5	31.5	1.49E-04	0.25	2	111.7	1.0	1.08E-04	0.19
	300	1	169.9	26.0	1.48E-04	0.25	2	163.2	18.6	1.39E-04	0.24
	350	1	171.1	19.4	1.46E-04	0.25	2	171.5	9.9	1.71E-04	0.30
	380	1	–	–	–	–	2	–	–	–	–
	400	1	172.7	11.4	1.50E-04	0.25	2	175.5	5.2	1.65E-04	0.29
	420	1	179.5	9.6	1.49E-04	0.25	2	–	–	–	–
	450	1	177.7	6.4	1.49E-04	0.25	2	183.4	2.2	2.00E-04	0.35
	480	1	99.9	24.1	1.62E-04	0.27	2	183.1	0.6	1.74E-04	0.31
	500	1	–	–	–	–	2	–	–	–	–
	520	1	183.5	6.3	1.32E-04	0.22	2	180.3	2.4	1.07E-04	0.19
	550	1	171.9	9.9	9.73E-05	0.16	2	175.1	-2.1	9.99E-05	0.18
	580	1	159.5	17.4	9.10E-05	0.15	2	–	–	–	–
	600	1	168.5	1.6	7.63E-05	0.13	2	147.5	-7.4	2.11E-05	0.04
	620	1	–	–	–	–	2	–	–	–	–
	650	1	–	–	–	–	2	–	–	–	–
	680	1	–	–	–	–	2	–	–	–	–
CLK11-PM55	0	1	2.4	1.0	7.85E-04	1.00	2	0.8	7.4	7.50E-04	1.00
	100	1	3.8	4.6	5.75E-04	0.73	2	4.8	7.7	6.72E-04	0.90
	150	1	2.3	3.7	4.02E-04	0.51	2	6.5	7.5	3.20E-04	0.43
	200	1	8.4	7.5	1.07E-04	0.14	2	7.6	11.3	2.70E-04	0.36
	250	1	155.6	18.8	2.39E-05	0.03	2	95.3	36.8	2.80E-05	0.04
	300	1	164.7	4.3	4.86E-05	0.06	2	121.3	34.7	3.41E-05	0.05
	350	1	167.8	2.9	6.67E-05	0.08	2	167.9	3.5	6.11E-05	0.08
	380	1	–	–	–	–	2	–	–	–	–
	400	1	168.9	1.4	6.76E-05	0.09	2	154.2	11.5	6.46E-05	0.09
	420	1	176.6	0.0	7.96E-05	0.10	2	166.7	0.5	9.31E-05	0.12
	450	1	176.0	0.5	8.12E-05	0.10	2	164.7	15.5	1.04E-04	0.14
	480	1	76.2	46.3	1.06E-04	0.14	2	180.7	2.9	9.14E-05	0.12
	500	1	–	–	–	–	2	–	–	–	–
	520	1	182.1	0.7	8.24E-05	0.10	2	181.6	-1.8	8.76E-05	0.12
	550	1	177.6	4.5	5.38E-05	0.07	2	169.2	-20.4	7.15E-05	0.10
	580	1	162.5	66.8	3.90E-05	0.05	2	–	–	–	–
	600	1	188.6	2.7	5.95E-05	0.08	2	167.6	-1.1	1.00E-05	0.01
	620	1	–	–	–	–	2	–	–	–	–
	650	1	–	–	–	–	2	–	–	–	–
	680	1	–	–	–	–	2	–	–	–	–

Table 7. continued

Sample	Demag field (°C)	Run	Dec.	Inc.	Intensity (emu/cc)	I/I_o	Run	Dec.	Inc.	Intensity (emu/cc)	I/I_o
CLK11-PM56	0	1	–	–	–	–	2	–	–	–	–
	100	1	–	–	–	–	2	–	–	–	–
	150	1	–	–	–	–	2	–	–	–	–
	200	1	–	–	–	–	2	–	–	–	–
	250	1	–	–	–	–	2	–	–	–	–
	300	1	–	–	–	–	2	–	–	–	–
	350	1	–	–	–	–	2	–	–	–	–
	380	1	–	–	–	–	2	–	–	–	–
	400	1	–	–	–	–	2	–	–	–	–
	420	1	–	–	–	–	2	–	–	–	–
	450	1	–	–	–	–	2	–	–	–	–
	480	1	–	–	–	–	2	–	–	–	–
	500	1	–	–	–	–	2	–	–	–	–
	520	1	–	–	–	–	2	–	–	–	–
	550	1	–	–	–	–	2	–	–	–	–
	580	1	–	–	–	–	2	–	–	–	–
	600	1	–	–	–	–	2	–	–	–	–
	620	1	–	–	–	–	2	–	–	–	–
	650	1	–	–	–	–	2	–	–	–	–
	680	1	–	–	–	–	2	–	–	–	–
CLK11-PM57	0	1	6.0	7.9	1.58E-03	1.00	2	13.3	6.0	1.34E-03	1.00
	100	1	3.1	9.1	1.32E-03	0.83	2	11.8	4.9	1.02E-03	0.76
	150	1	7.0	12.7	1.06E-03	0.67	2	7.7	6.6	7.09E-04	0.53
	200	1	8.8	15.2	5.95E-04	0.38	2	16.5	20.0	2.30E-04	0.17
	250	1	8.9	22.4	2.04E-04	0.13	2	16.2	26.0	1.37E-04	0.10
	300	1	14.6	25.2	1.22E-04	0.08	2	19.0	28.8	8.41E-05	0.06
	350	1	2.9	30.0	6.32E-05	0.04	2	72.6	68.3	2.40E-05	0.02
	380	1	–	–	–	–	2	–	–	–	–
	400	1	356.4	-4.8	4.61E-05	0.03	2	115.4	40.9	2.09E-05	0.02
	420	1	57.6	22.5	3.19E-05	0.02	2	160.2	26.5	2.50E-05	0.02
	450	1	296.1	-46.1	1.42E-05	0.01	2	176.3	67.4	1.24E-05	0.01
	480	1	188.2	-50.8	6.97E-05	0.04	2	105.0	32.8	1.16E-05	0.01
	500	1	–	–	–	–	2	–	–	–	–
	520	1	18.1	5.9	2.01E-05	0.01	2	154.3	24.0	1.20E-05	0.01
	550	1	106.4	10.5	4.50E-05	0.03	2	108.0	64.4	3.65E-05	0.03
	580	1	128.2	-14.6	4.71E-05	0.03	2	–	–	–	–
	600	1	254.4	-40.3	5.06E-05	0.03	2	191.9	-11.1	2.02E-05	0.02
	620	1	–	–	–	–	2	–	–	–	–
	650	1	–	–	–	–	2	–	–	–	–
	680	1	–	–	–	–	2	–	–	–	–
CLK11-PM58	0	1	13.5	-5.9	2.21E-04	1.00	2	5.9	8.3	2.00E-04	1.00
	100	1	12.6	-5.5	1.58E-04	0.71	2	155.7	36.7	7.82E-05	0.39
	150	1	39.9	-9.7	6.46E-05	0.29	2	171.3	13.2	2.69E-04	1.35
	200	1	80.5	2.0	3.64E-05	0.16	2	176.3	6.2	4.84E-04	2.42
	250	1	174.7	6.3	2.92E-04	1.32	2	172.8	4.1	4.60E-04	2.30
	300	1	175.2	1.9	3.82E-04	1.73	2	174.5	1.2	3.24E-04	1.62
	350	1	172.1	-0.9	3.88E-04	1.76	2	180.2	3.3	2.01E-04	1.00
	380	1	170.3	-1.6	4.33E-04	1.96	2	–	–	–	–
	400	1	–	–	–	–	2	181.6	-2.7	1.67E-04	0.83
	420	1	173.7	-3.5	4.14E-04	1.87	2	189.6	-4.9	1.47E-04	0.74
	450	1	174.4	-7.3	2.84E-04	1.29	2	173.9	1.4	1.19E-04	0.60
	480	1	173.0	-4.5	7.60E-05	0.34	2	178.5	-5.7	1.01E-04	0.50
	500	1	174.9	-7.9	6.28E-05	0.28	2	–	–	–	–
	520	1	220.3	-22.4	3.00E-05	0.14	2	193.8	2.8	6.75E-05	0.34
	550	1	213.2	-27.6	3.84E-05	0.17	2	178.3	-10.3	7.21E-05	0.36
	580	1	–	–	–	–	2	–	–	–	–
	600	1	138.9	64.6	4.53E-05	0.21	2	156.7	7.9	2.62E-05	0.13
	620	1	–	–	–	–	2	–	–	–	–
	650	1	2.8	-36.2	8.09E-05	0.37	2	–	–	–	–
	680	1	–	–	–	–	2	–	–	–	–

Table 7. continued

Sample	Demag field (°C)	Run	Dec.	Inc.	Intensity (emu/cc)	I/I_o	Run	Dec.	Inc.	Intensity (emu/cc)	I/I_o
CLK11-PM59	0	1	187.8	14.2	4.12E-04	1.00	2	183.9	10.6	3.46E-04	1.00
	100	1	190.0	8.7	5.57E-04	1.35	2	179.9	9.0	5.36E-04	1.55
	150	1	193.7	6.0	7.10E-04	1.72	2	181.7	7.0	5.82E-04	1.68
	200	1	189.2	10.6	6.44E-04	1.56	2	181.3	7.6	6.96E-04	2.02
	250	1	192.7	6.0	6.82E-04	1.66	2	181.7	5.9	6.80E-04	1.97
	300	1	190.9	4.4	6.08E-04	1.48	2	180.6	7.0	4.07E-04	1.18
	350	1	187.9	-0.2	5.23E-04	1.27	2	173.1	9.4	3.87E-04	1.12
	380	1	–	–	–	–	2	–	–	–	–
	400	1	194.5	0.8	3.35E-04	0.81	2	181.6	4.6	2.11E-04	0.61
	420	1	194.0	-3.2	3.24E-04	0.79	2	193.6	-7.2	1.75E-04	0.51
	450	1	198.9	-0.2	2.57E-04	0.62	2	183.5	-0.8	1.04E-04	0.30
	480	1	196.0	2.1	9.76E-05	0.24	2	165.8	-6.2	9.18E-05	0.27
	500	1	–	–	–	–	2	–	–	–	–
	520	1	193.8	-11.0	1.04E-04	0.25	2	187.8	-1.1	6.56E-05	0.19
	550	1	155.3	21.6	7.43E-05	0.18	2	184.1	0.1	1.06E-04	0.31
	580	1	195.1	-38.4	2.27E-05	0.06	2	–	–	–	–
	600	1	164.5	-16.2	3.78E-05	0.09	2	121.9	-21.4	1.60E-05	0.05
	620	1	–	–	–	–	2	–	–	–	–
	650	1	–	–	–	–	2	–	–	–	–
	680	1	–	–	–	–	2	–	–	–	–
CLK11-PM60	0	1	163.5	5.7	4.12E-04	1.00	2	170.0	0.8	3.29E-04	1.00
	100	1	175.6	1.7	5.87E-04	1.42	2	177.1	3.3	4.75E-04	1.44
	150	1	186.2	1.1	9.24E-04	2.24	2	182.6	-1.1	6.96E-04	2.12
	200	1	183.1	-0.1	8.85E-04	2.15	2	185.8	-0.7	7.23E-04	2.20
	250	1	182.7	-1.1	7.41E-04	1.80	2	187.7	-3.6	4.79E-04	1.46
	300	1	182.4	3.9	6.03E-04	1.46	2	182.2	-0.4	3.81E-04	1.16
	350	1	185.0	1.1	4.40E-04	1.07	2	185.1	-4.8	2.11E-04	0.64
	380	1	–	–	–	–	2	–	–	–	–
	400	1	183.1	7.6	3.10E-04	0.75	2	183.1	2.1	1.80E-04	0.55
	420	1	183.8	0.2	2.78E-04	0.67	2	183.8	-3.1	1.18E-04	0.36
	450	1	189.4	-1.9	2.24E-04	0.54	2	190.9	-3.5	1.14E-04	0.35
	480	1	182.8	1.7	1.28E-04	0.31	2	182.6	10.9	1.10E-04	0.33
	500	1	–	–	–	–	2	–	–	–	–
	520	1	185.9	0.4	4.91E-05	0.12	2	171.5	-4.1	9.00E-05	0.27
	550	1	193.6	19.0	6.26E-05	0.15	2	293.5	-39.8	2.28E-03	6.92
	580	1	183.5	17.6	3.96E-05	0.10	2	–	–	–	–
	600	1	162.7	-16.1	5.86E-05	0.14	2	165.2	-12.3	7.89E-05	0.24
	620	1	–	–	–	–	2	–	–	–	–
	650	1	–	–	–	–	2	177.3	17.5	4.44E-05	0.14
	680	1	–	–	–	–	2	–	–	–	–
CLK11-PM61	0	1	–	–	–	–	2	–	–	–	–
	100	1	–	–	–	–	2	–	–	–	–
	150	1	–	–	–	–	2	–	–	–	–
	200	1	–	–	–	–	2	–	–	–	–
	250	1	–	–	–	–	2	–	–	–	–
	300	1	–	–	–	–	2	–	–	–	–
	350	1	–	–	–	–	2	–	–	–	–
	380	1	–	–	–	–	2	–	–	–	–
	400	1	–	–	–	–	2	–	–	–	–
	420	1	–	–	–	–	2	–	–	–	–
	450	1	–	–	–	–	2	–	–	–	–
	480	1	–	–	–	–	2	–	–	–	–
	500	1	–	–	–	–	2	–	–	–	–
	520	1	–	–	–	–	2	–	–	–	–
	550	1	–	–	–	–	2	–	–	–	–
	580	1	–	–	–	–	2	–	–	–	–
	600	1	–	–	–	–	2	–	–	–	–
	620	1	–	–	–	–	2	–	–	–	–
	650	1	–	–	–	–	2	–	–	–	–
	680	1	–	–	–	–	2	–	–	–	–

Table 7. continued

Sample	Demag field (°C)	Run	Dec.	Inc.	Intensity (emu/cc)	I/I$_o$	Run	Dec.	Inc.	Intensity (emu/cc)	I/I$_o$
CLK11-PM62	0	1	132.7	18.8	1.19E-04	1.00	2	121.3	6.2	1.15E-04	1.00
	100	1	141.2	10.1	1.32E-04	1.10	2	135.6	12.0	1.26E-04	1.09
	150	1	145.7	8.4	1.15E-04	0.96	2	136.0	10.6	1.24E-04	1.08
	200	1	140.2	8.9	1.26E-04	1.06	2	143.4	9.7	1.24E-04	1.08
	250	1	150.4	6.4	1.17E-04	0.98	2	140.6	12.5	1.14E-04	0.99
	300	1	150.9	6.6	9.99E-05	0.84	2	139.6	11.4	9.43E-05	0.82
	350	1	146.9	5.0	9.14E-05	0.77	2	139.2	12.2	9.58E-05	0.83
	380	1	–	–	–	–	2	–	–	–	–
	400	1	149.3	7.8	7.98E-05	0.67	2	138.0	13.4	8.43E-05	0.73
	420	1	148.7	7.6	8.09E-05	0.68	2	137.1	13.4	8.27E-05	0.72
	450	1	151.3	11.0	7.02E-05	0.59	2	142.2	13.0	7.02E-05	0.61
	480	1	146.3	10.5	5.58E-05	0.47	2	134.2	17.6	5.09E-05	0.44
	500	1	–	–	–	–	2	–	–	–	–
	520	1	152.7	7.9	3.88E-05	0.32	2	134.6	15.0	4.65E-05	0.40
	550	1	158.6	10.4	3.78E-05	0.32	2	146.7	11.4	2.99E-05	0.26
	580	1	140.2	6.0	3.65E-05	0.31	2	–	–	–	–
	600	1	154.7	17.0	1.81E-05	0.15	2	131.7	14.0	2.79E-05	0.24
	620	1	–	–	–	–	2	–	–	–	–
	650	1	169.4	34.1	4.22E-06	0.04	2	–	–	–	–
	680	1	–	–	–	–	2	–	–	–	–
CLK11-PM63	0	1	2.6	-12.5	1.56E-04	1.00	2	16.1	-15.4	1.68E-04	1.00
	100	1	15.1	-17.1	9.72E-05	0.62	2	21.1	-19.1	1.18E-04	0.70
	150	1	10.6	-19.0	6.37E-05	0.41	2	23.6	-19.4	9.52E-05	0.57
	200	1	25.3	-22.5	4.10E-05	0.26	2	40.4	-20.9	6.11E-05	0.36
	250	1	50.5	-26.2	2.62E-05	0.17	2	61.4	-22.9	3.93E-05	0.23
	300	1	73.8	-20.6	1.89E-05	0.12	2	86.2	-20.0	2.90E-05	0.17
	350	1	91.0	-10.1	1.68E-05	0.11	2	77.7	-29.6	2.76E-05	0.16
	380	1	–	–	–	–	2	–	–	–	–
	400	1	97.6	-11.8	1.37E-05	0.09	2	106.7	-10.5	2.12E-05	0.13
	420	1	101.0	-8.6	1.82E-05	0.12	2	–	–	–	–
	450	1	111.4	-11.5	1.35E-05	0.09	2	140.1	14.1	3.88E-05	0.23
	480	1	95.1	-8.4	1.60E-05	0.10	2	107.4	-9.4	2.51E-05	0.15
	500	1	–	–	–	–	2	–	–	–	–
	520	1	100.2	-26.8	6.84E-06	0.04	2	106.7	-6.4	1.35E-05	0.08
	550	1	86.3	-0.6	1.58E-05	0.10	2	130.1	-51.3	2.34E-05	0.14
	580	1	138.1	-9.3	1.72E-05	0.11	2	–	–	–	–
	600	1	208.0	3.3	4.98E-06	0.03	2	25.1	-4.0	1.31E-05	0.08
	620	1	–	–	–	–	2	–	–	–	–
	650	1	–	–	–	–	2	–	–	–	–
	680	1	–	–	–	–	2	–	–	–	–
CLK11-PM64	0	1	15.2	30.2	1.82E-04	1.00	2	336.6	69.1	6.93E-04	1.00
	100	1	26.1	33.2	1.31E-04	0.72	2	337.7	68.9	5.82E-04	0.84
	150	1	26.9	40.7	9.86E-05	0.54	2	324.6	73.0	4.95E-04	0.71
	200	1	65.4	54.6	6.12E-05	0.34	2	299.9	77.3	4.02E-04	0.58
	250	1	100.5	58.3	4.28E-05	0.24	2	255.3	78.5	2.99E-04	0.43
	300	1	114.5	56.6	3.26E-05	0.18	2	235.0	77.5	2.15E-04	0.31
	350	1	127.7	44.6	2.56E-05	0.14	2	232.5	76.0	1.95E-04	0.28
	380	1	–	–	–	–	2	–	–	–	–
	400	1	156.0	33.6	2.21E-05	0.12	2	229.9	77.5	1.97E-04	0.28
	420	1	151.1	28.8	2.18E-05	0.12	2	–	–	–	–
	450	1	150.3	27.8	2.08E-05	0.11	2	296.6	61.8	1.32E-04	0.19
	480	1	157.6	25.5	1.62E-05	0.09	2	190.9	47.1	1.66E-05	0.02
	500	1	–	–	–	–	2	–	–	–	–
	520	1	146.8	11.6	1.18E-05	0.06	2	151.3	23.5	1.26E-05	0.02
	550	1	130.8	14.6	1.34E-05	0.07	2	168.7	21.7	8.00E-06	0.01
	580	1	218.5	-8.1	1.45E-05	0.08	2	–	–	–	–
	600	1	106.3	32.3	8.47E-06	0.05	2	113.7	11.0	4.13E-05	0.06
	620	1	–	–	–	–	2	–	–	–	–
	650	1	–	–	–	–	2	–	–	–	–
	680	1	–	–	–	–	2	–	–	–	–

Table 7. continued

Sample	Demag field (°C)	Run	Dec.	Inc.	Intensity (emu/cc)	I/I$_o$	Run	Dec.	Inc.	Intensity (emu/cc)	I/I$_o$
CLK11-PM65	0	1	355.0	28.9	8.56E-04	1.00	2	344.0	-7.4	1.05E-03	1.00
	100	1	357.2	29.3	7.70E-04	0.90	2	341.8	-6.0	1.01E-03	0.96
	150	1	352.6	32.6	6.84E-04	0.80	2	340.7	-3.5	9.20E-04	0.88
	200	1	352.0	32.3	5.77E-04	0.67	2	339.6	-3.6	8.90E-04	0.85
	250	1	355.7	32.5	4.40E-04	0.51	2	340.5	-2.8	6.77E-04	0.65
	300	1	355.0	31.7	3.27E-04	0.38	2	340.4	-2.5	6.46E-04	0.62
	350	1	355.6	32.0	2.54E-04	0.30	2	336.0	-3.9	6.34E-04	0.60
	380	1	–	–	–	–	2	–	–	–	–
	400	1	358.7	35.5	1.73E-04	0.20	2	339.9	-2.2	3.40E-04	0.32
	420	1	358.2	33.5	1.79E-04	0.21	2	339.4	-3.2	2.19E-04	0.21
	450	1	356.9	36.5	1.36E-04	0.16	2	336.6	-6.8	2.34E-04	0.22
	480	1	332.9	41.7	1.27E-04	0.15	2	337.1	-3.5	1.90E-04	0.18
	500	1	–	–	–	–	2	–	–	–	–
	520	1	1.3	27.5	1.37E-04	0.16	2	339.7	-3.2	1.14E-04	0.11
	550	1	354.9	34.2	1.28E-04	0.15	2	335.4	-4.8	1.10E-04	0.10
	580	1	354.4	35.7	1.21E-04	0.14	2	–	–	–	–
	600	1	349.6	35.6	8.81E-05	0.10	2	342.2	-2.8	1.15E-04	0.11
	620	1	–	–	–	–	2	–	–	–	–
	650	1	12.6	8.2	1.43E-05	0.02	2	–	–	–	–
	680	1	–	–	–	–	2	–	–	–	–
CLK11-PM66	0	1	10.9	-11.0	1.61E-04	1.00	2	1.9	-5.6	1.47E-04	1.00
	100	1	8.7	-10.5	1.38E-04	0.86	2	5.7	-5.6	1.38E-04	0.94
	150	1	9.0	-9.9	1.19E-04	0.74	2	4.1	-1.9	1.04E-04	0.71
	200	1	7.8	-10.5	1.01E-04	0.63	2	4.1	-5.9	1.02E-04	0.69
	250	1	12.0	-10.7	9.36E-05	0.58	2	4.0	-6.0	6.99E-05	0.47
	300	1	13.6	-12.4	8.60E-05	0.54	2	1.6	-5.5	6.88E-05	0.47
	350	1	12.8	-13.3	4.11E-05	0.26	2	4.2	-7.2	4.46E-05	0.30
	380	1	–	–	–	–	2	–	–	–	–
	400	1	12.5	-13.2	3.09E-05	0.19	2	3.2	-6.9	3.93E-05	0.27
	420	1	19.4	-6.7	3.34E-05	0.21	2	4.4	-3.3	3.52E-05	0.24
	450	1	9.4	-13.7	2.34E-05	0.15	2	2.6	-6.0	3.21E-05	0.22
	480	1	8.6	-11.1	2.45E-05	0.15	2	359.1	-3.9	3.17E-05	0.22
	500	1	–	–	–	–	2	–	–	–	–
	520	1	13.0	-16.5	2.45E-05	0.15	2	6.8	-0.8	2.69E-05	0.18
	550	1	10.2	-15.2	2.46E-05	0.15	2	3.4	-5.1	2.74E-05	0.19
	580	1	15.9	-17.1	2.39E-05	0.15	2	–	–	–	–
	600	1	12.3	-16.9	2.29E-05	0.14	2	354.8	-5.3	1.20E-05	0.08
	620	1	–	–	–	–	2	–	–	–	–
	650	1	–	–	–	–	2	–	–	–	–
	680	1	–	–	–	–	2	–	–	–	–
CLK11-PM67	0	1	8.5	-18.5	3.74E-04	1.00	2	16.3	15.6	3.82E-04	1.00
	100	1	23.6	-25.2	2.03E-04	0.54	2	21.1	25.7	2.52E-04	0.66
	150	1	36.0	-47.7	1.07E-04	0.29	2	162.4	45.3	1.60E-04	0.42
	200	1	170.6	-33.8	1.29E-04	0.35	2	172.6	25.5	2.27E-04	0.59
	250	1	183.2	-16.3	2.94E-04	0.79	2	173.8	23.3	2.30E-04	0.60
	300	1	182.5	-14.3	2.55E-04	0.68	2	174.6	25.6	1.18E-04	0.31
	350	1	181.1	-10.4	2.54E-04	0.68	2	187.9	12.6	5.93E-05	0.16
	380	1	–	–	–	–	2	–	–	–	–
	400	1	184.0	-13.4	2.23E-04	0.60	2	188.7	2.9	3.43E-05	0.09
	420	1	183.4	-14.0	1.87E-04	0.50	2	183.2	26.3	1.74E-05	0.05
	450	1	183.9	-14.2	1.66E-04	0.44	2	221.4	20.4	1.86E-05	0.05
	480	1	188.7	-17.2	1.18E-04	0.32	2	208.9	69.5	7.05E-06	0.02
	500	1	–	–	–	–	2	–	–	–	–
	520	1	215.9	-10.9	4.34E-05	0.12	2	212.4	-0.2	2.84E-05	0.07
	550	1	178.0	-12.1	4.32E-05	0.12	2	232.0	47.0	1.22E-05	0.03
	580	1	260.7	-36.3	2.12E-05	0.06	2	–	–	–	–
	600	1	202.4	-19.8	3.62E-05	0.10	2	148.9	38.4	3.37E-05	0.09
	620	1	–	–	–	–	2	–	–	–	–
	650	1	–	–	–	–	2	–	–	–	–
	680	1	–	–	–	–	2	–	–	–	–

Table 7. continued

Sample	Demag field (°C)	Run	Dec.	Inc.	Intensity (emu/cc)	I/I$_o$	Run	Dec.	Inc.	Intensity (emu/cc)	I/I$_o$
CLK11-PM68	0	1	31.6	-8.2	1.28E-04	1.00	2	18.4	-0.7	9.49E-05	1.00
	100	1	31.2	-6.4	9.33E-05	0.73	2	16.8	4.8	6.62E-05	0.70
	150	1	46.6	-12.9	3.12E-05	0.24	2	21.1	9.9	4.11E-05	0.43
	200	1	130.9	-23.8	1.49E-05	0.12	2	29.3	10.4	2.12E-05	0.22
	250	1	109.9	-31.8	1.44E-05	0.11	2	40.4	10.1	9.73E-06	0.10
	300	1	122.1	-32.3	1.30E-05	0.10	2	33.3	4.1	6.22E-06	0.07
	350	1	134.5	-32.9	1.17E-05	0.09	2	3.5	-14.3	4.59E-06	0.05
	380	1	–	–	–	–	2	–	–	–	–
	400	1	160.9	-27.5	1.07E-05	0.08	2	6.2	1.2	6.05E-06	0.06
	420	1	145.4	-44.3	1.28E-05	0.10	2	30.9	-5.6	2.22E-06	0.02
	450	1	159.1	-33.4	1.51E-05	0.12	2	335.2	38.0	2.02E-06	0.02
	480	1	168.4	-12.5	2.14E-05	0.17	2	60.1	39.5	1.84E-06	0.02
	500	1	–	–	–	–	2	–	–	–	–
	520	1	203.2	-19.9	1.51E-05	0.12	2	299.8	36.1	4.02E-06	0.04
	550	1	178.3	-4.4	2.24E-05	0.17	2	309.6	15.8	4.53E-06	0.05
	580	1	181.3	-10.4	1.16E-05	0.09	2	–	–	–	–
	600	1	179.1	-26.1	6.52E-06	0.05	2	258.3	-9.0	5.20E-06	0.05
	620	1	–	–	–	–	2	–	–	–	–
	650	1	–	–	–	–	2	–	–	–	–
	680	1	–	–	–	–	2	–	–	–	–
CLK11-PM69	0	1	190.1	-0.8	3.76E-04	1.00	2	187.2	-5.7	3.71E-04	1.00
	100	1	187.3	-1.3	5.51E-04	1.46	2	182.1	-7.5	4.05E-04	1.09
	150	1	185.3	-0.3	7.43E-04	1.98	2	180.5	-3.2	4.58E-04	1.23
	200	1	183.2	-1.7	8.06E-04	2.14	2	173.6	-3.7	6.95E-04	1.87
	250	1	189.0	0.5	6.85E-04	1.82	2	177.9	-3.5	6.84E-04	1.84
	300	1	185.9	2.6	5.52E-04	1.47	2	178.0	-5.2	3.83E-04	1.03
	350	1	185.0	-0.8	5.34E-04	1.42	2	177.3	-5.6	3.73E-04	1.00
	380	1	–	–	–	–	2	–	–	–	–
	400	1	188.1	2.7	3.72E-04	0.99	2	176.1	-4.9	2.27E-04	0.61
	420	1	183.0	-2.5	3.64E-04	0.97	2	174.2	-3.6	2.12E-04	0.57
	450	1	187.7	-0.4	3.00E-04	0.80	2	178.5	-6.4	1.63E-04	0.44
	480	1	190.3	-7.0	1.67E-04	0.44	2	178.5	-2.0	1.54E-04	0.41
	500	1	–	–	–	–	2	–	–	–	–
	520	1	194.6	-3.3	1.32E-04	0.35	2	167.6	-3.3	1.16E-04	0.31
	550	1	178.4	2.4	1.40E-04	0.37	2	188.1	-0.2	1.21E-04	0.33
	580	1	175.8	-5.5	1.08E-04	0.29	2	–	–	–	–
	600	1	206.1	-7.5	7.47E-05	0.20	2	146.0	4.0	1.24E-04	0.33
	620	1	–	–	–	–	2	–	–	–	–
	650	1	–	–	–	–	2	120.3	-29.4	6.57E-06	0.02
	680	1	–	–	–	–	2	–	–	–	–
41-1	0	1	20.4	-43.1	6.44E-04	1.00	2	25.2	-13.7	6.51E-04	1.00
	100	1	24.2	-43.6	5.27E-04	0.82	2	27.9	-13.5	5.05E-04	0.78
	150	1	37.5	-48.8	3.63E-04	0.56	2	34.5	-16.2	3.77E-04	0.58
	200	1	68.5	-52.6	2.12E-04	0.33	2	48.5	-21.8	2.20E-04	0.34
	250	1	114.9	-42.7	1.29E-04	0.20	2	73.5	-29.5	1.20E-04	0.18
	300	1	118.8	-38.8	9.91E-05	0.15	2	100.7	-28.2	8.59E-05	0.13
	350	1	120.4	-36.9	9.00E-05	0.14	2	101.3	-30.3	8.15E-05	0.13
	380	1	–	–	–	–	2	–	–	–	–
	400	1	128.0	-32.8	7.45E-05	0.12	2	129.2	-30.5	6.57E-05	0.10
	420	1	128.4	-29.6	7.39E-05	0.11	2	–	–	–	–
	450	1	133.8	-27.6	6.66E-05	0.10	2	158.5	-45.0	5.55E-05	0.09
	480	1	116.8	-23.4	5.03E-05	0.08	2	134.9	-39.9	8.31E-05	0.13
	500	1	–	–	–	–	2	–	–	–	–
	520	1	144.3	-19.7	4.20E-05	0.07	2	131.7	-37.2	2.67E-05	0.04
	550	1	149.7	-49.6	2.05E-05	0.03	2	55.0	-3.2	4.74E-05	0.07
	580	1	121.2	-49.0	1.24E-05	0.02	2	–	–	–	–
	600	1	136.9	-16.9	1.60E-05	0.02	2	182.8	-33.3	1.56E-05	0.02
	620	1	–	–	–	–	2	–	–	–	–
	650	1	–	–	–	–	2	–	–	–	–
	680	1	–	–	–	–	2	–	–	–	–

Table 7. continued

Sample	Demag field (°C)	Run	Dec.	Inc.	Intensity (emu/cc)	I/I$_o$	Run	Dec.	Inc.	Intensity (emu/cc)	I/I$_o$
41-2	0	1	22.4	-60.4	8.57E-06	1.00	2	356.2	-59.9	1.05E-05	1.00
	100	1	163.4	-63.4	4.29E-06	0.50	2	340.1	-55.2	7.07E-06	0.67
	150	1	184.9	-41.9	4.44E-06	0.52	2	272.0	-54.0	3.14E-06	0.30
	200	1	164.8	-30.2	4.06E-06	0.47	2	273.7	-56.8	2.89E-06	0.28
	250	1	170.7	-33.2	2.80E-06	0.33	2	251.9	-30.9	2.21E-06	0.21
	300	1	168.3	-30.7	2.10E-06	0.25	2	262.3	-39.7	2.07E-06	0.20
	350	1	174.6	-16.0	2.17E-06	0.25	2	275.8	-54.8	1.79E-06	0.17
	380	1	–	–	–	–	2	–	–	–	–
	400	1	150.0	-25.2	1.28E-06	0.15	2	300.7	-33.1	1.58E-06	0.15
	420	1	178.4	-30.7	1.00E-06	0.12	2	273.3	-30.9	1.41E-06	0.13
	450	1	194.5	-25.1	1.22E-06	0.14	2	331.8	-13.5	8.69E-07	0.08
	480	1	185.3	-37.2	1.97E-06	0.23	2	338.5	-31.6	8.89E-07	0.08
	500	1	–	–	–	–	2	–	–	–	–
	520	1	91.2	-32.5	1.50E-06	0.17	2	35.5	-64.2	6.95E-07	0.07
	550	1	59.1	-25.3	1.22E-06	0.14	2	254.0	-22.0	1.52E-06	0.14
	580	1	187.8	-42.7	1.74E-06	0.20	2	–	–	–	–
	600	1	24.5	-62.6	4.01E-07	0.05	2	287.5	-40.1	1.82E-06	0.17
	620	1	–	–	–	–	2	–	–	–	–
	650	1	76.1	-74.0	4.80E-07	0.06	2	–	–	–	–
	680	1	–	–	–	–	2	–	–	–	–
41-3	0	1	5.6	-51.0	9.83E-06	1.00	2	24.2	-37.8	9.49E-06	1.00
	100	1	171.6	-74.9	3.88E-06	0.40	2	18.4	-46.6	5.03E-06	0.53
	150	1	191.7	-40.4	4.56E-06	0.46	2	76.8	-80.5	2.46E-06	0.26
	200	1	172.2	-28.0	5.15E-06	0.52	2	183.4	-32.4	3.03E-06	0.32
	250	1	178.9	-25.6	3.56E-06	0.36	2	182.2	-31.6	2.93E-06	0.31
	300	1	174.9	-24.6	2.85E-06	0.29	2	185.4	-27.8	2.19E-06	0.23
	350	1	163.0	-16.1	2.84E-06	0.29	2	191.7	-46.7	2.38E-06	0.25
	380	1	–	–	–	–	2	–	–	–	–
	400	1	173.4	-20.0	1.86E-06	0.19	2	196.8	-43.7	1.63E-06	0.17
	420	1	174.5	-18.4	2.35E-06	0.24	2	208.6	-59.4	1.26E-06	0.13
	450	1	171.1	-25.5	2.12E-06	0.22	2	210.2	-38.5	8.25E-07	0.09
	480	1	174.5	-30.2	2.04E-06	0.21	2	296.4	-33.0	1.02E-06	0.11
	500	1	–	–	–	–	2	–	–	–	–
	520	1	187.5	-40.6	1.90E-06	0.19	2	155.4	-68.4	8.56E-07	0.09
	550	1	163.0	-7.4	3.33E-06	0.34	2	335.6	9.4	2.97E-07	0.03
	580	1	211.8	-34.2	2.29E-06	0.23	2	–	–	–	–
	600	1	177.6	-17.7	1.75E-06	0.18	2	10.6	12.4	9.50E-07	0.10
	620	1	–	–	–	–	2	–	–	–	–
	650	1	–	–	–	–	2	–	–	–	–
	680	1	–	–	–	–	2	–	–	–	–
41-4	0	1	10.6	-45.4	2.29E-06	1.00	2	14.3	-26.1	2.69E-06	1.00
	100	1	128.3	-67.2	1.01E-06	0.44	2	151.8	-44.1	9.17E-07	0.34
	150	1	132.5	-53.8	1.11E-06	0.48	2	151.4	-49.0	9.74E-07	0.36
	200	1	160.7	-45.9	1.07E-06	0.47	2	170.0	-25.1	1.14E-06	0.42
	250	1	174.7	-32.7	6.65E-07	0.29	2	107.1	-54.5	6.97E-07	0.26
	300	1	176.2	-35.6	5.00E-07	0.22	2	177.1	-12.5	6.49E-07	0.24
	350	1	161.2	-42.4	3.20E-07	0.14	2	172.3	-16.0	6.21E-07	0.23
	380	1	–	–	–	–	2	–	–	–	–
	400	1	155.5	-39.3	3.22E-07	0.14	2	211.3	-5.0	2.04E-07	0.08
	420	1	211.8	-36.9	2.12E-07	0.09	2	–	–	–	–
	450	1	237.6	-51.9	2.02E-07	0.09	2	223.7	-50.6	7.16E-07	0.27
	480	1	25.3	-80.9	3.54E-07	0.15	2	351.5	-33.0	7.52E-07	0.28
	500	1	–	–	–	–	2	–	–	–	–
	520	1	277.9	-72.6	3.22E-07	0.14	2	44.1	-40.6	2.51E-07	0.09
	550	1	40.9	-43.2	4.18E-07	0.18	2	295.5	-43.0	1.53E-06	0.57
	580	1	315.1	-31.2	1.14E-06	0.50	2	–	–	–	–
	600	1	295.9	-28.0	3.21E-07	0.14	2	123.1	52.0	1.45E-07	0.05
	620	1	–	–	–	–	2	–	–	–	–
	650	1	184.0	-45.6	2.64E-07	0.12	2	–	–	–	–
	680	1	–	–	–	–	2	–	–	–	–

Table 7. continued

Sample	Demag field (°C)	Run	Dec.	Inc.	Intensity (emu/cc)	I/I$_o$	Run	Dec.	Inc.	Intensity (emu/cc)	I/I$_o$
41-5	0	1	49.9	-67.0	5.31E-06	1.00	2	–	–	–	–
	100	1	163.4	-44.2	2.75E-06	0.52	2	–	–	–	–
	150	1	180.3	-23.2	3.98E-06	0.75	2	–	–	–	–
	200	1	179.5	-13.4	3.92E-06	0.74	2	–	–	–	–
	250	1	178.3	-5.3	3.16E-06	0.60	2	–	–	–	–
	300	1	183.3	-4.8	2.71E-06	0.51	2	–	–	–	–
	350	1	180.8	-5.4	9.65E-07	0.18	2	–	–	–	–
	380	1	–	–	–	–	2	–	–	–	–
	400	1	144.7	-33.7	3.09E-07	0.06	2	–	–	–	–
	420	1	210.9	-54.1	3.05E-07	0.06	2	–	–	–	–
	450	1	306.8	-21.5	3.27E-07	0.06	2	–	–	–	–
	480	1	7.7	-42.6	1.27E-06	0.24	2	–	–	–	–
	500	1	–	–	–	–	2	–	–	–	–
	520	1	359.1	-55.6	9.81E-07	0.18	2	–	–	–	–
	550	1	249.9	-44.5	1.48E-06	0.28	2	–	–	–	–
	580	1	317.5	-38.4	2.71E-06	0.51	2	–	–	–	–
	600	1	289.5	-23.7	1.24E-06	0.23	2	–	–	–	–
	620	1	–	–	–	–	2	–	–	–	–
	650	1	21.3	2.8	1.12E-06	0.21	2	–	–	–	–
	680	1	–	–	–	–	2	–	–	–	–
41-6	0	1	241.9	-83.1	3.75E-05	1.00	2	303.4	-82.3	4.60E-05	1.00
	100	1	212.3	-66.6	4.22E-05	1.12	2	202.7	-60.2	4.43E-05	0.96
	150	1	204.6	-62.2	4.36E-05	1.16	2	196.0	-46.1	4.97E-05	1.08
	200	1	200.4	-55.3	4.72E-05	1.26	2	197.1	-27.6	6.23E-05	1.36
	250	1	184.5	-38.6	5.12E-05	1.36	2	195.3	-26.1	6.37E-05	1.39
	300	1	193.5	-39.4	4.88E-05	1.30	2	195.0	-19.3	6.49E-05	1.41
	350	1	194.1	-34.1	4.32E-05	1.15	2	193.3	-20.9	6.39E-05	1.39
	380	1	–	–	–	–	2	–	–	–	–
	400	1	192.7	-32.8	3.84E-05	1.02	2	192.2	-16.8	5.69E-05	1.24
	420	1	192.4	-33.7	3.76E-05	1.00	2	193.9	-15.9	5.76E-05	1.25
	450	1	193.5	-33.6	3.55E-05	0.95	2	195.5	-14.9	4.80E-05	1.05
	480	1	193.8	-35.4	3.44E-05	0.92	2	192.4	-10.7	4.54E-05	0.99
	500	1	–	–	–	–	2	–	–	–	–
	520	1	189.1	-36.0	3.66E-05	0.98	2	191.2	-13.5	4.31E-05	0.94
	550	1	193.8	-32.8	3.64E-05	0.97	2	191.6	-15.2	4.08E-05	0.89
	580	1	185.3	-35.3	3.47E-05	0.93	2	–	–	–	–
	600	1	187.6	-31.6	3.60E-05	0.96	2	199.8	-13.4	4.32E-05	0.94
	620	1	–	–	–	–	2	–	–	–	–
	650	1	178.4	-10.0	4.75E-06	0.13	2	184.1	-12.1	2.92E-05	0.64
	680	1	–	–	–	–	2	–	–	–	–
41-7	0	1	359.2	-5.2	1.99E-05	1.00	2	15.0	9.7	1.66E-05	1.00
	100	1	1.7	-1.3	7.87E-06	0.40	2	6.0	5.0	7.65E-06	0.46
	150	1	349.9	-6.2	5.15E-06	0.26	2	350.9	-3.3	2.45E-06	0.15
	200	1	354.8	2.9	2.69E-06	0.14	2	45.5	-46.5	4.25E-06	0.26
	250	1	6.4	1.1	1.65E-06	0.08	2	340.9	-66.6	1.43E-06	0.09
	300	1	327.3	-35.3	1.42E-06	0.07	2	326.5	-1.5	3.44E-06	0.21
	350	1	354.8	-45.2	4.70E-07	0.02	2	327.7	24.2	2.88E-07	0.02
	380	1	–	–	–	–	2	–	–	–	–
	400	1	342.1	-12.1	1.70E-06	0.09	2	198.6	-74.8	1.91E-06	0.12
	420	1	6.8	-14.6	2.23E-06	0.11	2	–	–	–	–
	450	1	80.3	-40.4	1.05E-06	0.05	2	286.9	-72.3	3.74E-06	0.23
	480	1	107.4	-16.0	8.75E-06	0.44	2	16.0	63.4	3.69E-06	0.22
	500	1	–	–	–	–	2	–	–	–	–
	520	1	263.5	-19.2	1.04E-06	0.05	2	308.5	9.9	8.48E-07	0.05
	550	1	237.1	-30.6	1.32E-06	0.07	2	76.2	-56.0	5.27E-06	0.32
	580	1	61.8	9.4	5.88E-06	0.30	2	–	–	–	–
	600	1	276.3	-37.7	3.48E-06	0.18	2	277.8	-52.9	1.79E-05	1.08
	620	1	–	–	–	–	2	–	–	–	–
	650	1	20.8	-36.8	9.58E-06	0.48	2	–	–	–	–
	680	1	–	–	–	–	2	–	–	–	–

Table 7. continued

Sample	Demag field (°C)	Run	Dec.	Inc.	Intensity (emu/cc)	I/I_o	Run	Dec.	Inc.	Intensity (emu/cc)	I/I_o
41-8	0	1	294.6	-72.7	9.64E-06	1.00	2	201.0	-8.5	1.82E-05	1.00
	100	1	187.2	-41.5	2.15E-05	2.23	2	201.8	8.6	3.39E-05	1.86
	150	1	187.0	-35.7	2.72E-05	2.82	2	200.6	11.7	3.57E-05	1.96
	200	1	185.9	-32.6	2.95E-05	3.06	2	200.3	12.9	4.02E-05	2.21
	250	1	185.4	-30.8	2.96E-05	3.07	2	195.7	14.4	3.41E-05	1.87
	300	1	184.7	-32.7	2.74E-05	2.84	2	196.1	15.3	2.99E-05	1.64
	350	1	189.3	-30.8	2.38E-05	2.46	2	200.5	-1.3	1.50E-05	0.82
	380	1	–	–	–	–	2	–	–	–	–
	400	1	185.1	-31.5	2.22E-05	2.30	2	195.5	3.5	1.62E-05	0.89
	420	1	194.3	-34.1	1.88E-05	1.95	2	200.5	12.9	1.18E-05	0.65
	450	1	189.3	-33.7	1.68E-05	1.75	2	182.1	17.5	6.96E-06	0.38
	480	1	223.2	-28.1	2.53E-05	2.63	2	224.1	4.1	5.92E-06	0.33
	500	1	–	–	–	–	2	–	–	–	–
	520	1	184.9	-31.6	1.37E-05	1.42	2	285.1	-9.7	4.09E-06	0.22
	550	1	171.1	-40.6	1.21E-05	1.26	2	288.2	12.4	3.08E-06	0.17
	580	1	306.6	-3.6	8.54E-06	0.89	2	–	–	–	–
	600	1	197.2	-33.1	1.09E-05	1.13	2	330.6	48.9	1.74E-06	0.10
	620	1	–	–	–	–	2	–	–	–	–
	650	1	92.0	8.3	3.02E-06	0.31	2	–	–	–	–
	680	1	–	–	–	–	2	–	–	–	–
41-9	0	1	–	–	–	–	2	–	–	–	–
	100	1	–	–	–	–	2	–	–	–	–
	150	1	–	–	–	–	2	–	–	–	–
	200	1	–	–	–	–	2	–	–	–	–
	250	1	–	–	–	–	2	–	–	–	–
	300	1	–	–	–	–	2	–	–	–	–
	350	1	–	–	–	–	2	–	–	–	–
	380	1	–	–	–	–	2	–	–	–	–
	400	1	–	–	–	–	2	–	–	–	–
	420	1	–	–	–	–	2	–	–	–	–
	450	1	–	–	–	–	2	–	–	–	–
	480	1	–	–	–	–	2	–	–	–	–
	500	1	–	–	–	–	2	–	–	–	–
	520	1	–	–	–	–	2	–	–	–	–
	550	1	–	–	–	–	2	–	–	–	–
	580	1	–	–	–	–	2	–	–	–	–
	600	1	–	–	–	–	2	–	–	–	–
	620	1	–	–	–	–	2	–	–	–	–
	650	1	–	–	–	–	2	–	–	–	–
	680	1	–	–	–	–	2	–	–	–	–
41-10	0	1	226.7	-51.8	1.28E-05	1.00	2	225.2	-49.1	1.19E-05	1.00
	100	1	213.0	-24.0	1.52E-05	1.19	2	202.1	-17.3	1.54E-05	1.29
	150	1	211.1	-16.5	1.77E-05	1.39	2	200.2	-10.8	1.71E-05	1.43
	200	1	209.1	-11.6	1.83E-05	1.43	2	198.1	-4.2	1.70E-05	1.43
	250	1	207.9	-10.0	1.76E-05	1.38	2	194.3	-4.6	1.54E-05	1.29
	300	1	203.9	-11.6	1.54E-05	1.21	2	186.4	-3.7	9.58E-06	0.80
	350	1	209.1	-9.5	1.36E-05	1.06	2	189.2	-5.1	9.45E-06	0.79
	380	1	–	–	–	–	2	–	–	–	–
	400	1	206.3	-3.8	2.10E-06	0.16	2	192.3	-2.4	5.17E-06	0.43
	420	1	239.8	-17.0	3.32E-06	0.26	2	215.0	4.3	5.30E-06	0.44
	450	1	210.3	-13.1	1.42E-06	0.11	2	197.7	3.0	3.68E-06	0.31
	480	1	41.9	-3.2	7.77E-06	0.61	2	145.3	9.3	6.00E-07	0.05
	500	1	–	–	–	–	2	–	–	–	–
	520	1	11.8	-50.4	5.07E-07	0.04	2	281.5	-21.0	2.85E-07	0.02
	550	1	207.2	-21.2	7.85E-07	0.06	2	218.6	-25.2	8.87E-07	0.07
	580	1	177.3	-65.6	3.13E-07	0.02	2	–	–	–	–
	600	1	201.8	-13.5	2.12E-07	0.02	2	12.3	-24.9	9.27E-07	0.08
	620	1	–	–	–	–	2	–	–	–	–
	650	1	–	–	–	–	2	–	–	–	–
	680	1	–	–	–	–	2	–	–	–	–

Table 7. continued

Sample	Demag field (°C)	Run	Dec.	Inc.	Intensity (emu/cc)	I/I$_o$	Run	Dec.	Inc.	Intensity (emu/cc)	I/I$_o$
41-11	0	1	196.5	-35.0	4.75E-05	1.00	2	206.9	-23.7	5.24E-05	1.00
	100	1	201.5	-24.2	5.16E-05	1.09	2	212.9	-7.8	5.38E-05	1.03
	150	1	202.1	-10.8	5.75E-05	1.21	2	209.7	1.6	5.62E-05	1.07
	200	1	199.5	-11.0	5.62E-05	1.18	2	211.3	4.0	4.71E-05	0.90
	250	1	200.0	-4.1	5.50E-05	1.16	2	213.7	3.8	4.44E-05	0.85
	300	1	203.8	-6.3	3.50E-05	0.74	2	211.9	2.8	2.95E-05	0.56
	350	1	204.3	-6.0	2.85E-05	0.60	2	208.5	3.1	2.88E-05	0.55
	380	1	–	–	–	–	2	–	–	–	–
	400	1	210.4	-2.4	2.72E-05	0.57	2	–	–	–	–
	420	1	195.8	-2.7	2.07E-05	0.44	2	–	–	–	–
	450	1	201.8	-4.6	1.77E-05	0.37	2	–	–	–	–
	480	1	48.6	13.5	8.96E-05	1.88	2	–	–	–	–
	500	1	–	–	–	–	2	–	–	–	–
	520	1	192.7	-9.2	9.45E-06	0.20	2	–	–	–	–
	550	1	210.0	-12.4	9.11E-06	0.19	2	–	–	–	–
	580	1	235.0	-12.2	2.96E-06	0.06	2	–	–	–	–
	600	1	174.6	24.7	1.16E-06	0.02	2	–	–	–	–
	620	1	–	–	–	–	2	–	–	–	–
	650	1	–	–	–	–	2	–	–	–	–
	680	1	–	–	–	–	2	–	–	–	–
41-12	0	1	232.2	-24.3	5.83E-05	1.00	2	248.2	-38.1	4.67E-05	1.00
	100	1	232.4	-6.1	7.35E-05	1.26	2	226.9	-19.9	5.12E-05	1.10
	150	1	229.2	-2.8	7.68E-05	1.32	2	227.3	-13.5	5.43E-05	1.16
	200	1	228.3	1.7	7.61E-05	1.30	2	219.9	-5.8	5.87E-05	1.26
	250	1	227.4	2.9	6.78E-05	1.16	2	220.0	-3.4	5.51E-05	1.18
	300	1	229.5	3.3	6.05E-05	1.04	2	220.0	-2.0	5.00E-05	1.07
	350	1	233.1	4.0	5.38E-05	0.92	2	209.3	-6.3	5.17E-05	1.11
	380	1	–	–	–	–	2	–	–	–	–
	400	1	228.5	4.1	4.88E-05	0.84	2	224.3	-2.6	4.46E-05	0.96
	420	1	229.7	4.7	4.55E-05	0.78	2	–	–	–	–
	450	1	232.7	4.5	3.95E-05	0.68	2	179.2	10.6	5.56E-05	1.19
	480	1	6.5	19.4	4.20E-04	7.21	2	226.0	-4.3	2.99E-05	0.64
	500	1	–	–	–	–	2	–	–	–	–
	520	1	240.4	7.8	2.44E-05	0.42	2	217.3	-0.8	2.88E-05	0.62
	550	1	231.0	4.8	2.97E-05	0.51	2	228.1	-38.3	2.34E-05	0.50
	580	1	289.2	7.0	1.25E-05	0.21	2	–	–	–	–
	600	1	246.7	-13.7	7.49E-06	0.13	2	228.0	-11.0	8.09E-06	0.17
	620	1	–	–	–	–	2	–	–	–	–
	650	1	123.4	-30.4	3.56E-06	0.06	2	–	–	–	–
	680	1	–	–	–	–	2	–	–	–	–
41-13	0	1	255.1	-71.3	4.79E-04	1.00	2	230.6	-72.4	5.01E-04	1.00
	100	1	249.2	-62.1	4.35E-04	0.91	2	231.2	-66.3	4.61E-04	0.92
	150	1	232.9	-42.2	3.92E-04	0.82	2	220.4	-42.2	4.05E-04	0.81
	200	1	226.8	-24.4	3.82E-04	0.80	2	216.0	-27.4	4.04E-04	0.81
	250	1	223.4	-17.6	3.32E-04	0.69	2	215.1	-19.2	3.78E-04	0.76
	300	1	224.8	-16.9	2.74E-04	0.57	2	213.8	-20.1	3.35E-04	0.67
	350	1	225.7	-15.1	2.24E-04	0.47	2	212.3	-16.6	2.74E-04	0.55
	380	1	–	–	–	–	2	–	–	–	–
	400	1	222.9	-16.0	1.57E-04	0.33	2	214.4	-16.7	2.67E-04	0.53
	420	1	229.2	-14.7	1.31E-04	0.27	2	–	–	–	–
	450	1	229.9	-13.6	1.09E-04	0.23	2	149.7	59.4	1.84E-04	0.37
	480	1	156.9	-32.7	1.18E-04	0.25	2	222.6	-17.7	9.41E-05	0.19
	500	1	–	–	–	–	2	–	–	–	–
	520	1	224.8	-10.5	6.92E-05	0.14	2	227.2	-17.1	1.09E-04	0.22
	550	1	212.9	-5.0	7.81E-05	0.16	2	231.0	-22.2	5.13E-05	0.10
	580	1	220.4	-6.9	2.44E-05	0.05	2	–	–	–	–
	600	1	230.1	-8.3	4.65E-05	0.10	2	295.9	-0.8	5.58E-05	0.11
	620	1	–	–	–	–	2	–	–	–	–
	650	1	–	–	–	–	2	–	–	–	–
	680	1	–	–	–	–	2	–	–	–	–

Table 7. continued

Sample	Demag field (°C)	Run	Dec.	Inc.	Intensity (emu/cc)	I/I$_o$	Run	Dec.	Inc.	Intensity (emu/cc)	I/I$_o$
41-14	0	1	227.3	-34.8	1.09E-04	1.00	2	236.7	-38.2	8.70E-05	1.00
	100	1	220.8	-25.5	1.15E-04	1.06	2	224.8	-24.8	8.47E-05	0.97
	150	1	218.1	-19.5	1.17E-04	1.07	2	220.7	-15.4	8.23E-05	0.95
	200	1	213.6	-13.3	1.15E-04	1.06	2	216.6	-12.3	8.04E-05	0.92
	250	1	213.7	-10.2	1.06E-04	0.98	2	212.8	-13.7	7.93E-05	0.91
	300	1	212.2	-11.3	8.72E-05	0.80	2	210.6	-10.6	5.83E-05	0.67
	350	1	212.1	-8.1	7.45E-05	0.68	2	209.3	-10.7	4.47E-05	0.51
	380	1	208.3	-9.2	6.03E-05	0.55	2	209.9	-10.4	4.07E-05	0.47
	400	1	216.9	-8.6	5.86E-05	0.54	2	207.7	-5.5	3.58E-05	0.41
	420	1	211.3	-10.1	4.59E-05	0.42	2	210.2	-6.3	3.31E-05	0.38
	450	1	350.5	-27.0	4.32E-05	0.40	2	207.6	-11.4	2.54E-05	0.29
	480	1	212.2	-8.4	3.21E-05	0.30	2	217.8	-6.8	2.48E-05	0.28
	500	1	228.7	-6.2	3.58E-05	0.33	2	230.5	-5.7	2.24E-05	0.26
	520	1	205.3	-3.8	2.41E-05	0.22	2	203.6	10.1	5.95E-06	0.07
	550	1	196.9	-10.5	1.73E-05	0.16	2	–	–	–	–
	580	1	–	–	–	–	2	–	–	–	–
	600	1	–	–	–	–	2	–	–	–	–
	620	1	–	–	–	–	2	–	–	–	–
	650	1	–	–	–	–	2	–	–	–	–
	680	1	–	–	–	–	2	–	–	–	–
41-15	0	1	–	–	–	–	2	–	–	–	–
	100	1	–	–	–	–	2	–	–	–	–
	150	1	–	–	–	–	2	–	–	–	–
	200	1	–	–	–	–	2	–	–	–	–
	250	1	–	–	–	–	2	–	–	–	–
	300	1	–	–	–	–	2	–	–	–	–
	350	1	–	–	–	–	2	–	–	–	–
	380	1	–	–	–	–	2	–	–	–	–
	400	1	–	–	–	–	2	–	–	–	–
	420	1	–	–	–	–	2	–	–	–	–
	450	1	–	–	–	–	2	–	–	–	–
	480	1	–	–	–	–	2	–	–	–	–
	500	1	–	–	–	–	2	–	–	–	–
	520	1	–	–	–	–	2	–	–	–	–
	550	1	–	–	–	–	2	–	–	–	–
	580	1	–	–	–	–	2	–	–	–	–
	600	1	–	–	–	–	2	–	–	–	–
	620	1	–	–	–	–	2	–	–	–	–
	650	1	–	–	–	–	2	–	–	–	–
	680	1	–	–	–	–	2	–	–	–	–
41-16	0	1	235.0	-60.7	3.62E-04	1.00	2	92.6	-24.2	3.68E-04	1.00
	100	1	215.3	-41.0	3.68E-04	1.02	2	123.6	-13.1	2.89E-04	0.79
	150	1	196.9	-14.2	4.75E-04	1.31	2	141.1	-1.6	3.14E-04	0.85
	200	1	198.8	-2.0	5.62E-04	1.55	2	153.8	5.4	3.32E-04	0.90
	250	1	195.2	3.6	5.64E-04	1.56	2	156.6	10.0	3.02E-04	0.82
	300	1	194.6	5.1	5.04E-04	1.39	2	168.6	14.7	2.59E-04	0.70
	350	1	193.2	1.3	3.49E-04	0.97	2	167.5	7.2	1.98E-04	0.54
	380	1	–	–	–	–	2	–	–	–	–
	400	1	189.3	-1.9	2.65E-04	0.73	2	169.0	11.0	1.27E-04	0.35
	420	1	188.2	5.5	2.35E-04	0.65	2	166.8	8.1	1.10E-04	0.30
	450	1	196.4	5.8	1.96E-04	0.54	2	177.3	22.5	6.03E-05	0.16
	480	1	176.0	-6.2	2.06E-04	0.57	2	162.4	2.8	6.25E-05	0.17
	500	1	–	–	–	–	2	–	–	–	–
	520	1	192.2	9.3	1.36E-04	0.38	2	190.4	8.1	7.27E-05	0.20
	550	1	205.9	7.2	1.46E-04	0.40	2	183.1	2.9	4.43E-05	0.12
	580	1	171.1	18.1	6.78E-05	0.19	2	–	–	–	–
	600	1	203.3	1.7	9.21E-05	0.25	2	175.6	4.9	7.89E-05	0.21
	620	1	–	–	–	–	2	–	–	–	–
	650	1	–	–	–	–	2	185.6	-1.8	3.24E-05	0.09
	680	1	–	–	–	–	2	–	–	–	–

Table 7. continued

Sample	Demag field (°C)	Run	Dec.	Inc.	Intensity (emu/cc)	I/I$_o$	Run	Dec.	Inc.	Intensity (emu/cc)	I/I$_o$
41-17	0	1	296.6	-41.5	3.03E-04	1.00	2	146.5	-85.7	2.16E-04	1.00
	100	1	300.7	-39.5	2.42E-04	0.80	2	185.5	-83.4	1.84E-04	0.85
	150	1	292.5	-37.1	1.94E-04	0.64	2	176.4	-74.8	1.03E-04	0.48
	200	1	293.6	-28.5	1.56E-04	0.51	2	172.7	-68.4	7.94E-05	0.37
	250	1	288.7	-23.4	1.23E-04	0.41	2	179.4	-49.4	5.15E-05	0.24
	300	1	288.1	-21.0	1.01E-04	0.33	2	169.5	-45.9	4.22E-05	0.20
	350	1	295.2	-21.1	8.19E-05	0.27	2	171.9	-43.5	2.84E-05	0.13
	380	1	–	–	–	–	2	–	–	–	–
	400	1	284.7	-18.9	6.57E-05	0.22	2	163.3	-37.1	1.77E-05	0.08
	420	1	293.1	-18.0	6.40E-05	0.21	2	–	–	–	–
	450	1	278.6	-17.5	4.13E-05	0.14	2	355.6	53.7	7.39E-05	0.34
	480	1	246.2	-9.4	4.37E-05	0.14	2	222.6	33.5	2.30E-06	0.01
	500	1	–	–	–	–	2	–	–	–	–
	520	1	265.1	0.2	2.86E-05	0.09	2	75.2	1.8	1.19E-05	0.05
	550	1	253.7	-0.3	2.16E-05	0.07	2	90.7	20.8	8.97E-06	0.04
	580	1	51.1	-27.2	3.85E-05	0.13	2	–	–	–	–
	600	1	248.6	-16.4	2.94E-05	0.10	2	333.2	-2.8	3.06E-05	0.14
	620	1	–	–	–	–	2	–	–	–	–
	650	1	–	–	–	–	2	–	–	–	–
	680	1	–	–	–	–	2	–	–	–	–
41-18	0	1	351.0	-12.1	3.41E-03	1.00	2	18.7	-1.9	3.63E-03	1.00
	100	1	347.4	-9.7	3.26E-03	0.96	2	17.4	0.4	3.00E-03	0.83
	150	1	347.7	-7.6	2.68E-03	0.79	2	20.0	1.6	2.85E-03	0.78
	200	1	350.9	-2.2	2.05E-03	0.60	2	21.4	9.1	1.50E-03	0.41
	250	1	354.0	-0.1	1.68E-03	0.49	2	22.9	11.2	1.04E-03	0.29
	300	1	350.1	3.8	1.17E-03	0.34	2	19.8	11.3	6.00E-04	0.17
	350	1	350.5	4.2	8.47E-04	0.25	2	13.9	4.2	5.64E-04	0.16
	380	1	–	–	–	–	2	–	–	–	–
	400	1	356.9	-5.2	6.72E-04	0.20	2	28.8	10.5	3.75E-04	0.10
	420	1	345.4	-3.2	6.76E-04	0.20	2	18.3	4.6	4.12E-04	0.11
	450	1	357.3	-5.3	5.40E-04	0.16	2	22.4	16.5	3.30E-04	0.09
	480	1	346.1	-53.1	4.16E-04	0.12	2	9.8	25.0	3.48E-04	0.10
	500	1	–	–	–	–	2	–	–	–	–
	520	1	353.9	-18.2	4.34E-04	0.13	2	30.1	20.7	3.03E-04	0.08
	550	1	335.8	-3.9	3.51E-04	0.10	2	51.5	25.9	2.32E-04	0.06
	580	1	279.5	36.6	7.05E-05	0.02	2	–	–	–	–
	600	1	350.8	-54.5	2.01E-04	0.06	2	40.6	13.1	1.43E-04	0.04
	620	1	–	–	–	–	2	–	–	–	–
	650	1	–	–	–	–	2	–	–	–	–
	680	1	–	–	–	–	2	–	–	–	–
41-19	0	1	97.7	-78.8	6.92E-05	1.00	2	–	–	–	–
	100	1	129.4	-77.7	6.74E-05	0.97	2	–	–	–	–
	150	1	167.4	-61.1	6.50E-05	0.94	2	–	–	–	–
	200	1	171.7	-36.3	7.24E-05	1.05	2	–	–	–	–
	250	1	179.4	-26.6	8.17E-05	1.18	2	–	–	–	–
	300	1	179.4	-9.6	9.49E-05	1.37	2	–	–	–	–
	350	1	177.8	-8.6	9.11E-05	1.32	2	–	–	–	–
	380	1	–	–	–	–	2	–	–	–	–
	400	1	182.2	-5.7	8.56E-05	1.24	2	–	–	–	–
	420	1	178.9	-3.8	8.31E-05	1.20	2	–	–	–	–
	450	1	185.2	-5.1	7.26E-05	1.05	2	–	–	–	–
	480	1	167.5	-14.2	5.25E-05	0.76	2	–	–	–	–
	500	1	–	–	–	–	2	–	–	–	–
	520	1	184.8	-9.1	6.18E-05	0.89	2	–	–	–	–
	550	1	182.7	-1.7	6.78E-05	0.98	2	–	–	–	–
	580	1	190.3	5.2	6.53E-05	0.94	2	–	–	–	–
	600	1	172.2	-9.7	4.85E-05	0.70	2	–	–	–	–
	620	1	–	–	–	–	2	–	–	–	–
	650	1	–	–	–	–	2	–	–	–	–
	680	1	–	–	–	–	2	–	–	–	–

APPENDIX E

PALEOMAGNETIC SAMPLE LOCATIONS AND
STRATIGRAPHIC POSITIONS

Table 8. Locations and stratigraphic positions of paleomagnetic samples collected in this study

Sample	Lithology or Tuff	Height above bottom of section (m)	Section	Latitude	Longitude
CLK11-PM8	Guo	–	–	4.2709	36.3468
CLK11-PM9	Guo	–	–	4.2705	36.3458
CLK11-PM10	Sub Ninikaa	–	–	4.0309	36.3453
CLK11-PM11	Guo	69	CLK10-S9	4.3819	36.3701
CLK11-PM12	Guo	72	CLK10-S9	4.3838	36.3696
CLK11-PM13	Kanyeris	–	CLK11-S3	4.3829	36.3636
CLK11-PM14	Tukunan	–	CLK10-S11	4.4043	36.3269
CLK11-PM15	Claystone	0	CLK11-S12	4.4204	36.3760
CLK11-PM16	Siltstone	2	CLK11-S12	4.4204	36.3760
CLK11-PM17	Claystone	4	CLK11-S12	4.4205	36.3760
CLK11-PM18	Claystone	6	CLK11-S12	4.4197	36.3767
CLK11-PM19	Claystone	7	CLK11-S12	4.4197	36.3767
CLK11-PM20	Siltstone	9	CLK11-S12	4.4197	36.3767
CLK11-PM21	Siltstone	12	CLK11-S12	4.4194	36.3767
CLK11-PM22	Claystone	16	CLK11-S12	4.4194	36.3767
CLK11-PM23	Fine sandstone	2	CLK11-S11	4.4183	36.3758
CLK11-PM24	Siltstone	5	CLK11-S11	4.4183	36.3758
CLK11-PM25	Fine sandstone	14	CLK11-S11	4.4179	36.3760
CLK11-PM26	Siltstone	29	CLK11-S11	4.4174	36.3755
CLK11-PM27	Claystone	37	CLK11-S11	4.4173	36.3755
CLK11-PM28	Moiti	41	CLK11-S11	4.4173	36.3754
CLK11-PM29	Kanyeris	–	–	4.2282	36.3145
CLK11-PM30	Siltstone	1	CLK11-S13	4.4085	36.3301
CLK11-PM31	Claystone	3	CLK11-S13	4.4085	36.3301
CLK11-PM32	Claystone	4	CLK11-S13	4.4085	36.3301
CLK11-PM33	Fine sandstone	7	CLK11-S13	4.4085	36.3301
CLK11-PM34	Siltstone	9	CLK11-S13	4.4085	36.3301
CLK11-PM35	Claystone	11	CLK11-S13	4.4085	36.3301
CLK11-PM36	Fine sandstone	12	CLK11-S13	4.4085	36.3301
CLK11-PM37	Fine sandstone	16	CLK11-S13	4.4085	36.3301
CLK11-PM38	Kanyeris	18	CLK11-S13	4.4083	36.3303
CLK11-PM39	Claystone	8	CLK11-S6	4.4159	36.3367
CLK11-PM40	Claystone	11	CLK11-S6	4.4159	36.3370
CLK11-PM41	Claystone	13	CLK11-S6	4.4158	36.3373
CLK11-PM42	Claystone	15	CLK11-S6	4.4158	36.3375
CLK11-PM43	Claystone	17	CLK11-S6	4.4158	36.3376

Table 8. continued

Sample	Lithology or Tuff	Height above bottom of section (m)	Section	Latitude	Longitude
CLK11-PM44	Claystone	20	CLK11-S6	4.4158	36.3376
CLK11-PM45	Wargolo	–	–	4.3893	36.3943
CLK11-PM46	Kisemei	0	CLK11-S2	4.3787	36.3700
CLK11-PM47	Fine sandstone	9	CLK10-S10	4.4043	36.3297
CLK11-PM48	Fine sandstone	10	CLK10-S10	4.4040	36.3299
CLK11-PM49	Fine sandstone	12	CLK10-S10	4.4040	36.3300
CLK11-PM50	Claystone	6	CLK10-S7	4.4119	36.3422
CLK11-PM51	Claystone	11	CLK10-S7	4.4119	36.3423
CLK11-PM52	Claystone	16	CLK10-S7	4.4119	36.3423
CLK11-PM53	Fine sandstone	0	CLK10-S4A	4.4132	36.3701
CLK11-PM54	Fine sandstone	1	CLK10-S4A	4.4132	36.3701
CLK11-PM55	Fine sandstone	3	CLK10-S4A	4.4132	36.3701
CLK11-PM56	Fine sandstone	3	CLK10-S4A	4.4132	36.3701
CLK11-PM57	Fine sandstone	4	CLK10-S4A	4.4132	36.3701
CLK11-PM58	Fine sandstone	6	CLK10-S4A	4.4131	36.3702
CLK11-PM59	Fine sandstone	8	CLK10-S4A	4.4131	36.3702
CLK11-PM60	Fine sandstone	12	CLK10-S4A	4.4130	36.3702
CLK11-PM61	Fine sandstone	16	CLK10-S4A	4.4129	36.3703
CLK11-PM62	Siltstone	–	–	4.2699	36.3469
CLK11-PM63	Siltstone	–	–	4.2699	36.3469
CLK11-PM64	Siltstone	–	–	4.2699	36.3469
CLK11-PM65	–	–	–	4.2370	36.3181
CLK11-PM66	Tuff	–	–	4.2370	36.3181
CLK11-PM67	Fine sandstone	64	CLK10-S9	4.3833	36.3712
CLK11-PM68	Mudstone	60	CLK10-S10	4.3834	36.3713
CLK11-PM69	Siltstone	56	CLK10-S11	4.3836	36.3715
41-1	Claystone	3	PNG-41.2	4.3077	36.3779
41-2	Claystone	6	PNG-41.3	4.3077	36.3779
41-3	Claystone	9	PNG-41.4	4.3078	36.3778
41-4	Claystone	16	PNG-41.5	4.3079	36.3777
41-5	Claystone	18	PNG-41.6	4.3079	36.3777
41-6	Claystone	25	PNG-41.7	4.3081	36.3775
41-7	Claystone	29	PNG-41.8	4.3083	36.3776
41-8	Claystone	32	PNG-41.9	4.3084	36.3776
41-9	Claystone	36	PNG-41.10	4.3084	36.3769
41-10	Claystone	40	PNG-41.11	4.3085	36.3768

Table 8. continued

Sample	Lithology or Tuff	Height above bottom of section (m)	Section	Latitude	Longitude
41-11	Claystone	43	PNG-41.12	4.3084	36.3764
41-12	Claystone	48	PNG-41.13	4.3085	36.3764
41-13	Claystone	55	PNG-41.14	4.3085	36.3762
41-14	Siltstone	57	PNG-41.15	4.3085	36.3762
41-15	Siltstone	60	PNG-41.16	4.3086	36.3760
41-16	Siltstone	65	PNG-41.17	4.3087	36.3760
41-17	Siltstone	75	PNG-41.18	4.3091	36.3758
41-18	Siltstone	86	PNG-41.19	4.3091	36.3758
41-19	Siltstone	79	PNG-41.20	4.3091	36.3758

REFERENCES

Alsop, G. I., and Marco, S., 2012, A large-scale radial pattern of seismogenic slumping towards the Dead Sea Basin: Journal of the Geological Society of London, v. 169, no. 1, p. 99–110.

Behrensmeyer, A. K., 1970, Preliminary geological interpretation of a new hominid site in the Lake Rudolf Basin: Nature (London), v. 226, no. 5242, p. 225–226.

Boschetto, H. B., Brown, F. H., and McDougall, I., 1992, Stratigraphy of the Lothidok Range, northern Kenya, and K/Ar ages of its Miocene primates: Journal of Human Evolution, v. 22, no. 1, p. 47–71.

Bowen, B. E., 1974, The Geology of the Upper Cenozoic Sediments in the East Rudolf Embayment of the Lake Rudolf Basin, Kenya: Iowa State University, 164 p.

Bowen, B. E., and Vondra, C. F., 1973, Stratigraphical Relationships of the Plio-Pleistocene Deposits, East Rudolf, Kenya: Nature (London), v. 242, no. 5397, p. 391–393.

Braun, D. R., Harris, J. W. K., Levin, N. E., McCoy, J. T., Herries, A. I. R., Bamford, M.K., Bishop, L. C., Richmond, B. G.,and Kibunjia, M., 2007, Early hominin diet included diverse terrestrial and aquatic animals 1.95 Ma in East Turkana, Kenya. Proceedings of the National Academy of Science, v. 107, p. 10002–10007.

Brown, F. H., and Cerling, T. E., 1982, Stratigraphical significance of the Tulu Bor Tuff of the Koobi Fora Formation: Nature (London), v. 299, no. 5880, p. 212–215.

Brown, F. H., and Feibel, C. S., 1986, Revision of lithostratigraphic nomenclature in the Koobi Fora region, Kenya: Journal of the Geological Society of London, v. 143, no. 2, p. 297–310.

Brown, F. H., and Feibel, C. S., 1991, Stratigraphy, depositional enviornments, and paleogeography of the Koobi Fora Formation, Oxford, Clarendon Press, Koobi Fora Research Project, Volume 3, The Fossil Ungulates: Geology, Fossil Artiodactyls, and Paleoenvironments, p. 1–30.

Brown, F. H., and Fuller, C. R., 2008, Stratigraphy and tephra of the Kibish Formation, southwestern Ethiopia: Journal of Human Evolution, v. 55, no. 3, p. 366–403.

Brown, F. H., Haileab, B., and McDougall, I., 2006, Sequence of tuffs between the KBS Tuff and the Chari Tuff in the Turkana Basin, Kenya and Ethiopia: Journal of the Geological Society of London, v. 163, no. 1, p. 185–204.

Brown, F. H., and McDougall, I., 2011. Geochronology of the Turkana Depression of northern Kenya and southern Ethiopia. Evolutionary Anthropology, v. 20, p. 217–227.

Brown, F. H., Shuey, R. T., and Croes, M. K., 1978, Magnetostratigraphy of the Shungura and Usno formations, southwestern Ethiopia; new data and comprehensive reanalysis: Geophysical Journal of the Royal Astronomical Society, v. 54, no. 3, p. 519–538.

Bruhn, R. L., Brown, F. H., Gathogo, P. N., and Haileab, B., 2011, Pliocene volcano-tectonics and paleogeography of the Turkana Basin, Kenya and Ethiopia: Journal of African Earth Sciences, v. 59, no. 2–3, p. 295–312.

Buchanan, M. J., 2010, Stratigraphic and structural geology of Area 117, Koobi Fora Region, northern Kenya [M.S. 1476646]: The University of Utah, 153 p.

Cerling, T. E., and Brown, F. H., 1982, Tuffaceous marker horizons in the Koobi Fora region and the Lower Omo Valley: Nature (London), v. 299, no. 5880, p. 216–221.

deMenocal, P. B., and Brown, F. H., 1999. Pliocene tephra correlations between East African hominid localities, the Gulf of Aden, and the Arabian Sea, Hominid Evolution and Climatic change in the Europe, v. 1. The Evolution of Neogene Terrestrial Ecosystems in Europe, Cambridge University Press, p. 23–54.

Ebinger, C. J., Yemane, T., Harding, D. J., Tesfaye, S., Kelley, S., and Rex, D., 2000, Rift deflection, migration, and propagation: Linkage of the Ethiopian and Eastern rifts, Africa: Bulletin of the Geological Society of America, v. 112, no. 2, p. 163–176.

Feibel, C. S., 1988, Paleoenvironments of the Koobi Fora Formation, Turkana Basin, northern Kenya [Doctoral Ph. D dissertation]: University of Utah, 337 p.

Feibel, C. S., Harris, J. M., and Brown, F. H., 1991, Paleoenvironmental context for the Late Neogene of the Turkana Basin, Oxford, Clarendon Press, Koobi Fora Research Project, Volume 3, The Fossil Ungulates: Geology, Fossil Artiodactyls, and Palaeoenvironments, p. 321–370.

Fuchs, V. E., 1934, The geological work of the Cambridge Expedition to the East African lakes, 1930-31: Geological Magazine, v. 71, no. 837, p. 97–112.

Gathogo, P. N., 2003, Stratigraphy and Paleoenvironments of the Koobi Fora Formation of the Ileret Area, Northern Kenya, University of Utah, 160 p.

Gathogo, P. N., and Brown, F. H., 2006, Stratigraphy of the Koobi Fora Formation (Pliocene and Pleistocene) in the Ileret region of northern Kenya: Journal of African Earth Sciences, v. 45, no. 4-5, p. 369–390.

Gathogo, P. N., Brown, F. H., and McDougall, I., 2008, Stratigraphy of the Koobi Fora Formation (Pliocene and Pleistocene) in the Loiyangalani region of northern Kenya: Journal of African Earth Sciences, v. 51, no. 5, p. 277–297.

Gibert, L., Sanz de Galdeano, C., Alfaro, P., Scott, G., and Lopez Garrido, A. C., 2005, Seismic-induced slump in early Pleistocene deltaic deposits of the Baza Basin (SE Spain): Sedimentary Geology, v. 179, no. 3–4, p. 279–294.

Gradstein, F. M., 2004, A geologic time scale 2004, Cambridge, United Kingdom (GBR), Cambridge University Press, Cambridge, 589 p.

Haileab, B., Brown, F. H., McDougall, I., and Gathogo, P. N., 2004, Gombe Group basalts and initiation of Pliocene deposition in the Turkana Depression, northern Kenya and southern Ethiopia: Geological Magazine, v. 141, no. 1, p. 41–53.

Harris, J. M., Leakey, M. G., and Brown, F. H., 2006, A Brief History of research at Koobi Fora, Northern Kenya, The American Society for Ethnohistory, v. 53, p. 35–69, Duke University Press, Durham, N.C.

Hillhouse, J. W., Cerling, T. E., and Brown, F. H., 1986, Magnetostratigraphy of the Koobi Fora Formation, Lake Turkana, Kenya: Journal of Geophysical Research, v. 91, no. B11, p. 11,581–11,595.

Hillhouse, J. W., Ndombi, J. W. M., Cox, A., and Brock, A., 1977, Additional results on palaeomagnetic stratigraphy of the Koobi Fora Formation, east of Lake Turkana (Lake Rudolf), Kenya: Nature (London), v. 265, no. 5593, p. 411–415.

Hynek, S. A., Brown, F. H., and Fernandez, D. P., 2011, A rapid method for hand picking potassium-rich feldspar from silicic tephra: Quaternary Geochronology, v. 6, no. 2, p. 285–288.

Key, R. M., and Watkins, R. T., 1988, Geology of the Sabarei Area: Mines and Geology Department, Republic of Kenya, 111, 57 p.

Kuiper, K., Deino, A., Hilgen, F., Krijgsman, W., Renne, P., Wijbrans, J., and Anonymous, 2008, Synchronizing rock clocks of Earth history: International Geological Congress, Abstracts = Congres Géologique International, Resumes, v. 33, p. Abstract 1349328.

Leakey, M. G., and Harris, J. M., 2003, Lothagam: The Dawn of Humanity in Eastern Africa: New York Columbia University Press, 678 p.

Leakey, M. G., and Leakey, R. E., 1978, Koobi Fora Reasearch Project Oxford, Clarendon Press, 191 p.

Leakey, R. E., 1970, New Hominid Remains and Early Artefacts Nature, v. 226, p. 223–226.

McDougall, I., and Brown, F. H., 2008, Geochronology of the pre-KBS Tuff sequence, Omo Group, Turkana Basin: Journal of the Geological Society of London, v. 165, no. 2, p. 549–562.

McDougall, I., and Feibel, C. S., 2003, Numerical Age control for the Miocene-Pliocene succession at Lothagam, a Hominoid-bearing sequence in the Northern Kenya Rift, *in* Leakey, M. G., John M., ed., Lothagam: The Dawn of Humanity in Eastern Africa: New York, Columbia University Press, p. 43–64.

Min, K., Mundil, R., Renne, P. R., and Ludwig, K. R., 2000, A test for systematic errors in $^{40}Ar/^{39}Ar$ geochronology through comparison with U/Pb analysis of a 1.1-Ga rhyolite: Geochimica et Cosmochimica Acta, v. 64, no. 1, p. 73–98.

Morley, C. K., 1999, Geoscience of Rift Systems - Evolution of East Africa: AAPG Studies in Geology No. 44, 242 p.

Morley, C. K., Ngenoh, D. K., and Ego, J. K., 1999a, Introduction to the East African Rift System, *in* Morley, C. K., ed., Geoscience of Rift Systems-Evolution of East Africa: Studies in Geology No. 44, p. 1–18.

Morley, C. K., Wescott, W. A., Stone, D. M., Harper, R. M., Wigger, S. T., Day, R. A., and Karanja, F. M., 1999b, Geology and Geophysics of the Western Turkana Basins, Kenya, *in* Morley, C. K., ed., Geoscience of Rift Systems-Evolution of East Africa: Studies in Geology No. 44, p. 19–54.

Morley, C. K., Wescott, W. A., Stone, D. M., Harper, R. M., Wigger, S. T., and Karanja, F. M., 1992, Tectonic evolution of the northern Kenyan Rift: Journal of the Geological Society of London, v. 149, Part 3, p. 333–348.

Owen, R. B., and Renaut, R. W., 1986, Sedimentology, stratigraphy and paleoenvironments of the Holocene Galana Boi Formation, NE Lake Turkana, Kenya, *in* Frostick, L. E., Renaut, R. W., Reid, I., and Tiercelin, J. J., eds., Sedimentation in the African rifts: Blackwell, Oxford, Geological Society Special Publication 25, p. 311–322.

Rosendahl, B. R., 1987, Architecture of continental rifts with special reference to East Africa: Annual Reviews of Earth and Planetary Science, v. 15, p. 445–503.

Salisbury, M. J., Jicha, B. R., de Silva, S. L., Singer, B. S., Jimenez, N. C., and Ort, M. H., 2011, ^{40}Ar/^{39}Ar chronostratigraphy of Altiplano-Puna volcanic complex ignimbrites reveals the development of a major magmatic province: Geological Society of America Bulletin, v. 123, no. 5–6, p. 821–840.

Shuey, R. T., Brown, F. H., and Croes, M. K., 1974, Magnetostratigraphy of the Shungura Formation, southwestern Ethiopia: Fine structure of the lower Matuyama polarity epoch: Earth and Planetary Science Letters, v. 23, no. 2, p. 249–260.

Tauxe, L., Butler, R. F., Van der Voo, R., and Banerjee, S. K., 2010, Essentials of paleomagnetism, Berkeley, CA, United States (USA), University of California Press, Berkeley, CA, Essentials of paleomagnetism, 489 p.

von Höhnel, L., 1894, Count Teleki and the Discovery of Lakes Rudolf and Stefanie, London, Green and Company, 435 p.

Watkins, R. T., 1983, The Geology of the Suregei-Asille district and the upper Bakate Valley, Northern Kenya [Ph. D. Thesis]: University of London, 390 p.

WoldeGabriel, G., Aronson, J. L., and Walter, R. C., 1990, Geology, geochronology, and rift basin development in the central sector of the Main Ethiopia Rift: Geological Society of America Bulletin, v. 102, no. 4, p. 439–458.